New combinatorial features of knots and virtual knots

Arnaud Mortier

THÈSE

En vue de l'obtention du

DOCTORAT DE L'UNIVERSITÉ DE TOULOUSE

Délivré par: Université Toulouse III – Paul Sabatier
École doctorale: Mathématiques Informatique Télécommunications (MITT)
Unité de recherche: UMR 5219
Discipline : Mathématiques

présentée par

Arnaud MORTIER

Nouveaux aspects combinatoires de théorie des nœuds et des nœuds virtuels

---

dirigée par Thomas FIEDLER

Soutenue le 12 juillet 2013 devant le jury composé de :

M. Christian Blanchet	Paris VII	examinateur
M. Thomas Fiedler	Toulouse III	directeur
M. Louis Funar	Institut Fourier	rapporteur
M. Gregor Masbaum	Paris VI	examinateur
M. Jean-Baptiste Meilhan	Institut Fourier	examinateur
M. Michael Polyak	Technion	rapporteur

Remerciements

Avant tout je présente mes excuses aux personnes qui m'ont accompagné ou soutenu durant les quatre dernières années, pour le grand nombre de formalités et d'euphé- mismes contenus dans ces remerciements. Il peut être très difficile de résumer en quelques mots la reconnaissance accumulée au cours d'une période aussi longue. Tout comme il est difficile de ne pas donner à de tels propos une allure d'épilogue.

Je remercie Thomas Fiedler. Pour la confiance qu'il n'a cessé d'avoir en moi, depuis le début et à travers des périodes très incertaines. Pour la souplesse et l'autonomie qu'il m'a laissées, sans être jamais à court de ressources, d'idées, de références, de contacts, lorsque le besoin pouvait s'en faire sentir. Pour être, enfin, l'instigateur d'une école d'hiver d'une richesse mathématique et humaine que je ne saurais décrire par des mots.

I wish to thank Misha Polyak. Because he accepted the task of being a referee to this thesis report. For the uninterrupted flow of his ideas merging topology, algebra and combinatorics, which were a great source of inspiration over the past years. For being, in some sense, my virtual co-advisor.

Je remercie Louis Funar et Gregor Masbaum pour avoir accepté de faire partie de mon jury, et Louis en particulier pour m'avoir donné son temps en relisant ce manuscrit.

À Jean-Baptiste Meilhan, je souhaiterais dire merci pour s'être intéressé à mon travail – et avoir sincèrement proposé d'être rapporteur de cette thèse, avant qu'une subtilité bureaucratique ne l'en empêche. Pour m'avoir invité à Grenoble, et permis de participer aux événements organisés dans le cadre de l'ANR VasKho.

Pour n'oublier aucun membre du jury, je souhaite exprimer ma profonde reconnaissance à Christian Blanchet, pour n'avoir jamais refusé une conversation, pour ses conseils (méta-)mathématiques et son soutien – qui m'a notamment permis de passer une année extrêmement enrichissante à Paris.

I would like to thank a number of people who accepted to share their ideas with me, namely Fionntan Roukema and Micah Chrisman with whom I had interesting conversations over the internet, and Matthew Hedden, Jean-François Barraud and Benjamin Audoux who are responsible for the little I know about Heegaard-Floer homology.

Je tiens à remercier Ana Lecuona, Hoel Queffelec et Catherine Gille pour une collaboration inoubliable, qui m'a fait découvrir à quel point il peut être non seulement agréable, mais aussi productif, de travailler en groupe.

De trois ans passés à Toulouse, je garderai le souvenir de Michel Boileau et Joseph Tapia, qui ont une tendance innée à négliger leurs intérêts personnels pour prêter une attention sincère au néophyte et tenter de lui transmettre leurs connaissances, ne fût-il capable d'en absorber qu'une quantité finie.

Je me souviendrai de Jacques Sauloy, Claire Dartyge, Philippe Monnier, Ahmed Zeriahi et Anne Cumenge avec qui ce fut un plaisir d'enseigner – plaisir qui a pu se révéler réciproque, notamment lorsque Jacques a amicalement tenté de me dissuader de déménager à Paris.

Un grand merci à mes coburettes Virginie, Claire et Valentina (par ordre alphabétique des noms de famille, comme c'est d'usage en mathématiques lorsqu'aucun autre ordre ne s'avère plus naturel), pour le café, les kalanchoes, la chauffeuse à sieste, la scopa, les dessins millénaires au tableau, la bonne humeur (meur, meur, meur-meur) qui a régné dans le bureau 105 pendant ces années, ponctuées par les passages éclair de Dima que je remercie pour les cours de russe et les cours de дурак (je l'écris en russe, les gens croiront que c'est une théorie mathématique très compliquée).

Merci à JC et Marie-Anne pour leur amitié, les soirées, le festival du cinéma d'Amérique latine, la coinche (qui est aussi une théorie mathématique très compliquée). Merci à Sébastien, Paul et Daniel pour les parties d'échecs, à Arnaud et Pascale pour les bons moments passés autour d'un pique-nique ou d'un barbecue. Merci à Gioia pour si bien porter son prénom.

Avant de continuer, le lecteur doit réaliser que la période de fin d'études doctorale est assez éprouvante. Surtout les 36 derniers mois, dirait Coluche. Afin de tenir psychologiquement, il est de bon aloi de réserver une place incompressible à l'humour et à l'invraisemblable. Je ne peux que respecter cet état d'esprit en remerciant les personnes qui m'ont accompagné durant cette période et notamment les occupants des bureaux 7C08 puis 750, qui étaient pour beaucoup dans une situation similaire, et sans lesquelles la survie n'aurait pas été acquise.

Merci à LH et Lukas pour d'enrichissantes conversations, notamment sur les 3-coloriages de graphes bipartites, et sur les meilleures proportions thé/café dans lesquelles il convient d'arroser un cactus à raquettes. À Hoel pour sa preuve élégante de la primalité de 2013 (ainsi que d'autres nombres dont les mathématiciens ont longtemps mis en doute le caractère premier en raison de leur divisibilité par 2). À Elodie, pour ses connaissances en labyrinthes administratifs, pour la logistique pain/nutella/sopalin des pauses café, et pour les regards noirs qu'elle m'a valus en envoyant des e-mails calomnieux à ma femme. À Roro, le Chinois du Cambodge qui sait parler aux filles (en langage des singes), pour avoir porté mes slips (afin de donner un coup de main lors de mon déménagement à Paris), pour les week-ends studieux à Sophie Germain, et enfin pour m'avoir promis une côte de bœuf pour figurer dans ces remerciements. À Christophe, pour ses macarons ratés, pour les pauses chocolat aux horaires très stricts, pour croire sérieusement que des gens s'enferment dans les bureaux de Sophie Germain pour y développer des photos. À Xin, Sary et Alexandre, pour avoir préservé une part de sagesse dans le quotidien des doctorants.

Une pensée particulière à destination de Pascal Chiettini, secrétaire dont l'efficacité comme la disponibilité ne semblent pas avoir de limites.

Enfin, merci à ma famille, mes parents, Vika, pour me supporter, pour croire en moi, pour me garder dans le droit chemin. Vika, sans toi ce manuscrit ne serait pas. Je te dois un café.

Большое спасибо Галине Лебедь за то, что она приняла меня в свою семью.

Contents

Chapter 1

Introduction

Gauss diagrams

A Gauss diagram is the result of unknotting a knot diagram in the plane, using arrows to remember which couples of points of the circle were originally crossed. To make the construction *faithful* – that is, with no essential loss of information –, one also remembers the over/under datum and the local writhes of the crossings.

One observes that not all Gauss diagrams actually come from knots. By forgetting the 3-space and the actual knots, considering only Gauss diagrams and their combinatorics (also made of "Reidemeister moves"), one obtains the *virtual knot theory*, developed by Kauffman [17] in the late 90's. It happens that virtual knots can also be understood in terms of knot diagrams in the plane, with usual and *virtual* crossings, subject to usual, *virtual* and *mixed* Reidemeister moves. These last two additional kinds of moves are precisely those leaving the underlying Gauss diagram unchanged. Together, they are equivalent to the single *detour move*, which is global – one or the other viewpoint can be more convenient depending on the situation. An important result of Kauffman [17] states that the additional virtual moves cannot connect different usual knot types.

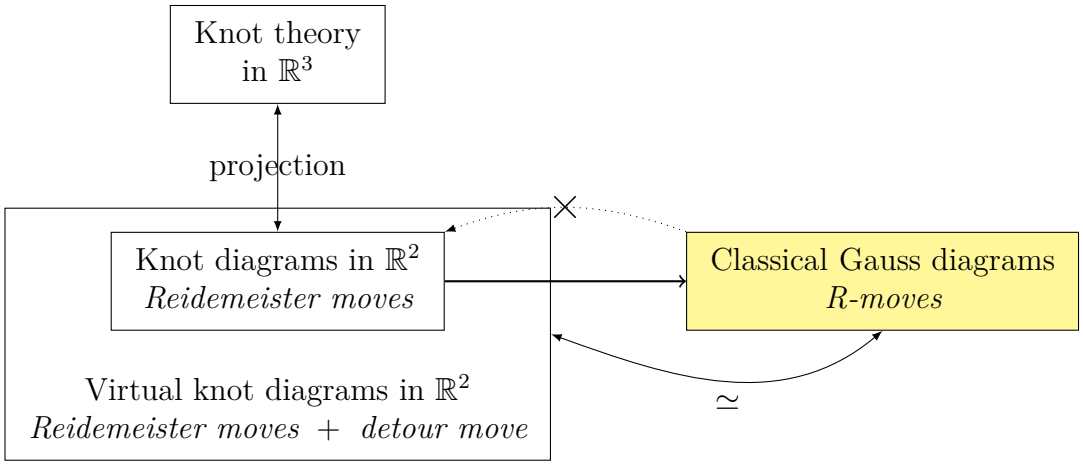

In Chapter 2, we aim at generalizing this scheme following the initial idea of replacing the projection $\mathbb{R}^3 \to \mathbb{R}^2$ with a real line bundle over an arbitrary surface Σ – which is called a *thickened surface*.

To circumvent algebraic issues about conjugacy in free groups, the knots considered have all of their usual crossings lying over a fixed contractible subset of Σ. Also, every usual Reidemeister move can be made to happen over that set by an adequate diagram isotopy. This splits the tasks into two parts: understanding the *local* Reidemeister moves (which are nothing more than what one is used to), and understanding the *global* diagram isotopies and detour moves. It is shown that these global moves are essentially generated by the elementary move taking a real crossing and moving it all along a given loop in Σ.

From the Gauss diagram viewpoint – assuming for now that Σ is orientable:

- → Gathering all the real crossings over a disc allows one to color the edges (the parts of the circle between two consecutive arrow ends) with elements of $\pi = \pi_1(\Sigma)$.
- → The Reidemeister moves are the same as usual, with the requirement that the edges involved must be marked the unit $1 \in \pi$.
- → As before, the detour moves do not change the diagram at all.
- → There is a new *conjugacy move* corresponding to an elementary global move. It changes the π-markings of the four edges adjacent to an arrow.

The case of non orientable surfaces requires only little more effort: some of the Gauss diagram decorations may not be globally defined, in which case the conjugacy move can change them too, according to their monodromy. When the total space of the bundle is assumed to be orientable, then there is only one monodromy morphism to consider, and it is given by the first Stiefel-Whitney class of the tangent bundle to Σ.

With all this in mind we define a new Gauss diagram theory, that depends only on an arbitrary group π and a homomorphism $w : \pi \to \mathbb{F}_2$ (Section 2.3). Just like the usual virtual knot theory gives up caring about the actual existence of knots, this "**virtual knot theory on a group**" ignores the existence of a surface on which to draw diagrams. As expected, for an arbitrary surface Σ, the input $\pi = \pi_1(\Sigma)$ and $w \equiv w_1(T\Sigma)$ (the first Stiefel-Whitney class) gives a theory that fully and faithfully encodes virtual knot diagrams on Σ up to Reidemeister moves, diagram isotopy and detour moves. It follows that when two surfaces happen to thicken into the same 3-manifold M – such as the annulus and the Moebius strip, one obtains *different "virtual" generalizations of knot theory in* M. However, when $\pi_1(M) \neq \{1\}$, it is not known whether the usual knot theory in M faithfully embeds into any of these virtual generalizations.

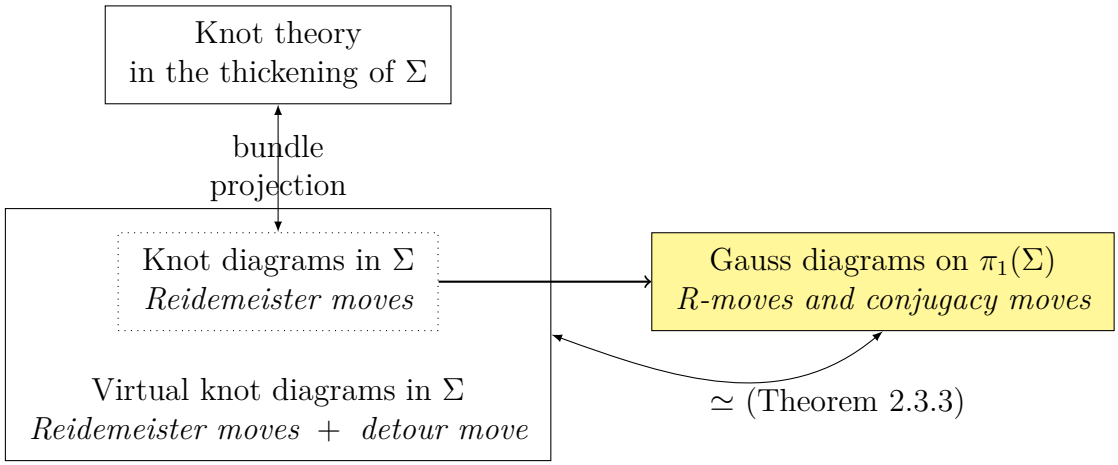

A slightly more compact version is defined when the group π is abelian, inspired by T.Fiedler's diagrams decorated with elements of $H_1(\Sigma)$ [10, 9]. It allows one to get rid of the conjugacy moves, with no loss of information. In general, a description of the orbits of the conjugacy moves by diagrams with finitely many decorations is not known. It is related to the existence of an algorithm to decide whether two given Gauss diagrams are related by conjugacy moves. We discuss that question in Subsection 2.3.1 – paragraph *About the orbits of w-moves*.

Finite type invariants

Besides the encoding of knot diagrams, a major feature of Gauss diagrams is that they provide a combinatorial description of Vassiliev's finite type invariants. This so called theory of *Gauss diagram formulas* was developed by M.Polyak and O.Viro [27], and independently by T.Fiedler [9]. A few formulas due to J.Lannes [19] for the invariants up to degree three do the same computations and came up simultaneously, though without the powerful diagrammatic aspect. All of these invariants are of finite type in the sense of Vassiliev. An important theorem of M.Goussarov [13] states that conversely, in the classical case of knots in $\mathbb{R}^3$, every Vassiliev invariant happens as a Gauss diagram formula.

Roughly, a Gauss diagram formula computes a weighted sum of the subdiagrams of its variable. An important particular case is that of *arrow diagram formulas*, whose weights satisfy the following rule: *if two diagrams differ only by the signs of their arrows, then either their weights are* 0*, or the ratio of their weights is equal to the ratio of the products of their signs.* Historically, this particular case was the first to appear (see [27]). Most examples still belong in this case at the time of writing (see [3], [4], [15]).

One observes that these invariants are naturally defined, as maps, on the set of all Gauss diagrams. It raises the question: which of them do also define invariants of virtual knots? This question is investigated in [14], where it is shown that the $\mathbb{Q}$-space of virtual Gauss diagram formulas identifies with the dual of the *Polyak algebra* from [25]. Also in [14], an alternative notion of *finite-type* is developed, axiomatizing those virtual knot invariants that come from Gauss diagram formulas.

Besides this virtual direction, a number of generalizations of Gauss diagram formulas have been made for knot diagrams in a surface Σ, using different kinds of

additional decorations – for instance free homotopy classes of loops in Σ [15], and elements of quotients of $H_1(\Sigma)$ [10]. All of these frameworks are "contained" the above Gauss diagram theory on a group.

Chapter 3 is devoted to the study of the virtual invariants in the framework of Gauss diagrams on a group. It generalizes [22] where only the case of knot diagrams in $\mathbb{R} \times \mathbb{S}^1$ was considered.

We formalize the fact that it should *contain* the existing theories by describing appropriate "symmetry preserving" maps: a space with few information and lots of symmetries injects into a space with more information and less symmetries.

A Polyak algebra is constructed. It allows one to observe numerous relations between arrow diagram formulas and *homogeneous* Gauss diagram formulas, which finally lead to show that these two notions coincide (Theorem 3.2.24). Special invariance criteria follow for arrow diagram formulas. In particular, the Reidemeister III criterion (Theorem 3.3.9) gives an interpretation and a proof of a conjecture of M.Polyak, which predicts that arrow diagram formulas should be the kernel of a map with values in some space of degenerate diagrams. Subsection 3.3.4 contains a topological point of view on this map, at the intersection between M.Polyak and V.A.Vassiliev's ideas. This point of view is the most likely to give rise to a full cohomology theory, in which the above map would be the 0-coboundary.

Once the invariance criteria have been described at the top-level (that of arrow diagrams on a group), thanks to the symmetry-preserving injections one directly obtains criteria for all the kinds of invariants that lie "below". Chapter 3 ends with examples that take advantage of this fact. In particular, we give an alternative proof to Grishanov-Vassiliev's theorem on planar arrow diagram formulas [15] and slightly improve it.

Detection of closed braids in the solid torus

The closed braid problem is the following: given a knot diagram in the annulus $\mathbb{R} \times \mathbb{S}^1$, how to tell if it represents a knot that is isotopic to a closed braid in the solid torus [16]?

In [10], T.Fiedler suggests an attempt to answer that question by evaluating specific finite-type invariants, which conjecturally all vanish if and only if the knot is a closed braid. Only a few examples are constructed. The reason why the invariants from these examples vanish on closed braids is that they weight only diagrams that cannot happen as subdiagrams of a closed braid, because of the homology class of certain loops: those that run positively along the edges of the Gauss diagram (the *ER loops*).

Chapter 4 is a draft attempt to answer the closed braid problem by a direct study of the set of these loops.

A new kind of Gauss diagrams is introduced, no more decorated by elements of a group, but by words in a fixed presentation of that group. The difference is significant – and similar to the step between Gauss diagrams with π_1 decorations and those with only some h_1 decorations: the more information there is in the Gauss diagrams, the more accurate will be their topological matches.

It is shown that being a virtual closed braid diagram in the annulus is char-

acterized by the fact that all ER loops must have a positive homology class in $\mathbb{Z} \simeq H_1(\mathbb{R} \times \mathbb{S}^1)$ – a property called *braid-admissibility* already in [10]. We conjecture that for diagrams with minimal number of crossings, not being in a closed braid position implies not being equivalent to a closed braid diagram modulo Reidemeister moves. A few aspects and possible plans towards that conjecture are discussed at the end of the chapter.

Invariants of non generic homotopies

V.A.Vassiliev introduced the finite-type knot invariants by studying the topology of the infinite dimensional stratified space of all smooth immersions of a circle in $\mathbb{R}^3$. To define these invariants, one considers only those strata of the discriminant that correspond to singular knots with a finite number of ordinary double points.

In Chapter 5, we investigate what can happen if one avoids these strata and instead consider those with ordinary *triple* points. M.Heusener has proved that any knot can be unknotted by a homotopy that meets the discriminant only in such strata, even if one only allows some directions in which to cross these strata, called *coherent* – that is, when on both sides of the singularity, the three crossings of the knot diagram have the same local writhe.

By adding up all the writhe increases encountered *at triple points* during such a homotopy, one obtains an invariant of triple homotopies (in a sense that is made precise by defining homotopies of triple homotopies), that is shown to be non-trivial.

We show that a twisted (or weighted) form of the above invariant gives a formula for the "derivative" of the Casson invariant for knots, with respect to coherent triple points. A number of (unanswered) questions arise from there: is it possible to define a complete finite-type theory with respect to coherent triple points? How is it related to Vassiliev's finite-type invariant theory?

1.1 Conventions

Pictures with incomplete diagrams

When several incomplete diagrams are represented side by side in a picture, or in one and the same equation, it is to be understood that

1. Every unseen part – including missing decorations, such as local orientations – is the same for all diagrams.
2. The picture is valid no matter what are those unseen parts, unless otherwise specified in the caption under the picture.

"Real" objects

The word "real" will be used to label a usual crossing in a knot diagram, or a knot diagram that only contains usual crossings, or a Gauss diagram that is represented by such a knot diagram. This terminology is justified by two reasons. First, the contrast with the word "virtual", that labels the second kind of crossings encountered

in Gauss diagram theory. Second, a *real* crossing, in a diagram drawn on a surface Σ, is a double point of an immersion whose two smooth branches have been locally pushed inside a *real* line bundle over Σ.

I deeply apologize to the reader who is familiar with another terminology.

Notations

A notation that is absent from this list is usually specific to a section.

D: a knot diagram.
G: a Gauss diagram or an abelian Gauss diagram.
K: a knot, or the circle of a Gauss diagram.
R-I, R-II, R-III: Reidemeister moves of knot diagrams.
R_1, R_2, R_3: R-moves of Gauss diagrams – matching the Reidemeister moves.
ν: a knot invariant.
$\mathcal{G}$: a linear combination of Gauss diagrams.
$\mathfrak{G}_n$: the $\mathbb{Q}$-space freely generated by degree n Gauss diagrams.
$\mathfrak{G}_{\leq n}$: the direct sum of all $\mathfrak{G}_k$'s for $k \leq n$.
$\mathfrak{G}$: the direct limit of the $\mathfrak{G}_{\leq n}$'s with the natural inclusions.
$\mathfrak{G}_\bullet$: similar to $\mathfrak{G}$, where the Gauss diagrams have a preferred edge (Definition 3.3.1).
$\mathfrak{DG}$: similar to $\mathfrak{G}$, with degenerate diagrams (Definition 3.3.1).
$\widehat{\mathfrak{G}}$: the $\mathbb{Q}$-space of formal series of Gauss diagrams.

There are similar notations for arrow diagrams:
A, $\mathcal{A}$, $\mathfrak{A}_n$, $\mathfrak{A}_{\leq n}$, $\mathfrak{A}$, $\mathfrak{A}_\bullet$, $\mathfrak{DA}$, $\widehat{\mathfrak{A}}$.

π: an arbitrary group.
$h_1(\pi)$: the set of conjugacy classes in π.
g: an arbitrary element of π.
w: an arbitrary "weight" homomorphism $\pi \to \mathbb{F}_2$.
w_0: the trivial homomorphism $\pi \to \mathbb{F}_2$.
Σ: an arbitrary surface.
$h_1(\Sigma)$: the *set* of free homotopy classes of loops in Σ.
M: the total space of an oriented real line bundle over Σ.
When a surface Σ is considered, π is set to $\pi_1(\Sigma)$ and w is set to the first Stiefel-Whitney class of $T\Sigma$. This couple is called the weighted fundamental group *of Σ.*

μ: the decorating map $H_1(G) \to \pi$ of an *abelian Gauss diagram* G.
γ: a loop $\mathbb{S}^1 \to G$, or a homology class in $H_1(G)$.
A: an arrow of G.
e: an edge of G.
c: an arbitrary 1-cell of G, *i.e.* an arrow or an edge.

Chapter 2

Virtual knot theories

This chapter begins with a brief introduction to the classical settings of virtual knot theory via Gauss diagrams. The goal is to define Gauss diagrams in a large framework that contains virtual knot diagrams on an arbitrary surface.

Section 2.2 defines and studies (virtual) knot diagrams on an arbitrary surface Σ: these are tetravalent graphs embedded in Σ, some of whose double points (the "real" ones) are pushed and desingularized into a real line bundle over Σ. Defining Gauss diagrams requires a global notion for the branches at a real crossing to be one "over" the other, and a global notion of writhe of a crossing. It is shown that these notions can be defined simultaneously if and only if Σ is orientable. If it is not, we sacrifice the globality of one property, and take into account its monodromy. It is shown that when the total space of the bundle is orientable, the writhes are globally defined and the monodromy of the "over/under" datum is the first Stiefel-Whitney class of the tangent bundle to Σ, $w_1(\Sigma)$.

In Section 2.3 is given a definition of Gauss diagrams decorated by elements of a fixed group π, subject to usual Reidemeister moves, and to additional "conjugacy moves", depending on a fixed group homomorphism $w : \pi \to \mathbb{F}_2$. It is shown that when there is a surface Σ such that $\pi = \pi(\Sigma)$ and $w_1 = w_1(\Sigma)$, then there is a $1-1$ correspondence between Gauss diagrams and virtual knot diagrams, that induces a correspondence between the equivalence classes (virtual knot types) on both sides.

A lighter kind of Gauss diagrams, called *abelian*, is defined in Subsection 2.3.2 following the idea of T.Fiedler's $H_1(\Sigma)$-decorated diagrams ([9]) and shown to be equivalent to the above when π is abelian and w is trivial. The little drawback of this version is that it becomes more difficult to compute the homological decoration of an arbitrary loop. Two formulas are presented in 2.3.3 to sort this out, involving quite unexpected combinatorial tools.

2.1 The classical case

2.1.1 "Real" knots in $\mathbb{S}^3$ and their Gauss diagrams

In the classical sense, a *knot* denotes a smooth embedding of a circle, which is here always assumed to be oriented, into the 3-dimensional sphere. Knots are usually considered up to isotopy: a *knot type* is the orbit of a knot under the action

of $\mathrm{Diff}^+(\mathbb{S}^3)$, the group of positive (*i.e.* orientation preserving) diffeomorphisms of $\mathbb{S}^3$.

A significant part of knot theory goes through the study of *knot diagrams*, which are generic projections of knots on a plane (or a 2-dimensional sphere), whose double points are decorated with the datum of which branch is "over" the other. Such projections enable one to treat knots, and even knot types, as combinatorial objects: the *isotopy* equivalence relation, rather difficult to handle as such, splits into simple parts:

- → On the one hand, *diagram isotopy* – that is, the action of positive diffeomorphisms of the plane.
- → On the other hand, the so-called *Reidemeister moves*, which actually change the underlying tetravalent graph.

Reidemeister moves are depicted on Fig.2.1.

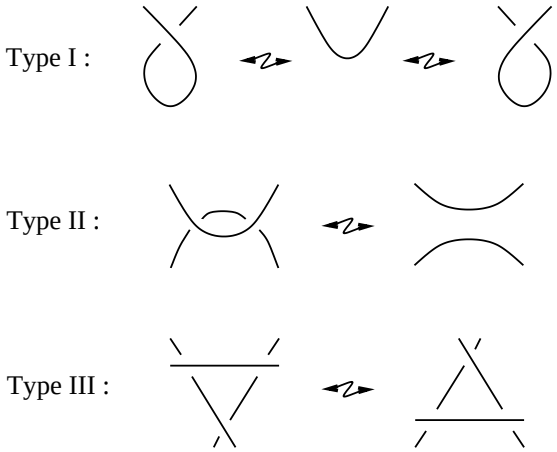

Figure 2.1: The three types of Reidemeister moves for knot diagrams

The theory of Gauss diagrams gets rid of the "diagram isotopy" part, to keep only the combinatorial skeleton.

Definition 2.1.1. A *classical Gauss diagram* is an equivalence class of an oriented circle in which a finite number of couples of points are linked by an abstract oriented arrow with a sign decoration, up to positive homeomorphism of the circle. A Gauss diagram with n arrows is said to be of *degree* n.

From a classical knot diagram D in $\mathbb{R}^2$, one obtains the *associated Gauss diagram* by considering a parametrization of D by an oriented circle, and connecting the preimages of each crossing by an arrow oriented from the underpassing to the overpassing point (the direction of the light from the picture to the eye), given as a sign the local writhe of the crossing (see Fig.2.2).

It will often happen that we regard Gauss diagrams as topological objects (drawing loops on them, considering their first homology). In that case, one must beware of the fact that *the arrows do not topologically intersect* – that is what is meant by "abstract". However, the fact that two arrows may *look like* they intersect is something combinatorially well-defined, and interesting for many purposes.

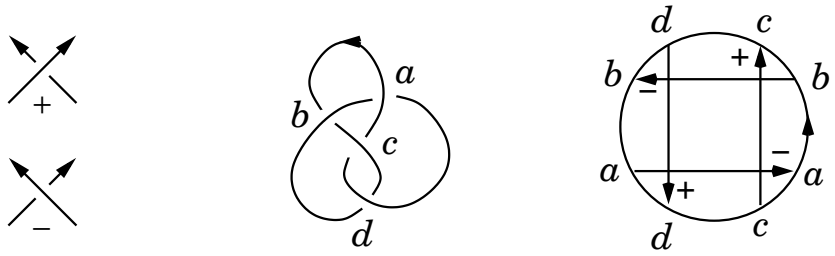

Figure 2.2: The writhe convention, a diagram of the figure eight knot, and its Gauss diagram – the letters are here only for the sake of clarity.

Definition-Lemma 2.1.2. *Two knot diagrams in the plane with the same Gauss diagram are isotopic to each other. In this regard, classical Gauss diagram theory is said to be* faithful *to real knot theory in* $\mathbb{S}^3$.

A *loop* in a Gauss diagram is a continuous map $\mathbb{S}^1 \to G$. Such a map is always homotopic to a locally injective one, so we will always assume loops to be locally injective: it is a helpful assumption to define combinatorial devices and properties. For instance, it makes sense to say that such a loop *turns left* at an arrow. Fig.2.3 shows 3 examples out of 8 possible local configurations.

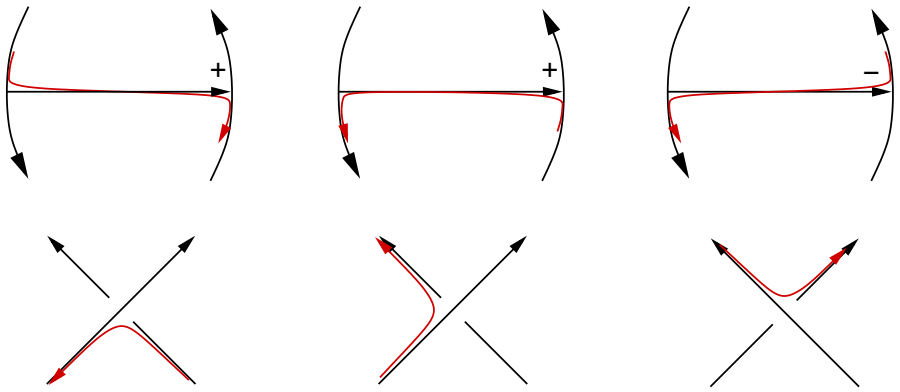

Figure 2.3: Paths turning left in a Gauss diagram and their knot diagrammatic version

In a knot diagram, it is possible to make two arcs cross each other by a Reidemeister II move if and only if these arcs *face* each other. Equivalently, there must be a path in the diagram that joins the two arcs and turns left at every crossing that it meets. Thus, one sees that Reidemeister II creating moves make sense in terms of Gauss diagrams.

In general, Gauss diagrams naturally enjoy a full set of Reidemeister moves. Fig.2.4 shows them without writhes, and Lemma 2.1.4 completes the picture.

Definition 2.1.3. In a classical Gauss diagram of degree n, the complementary of the arrows is made of $2n$ oriented components. These are called the *edges* of the diagram. In a diagram with no arrow, we still call the whole circle an edge.

Let e be an edge in a Gauss diagram, between two consecutive arrow ends that

do not belong to the same arrow. Put

$$\eta(e) = \begin{cases} +1 \text{ if the arrows that bound } e \text{ cross each other} \\ -1 \text{ otherwise} \end{cases},$$

and let $\uparrow(e)$ be the number of arrowheads at the boundary of e. Then define

$$\varepsilon(e) = \eta(e) \cdot (-1)^{\uparrow(e)}.$$

Finally, define the writhe $\mathrm{w}(e)$ as the product of the writhes of the two arrows at the boundary of e.

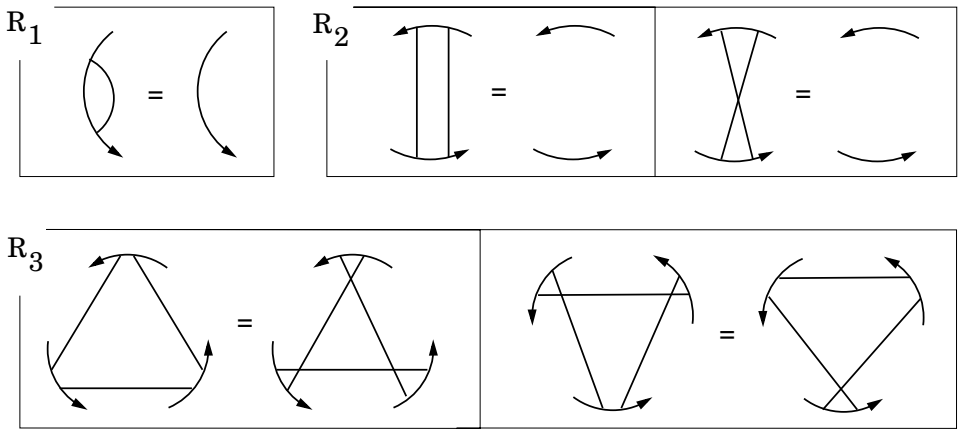

Figure 2.4: R-moves for Gauss diagrams (see Lemma 2.1.4 for the rules for the decorations)

Definition-Lemma 2.1.4. *Let D be a knot diagram with Gauss diagram G, such that G features a situation like on one of the pictures from Fig. 2.4 (say from table R_i, $1 \leq i \leq 3$). Then, the arcs/crossings of D corresponding to the edges/arrows of the local picture are in a position to perform a Reidemeister move of type* i *if and only if:*

- → $i = 1$. *No additional condition.*
- → $i = 2$. *The two arrows head to the same edge, and have opposite writhes, and there is a simple path joining the two visible edges, turning left at every arrow that it meets.*
- → $i = 3$. *The value of* $\mathrm{w}(e)\varepsilon(e)$ *is the same for all three visible edges e, and the values of* $\uparrow(e)$ *are pairwise different.*

A picture from Fig. 2.4 is called an R-move of real Gauss diagrams *as soon as it satisfies the above condition.*

Remark 2.1.5. The strange sign ε will show up again, not only in other kinds of R-moves, but in Section 3.3, where it plays a crucial role.

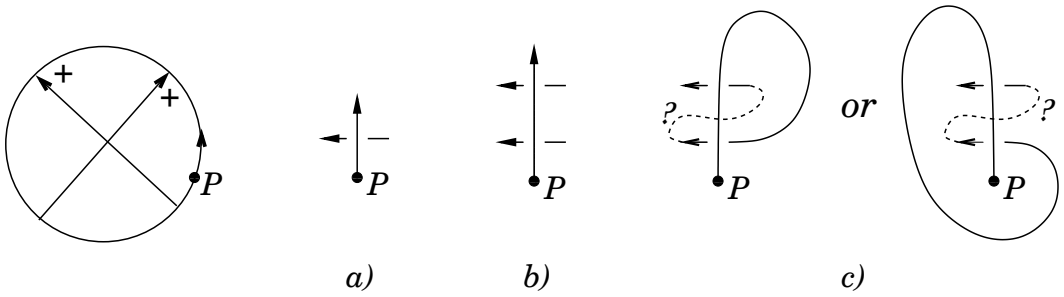

Figure 2.5: This one cannot come from a knot

2.1.2 The birth of virtual knot theory

Now a natural question is: "Is any classical Gauss diagram associated to some knot?", and the answer is no. The simplest example is pictured on Fig.2.5: try to draw a corresponding knot diagram, you will soon find it necessary to add a crossing where no arrow allows it.

This is how virtual knot theory begins: add whichever crossings you need to complete the picture, and draw a circle around them, to notify that these are not regular crossings. These so-called *virtual* crossings are subject to a new set of Reidemeister moves, precisely those that leave the underlying Gauss diagram unchanged (in particular, the last move depicted on Fig.2.6 is forbidden!).

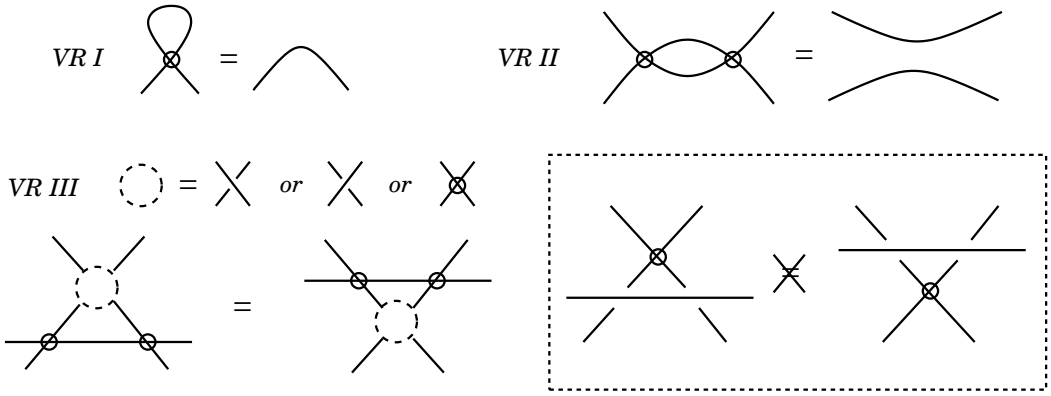

Figure 2.6: Virtual Reidemeister moves

Definition 2.1.6. A *detour move* is a boundary-fixing homotopy of an arc that goes through only virtual crossings. The arc may go across real crossings during the homotopy, and at the end it shall still contain only virtual crossings.

Fact. The full set of virtual Reidemeister moves (Fig.2.6) is equivalent to the detour move.

Finally, we see that virtual crossings are what they were meant to be: an artefact that enables knot-diagrammatic representations of (all) Gauss diagrams, with no gain or loss of information, as formalized below:

Definition-Lemma 2.1.7. *A classical Gauss diagram defines a unique virtual knot diagram in the plane, up to diagram isotopy and virtual Reidemeister moves (or detour moves). We say that classical Gauss diagram theory is* fully faithful *to virtual knot theory in the plane.*

Let us proceed to describing R-moves, with a virtual version of Lemma 2.1.4:

Definition-Lemma 2.1.8. *Let (D, G) be a couple like in Lemma 2.1.4 – though D is no more supposed to be real, and fix some edges/arrows of G matching a situation from Fig.2.4. Then,* up to detour moves*, the corresponding arcs/crossings of D are in a position to perform a* classical *Reidemeister move under the same necessary and sufficient conditions as in Lemma 2.1.4, except for Reidemeister II for which the "simple path condition" disappears.*

Again a picture from Fig. 2.4 is called an R-move of Gauss diagrams *if it satisfies the corresponding conditions.*

The two previous lemmas allow one to regard virtual knot theory as the theory of Gauss diagrams, up to R-moves, completely forgetting about actual knots.

Let us end this section by mentioning a theorem due to Kauffman, which definitely makes virtual knot theory satisfactory, because it really *contains* the classical theory:

Theorem 2.1.9 (Kauffman [17], see also [14])**.** *Any two knots in $\mathbb{S}^3$ with diagrams that may be linked by a sequence of real and virtual Reidemeister moves are isotopic.*

2.2 Knot diagrams on an arbitrary surface

One goal of this chapter is to examine when and how one can define a couple of equivalent theories "virtual knots − Gauss diagrams" that generalizes knot theory in an arbitrary 3-manifold M. What first appears is that a Gauss diagram depends on a projection; so it seems unavoidable to ask for the existence of a surface Σ (maybe with boundary, non orientable, or non compact), and a "nice" map $p : M \to \Sigma$. For the *over* and *under* branches at a crossing to be well-defined at least locally, the fibers of p need to be equipped with a total order: this leaves only the possiblity of a real line bundle.

2.2.1 Thickened surfaces

Let us now split the discussion according to the two kinds of decorations that one would expect to find on a Gauss diagram: signs (local writhes), and orientation of the arrows.

Local writhes

For a knot in an arbitrary real line bundle, there are situations in which it is possible to switch over and under in a crossing by a mere *diagram isotopy*. For instance, in the non-trivial line bundle over the annulus $\mathbb{S}^1 \times \mathbb{R}$, a full rotation of

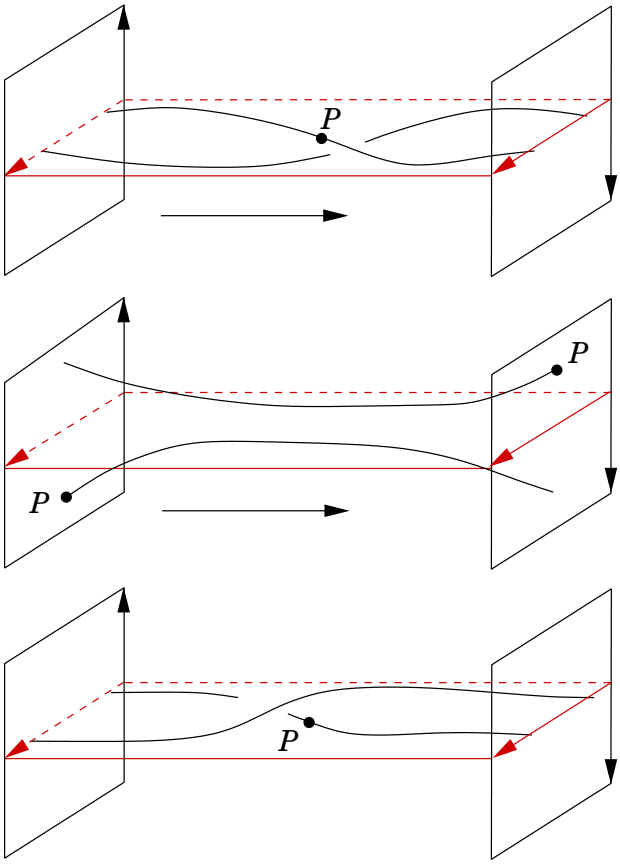

Figure 2.7: Non trivial line bundle over the annulus – as one reads from top to bottom, the knot moves towards the right of the picture.

the closure of the two-stranded elementary braid σ_1 turns it into the closure of σ_1^{-1} (Fig. 2.7).

Fig. 2.7 would be exactly the same (except for the gluing indications) if one considered the trivial line bundle over the Moebius strip. Note that this diagram would then represent a 2-component link. In fact, it is possible to embed this picture in *any non-orientable total space* of a line bundle over a surface.

This phenomenon reveals the fact that in these cases, there is no way to define the local writhe of a crossing.

Definition 2.2.1. We call a *thickened surface* a real line bundle over a surface, whose total space is orientable.

Definition-Lemma 2.2.2. *If $M \to \Sigma$ is a thickened surface, then its first Stiefel-Whitney class coincides with that of the tangent bundle to Σ. This class induces a homomorphism $w_1(\Sigma) : \pi_1(\Sigma) \to \mathbb{F}_2$. The couple $(\pi_1(\Sigma), w_1(\Sigma))$ is called the weighted fundamental group of Σ. Note that in particular the thickening of Σ is the trivial bundle $\Sigma \times \mathbb{R}$ if and only if Σ is orientable.*

There is a general definition of the writhe in these settings – see [7], Lemma 1. Let us repeat it for the sake of completeness.

Let $K : \mathbb{S}^1 \to M$ be an oriented knot in an *oriented* thickened surface $M \to \Sigma$, in generic position with respect to the bundle projection. Pick a double point p of the projection (*i.e.* a crossing), and choose an orientation of the fibre M_p. This orientation induces a total order on M_p, and defines an *over* branch and an *under* branch. By genericity, these may not be tangent through the projection, so the triple (under, over, fibre) defines an orientation on M.

Definition-Lemma 2.2.3. *The writhe of the crossing at p is set to $+1$ if the orientation defined above coincides with the fixed orientation of M, and -1 if not. This does not depend on the choice of an orientation of M_p.*

Remark 2.2.4. It appears that the writhe of a crossing depends on a choice, that of an orientation for M. The important thing is that this choice is *global*, so that it makes sense to compare the writhes of different crossings (they live in "the same" $\mathbb{Z}/2\mathbb{Z}$).

Arrow orientations

In the classical case, the orientations of the arrows in the Gauss diagram of a knot were defined according to which branch of each crossing was over the other. This assumed the choice of a position for the eye looking at the diagram, more formally an orientation for each fibre of the bundle.

For a knot in a general thickened surface, one can still orient the fibres over little neighborhoods of the crossings, thus defining an orientation for each arrow. But the fact of representing each all of these data with the same binary decoration, without any more information, implies that they can be compared – that they rely on a global definition (see Remark 2.2.4). This is possible only if the bundle is trivial, which, according to our definition of a thickened surface, happens only if the surface is orientable.

So it seems that one has a choice to make, either restricting one's attention to orientable surfaces, or taking into account the monodromy of whatever is not globally defined. Additional conjugacy moves will be needed when one defines Gauss diagrams – see section 2.3. The convention to consider only fibre bundles with an orientable total space is arbitrary, its only use is to reduce the number of monodromy morphisms to 1 *instead of* 2.

Fix an arbitrary surface Σ and denote its thickening by $M \to \Sigma$.

Definition 2.2.5. A *virtual knot diagram* on Σ is a generic immersion $\mathbb{S}^1 \to \Sigma$ whose every double point has been decorated

→ either with the designation "virtual" (which is nothing but a name),

→ or with a way to desingularize it locally into M, up to local isotopy.

These diagrams are subject to the usual Reidemeister moves depicted on Fig.2.1, and to detour moves (Definition 2.1.6), which are still equivalent to the set of virtual Reidemeister moves from Fig.2.6.

As before:

→ If one chooses an orientation for M, then the real crossings of a virtual knot diagram have a well-defined writhe.
→ There is no way to associate a classical Gauss diagram with such a knot, unless Σ is orientable.

2.2.2 Diagram isotopies and detour moves

Here by *knot diagram* we mean a virtual knot diagram on a fixed arbitrary surface Σ, as defined above. In this case a *diagram isotopy*, usually briefly denoted by $H : \mathrm{Id} \to h$, is the datum of a diffeomorphism h of Σ together with an isotopy from Id_Σ to h. A *detour move* is a boundary-fixing homotopy of an arc that, before and after the homotopy, goes through only virtual crossings (such an arc is called *totally virtual*). Though both of these processes seem rather simple, it will be useful to understand how they interact.

Lemma 2.2.6. *A knot diagram obtained from another by a sequence of diagram isotopies alternating with detour moves may always be obtained by a single diagram isotopy followed by detour moves.*

Proof. It is enough to show that a detour move d followed by a diagram isotopy $\mathrm{Id} \to h$ may be replaced with a diagram isotopy followed by a detour move (without changing the initial and final diagrams). The initial diagram is denoted by D.

Call α the totally virtual arc that is moved by the detour move. By definition, $d(\alpha)$ is boundary-fixing homotopic to α, and is totally virtual too. Thus, $h\,(d\,(\alpha))$ and $h(\alpha)$ are totally virtual and boundary-fixing homotopic to each other. Since $h\,(d\,(D))$ and $h(D)$ differ only by these two arcs, it follows that there is a detour move taking $h(D)$ to $h\,(d\,(D))$. □

Now an interesting question about diagram isotopies is when two of them lead to diagrams that are equivalent *under detour moves*. Here is a quite useful sufficient condition.

Definition 2.2.7. Let X and Y be two finite subsets of Σ with the same (positive) cardinality n. A *generalized braid* in $\Sigma \times [0,1]$ based on the sets X and Y is an embedding β of a disjoint union of segments, such that $\mathrm{Im}\,\beta \cap (\Sigma \times \{t\})$ has cardinality n for each t, coincides with X at $t = 0$ and with Y at $t = 1$.

Let D be a knot diagram and H a diagram isotopy. Let $p_1 \in P_1, \ldots, p_n \in P_n$ denote little neighborhoods of the real crossings of D, and set $\mathcal{P} = \cup P_i$. Then, $\coprod H(p_i, \cdot)$ defines a generalized braid ${}^H\beta$ in $\Sigma \times [0,1]$ with n strands based on the sets $\{p_1, \ldots, p_n\}$ and $\{h(p_1), \ldots, h(p_n)\}$. The strand of a braid β that intersects $\Sigma \times \{0\}$ at p_i is denoted by β_i.

Proposition 2.2.8. *Let D and H be as above. Then, up to detour moves, $h(D)$ only depends on D and the boundary fixing homotopy class of ${}^H\beta$.*

Proof. Let γ be a maximal smooth arc of D outside $\mathcal{P}$ (thus totally virtual). It begins at some P_i and ends at some P_j (of course it may happen that $j = i$). Using

little arcs inside of P_i and P_j to join the endpoints of γ with p_i and p_j, one obtains an oriented path ${}^H\beta_i^{-1}\gamma\,{}^H\beta_j$.

The obvious retraction of $\Sigma \times [0,1]$ onto $\Sigma \times \{1\}$ induces a map

$$\pi_1(\Sigma \times [0,1], h(\mathcal{P}) \times \{1\}) \longrightarrow \pi_1(\Sigma, h(\mathcal{P}))$$

that sends the class $\left[{}^H\beta_i^{-1}\gamma\,{}^H\beta_j\right]$ to $[h(\gamma)]$. Since the former class is unchanged under boundary-fixing homotopy of γ and ${}^H\beta$, so is the latter, which proves the result. □

This proposition states that the only relevant datum in a diagram isotopy of a virtual knot is the path followed by the real crossings along the isotopy, *up to homotopy*: the entanglement of these paths with each other or themselves does not matter. It follows that the crossings may be moved one at a time:

Corollary 2.2.9. *Let D be a knot diagram with its real crossings numbered from 1 to n, and let $H : \mathrm{Id} \to h$ be a diagram isotopy. Then there is a sequence of diagram isotopies $H_1, \ldots, H_n$, such that $h_n \ldots h_1(D)$ coincides with $h(D)$ up to detour moves, and such that H_i is the identity on a neighborhood of each real crossing but the i-th one.*

Remark 2.2.10. It is to be understood that the i-th crossing of $h_k \ldots h_1(D)$ is $h_k \ldots h_1(p_i)$.

Proof. Any generalized braid is (boundary-fixing) homotopic to a braid $\beta \subset \Sigma \times [0,1]$ such that the i-th strand is vertical before the time $\frac{i-1}{n}$ and vertical again after the time $\frac{i}{n}$. Take such a braid β that is homotopic to ${}^H\beta$. Any diagram isotopy H' such that $\beta = {}^{H'}\beta$ factorizes into a product $H_n \ldots H_1$ satisfying the last required condition. The fact that $h_n \ldots h_1(D)$ and $h(D)$ coincide up to detour moves is a consequence of Proposition 2.2.8. □

2.3 Virtual knot theory on a weighted group

In this section, we define a new Gauss diagram theory, that depends on an arbitrary group π and a homomorphism $w : \pi \to \mathbb{F}_2 \simeq \mathbb{Z}/2\mathbb{Z}$. These two data together are called a *weighted group*. When (π, w) is the weighted fundamental group of a surface (see Definition 2.2.2), this theory encodes, fully and faithfully, virtual knot diagrams on that surface.

2.3.1 General settings and the main theorem

Definition 2.3.1. Let π be an arbitrary group and w a homomorphism from π to $\mathbb{F}_2$. A *Gauss diagram on π* is a classical Gauss diagram decorated with

→ an element of π on each edge if the diagram has at least one arrow.

→ a single conjugacy class in π if the diagram is empty.

Such diagrams are subject to the usual types of R-moves, plus an additional *conjugacy move*, or *w-move* – the dependence on w arises only there. An equivalence class modulo all these moves is called a *virtual knot type on* (π, w)

A *subdiagram* of a Gauss diagram on π is the result of removing some of its arrows. Removing an arrow involves a merging of its (2, 3, or 4) adjacent edges, and the resulting single edge should be marked with the product in π of the former markings. If all the arrows have been removed, this product is not well-defined, but its conjugacy class is.

The notion of subdiagrams will not be used before Chapter 3, but it already allows explicit understanding of

1. The distinction between empty and non empty diagrams in the definition above.
2. The "merge $\rightsquigarrow$ multiply" principle, which is omnipresent, in particular in R-moves.

An R_1**-move** is the local addition or removal of an isolated arrow, surrounding an edge marked with the unit $1 \in \pi$. The markings of the affected edges must satisfy the rule indicated on Fig.2.8 (top-left). There are no conditions on the decorations of the arrows.

Exceptional case: If the isolated arrow is the only one in the diagram on the left, then the markings a and b on the picture actually correspond to the same edge, and the diagram on the right, with no arrow, must be decorated by $[a]$, the conjugacy class of a.

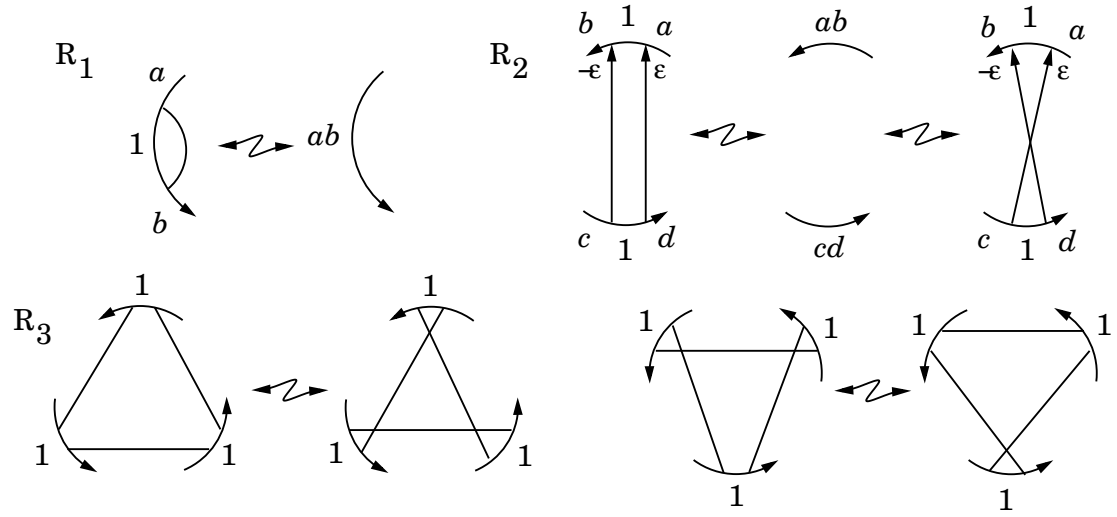

Figure 2.8: The R-moves for Gauss diagrams on a group – the exceptional cases and the rules for the missing decorations are made precise in Definition 2.3.1.

An R_2**-move** is the addition or removal of two arrows with opposite writhes and matching orientations as shown on Fig.2.8 (top-right). The surrounded edges must be decorated with 1, and the "merge $\rightsquigarrow$ multiply" rule should be satisfied.
Exceptional case of type 1: If the markings a and d (*resp.* b and c) correspond to the same edge, then the resulting marking shall be cab (*resp.* abd).
Exceptional case of type 2: If the middle diagram contains no arrow at all, *i.e.* a and d match and so do b and c, then the (only) marking of the middle diagram shall be $[ab]$.

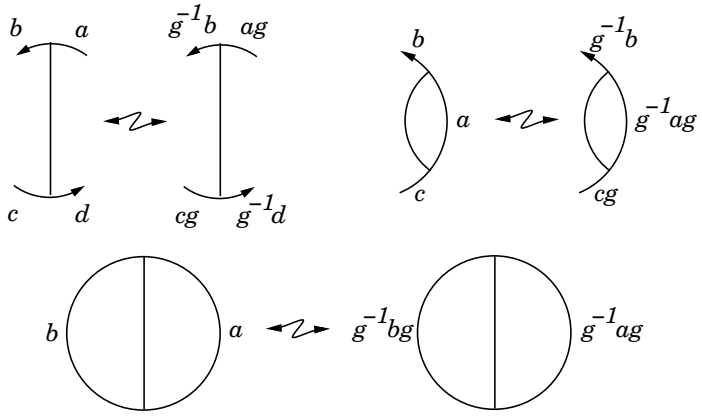

Figure 2.9: The general conjugacy move (top-left) and its two exceptional cases – in every case the orientation of the arrow switches if and only if $w(g) = -1$.

An R_3**-move** may be of the two types shown on Fig.2.8 (bottom left and right). The surrounded edges must be decorated by 1, the value of $w(\cdot)\varepsilon(\cdot)$ must be the same for all three of them, and the values of $\uparrow(\cdot)$ must be pairwise distinct (see Definition 2.1.3).

A **conjugacy move** depends on an element $g \in \pi$. It changes the markings of the adjacent edges to an arbitrary arrow as indicated on Fig.2.9. Besides, if $w(g) = -1$ then the orientation of the arrow is reversed – though its sign remains the same.

Remark 2.3.2. By composing R-moves and w-moves, it is possible to perform *generalized moves*, which look like R-moves but depend on w. Fig.2.10 shows some of them.

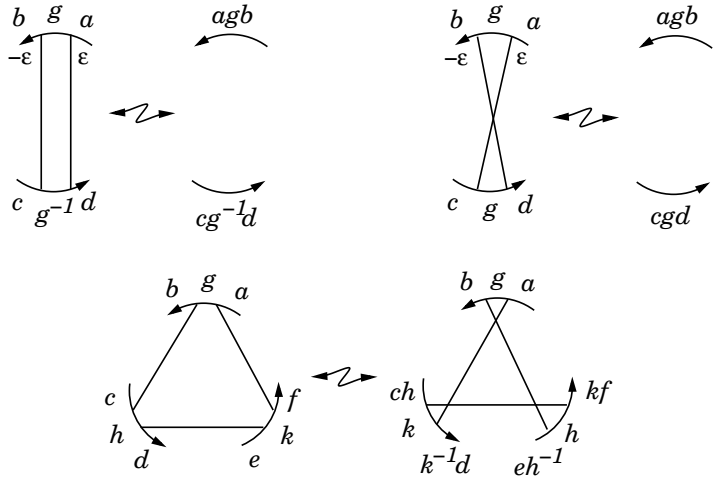

Figure 2.10: Some generalized moves – for the R_3 picture, it is assumed that $ghk = 1$. **Warning:** the rules for the arrow orientations in R_2 and R_3 depend on the value of $w(g)$.

Theorem 2.3.3. *Let (Σ, x) be an arbitrary surface with a base point, and denote by (π, w) the weighted fundamental group of (Σ, x) (see Definition 2.2.2). There is*

a $1-1$ *correspondence between Gauss diagrams on* π *up to R-moves and* w*-moves (i.e. virtual knot types on* (π, w)*), and virtual knot diagrams on* Σ *up to diagram isotopy, Reidemeister moves and detour moves (i.e. virtual knot types on* Σ*).*

Proof. Fix a subset X of Σ homeomorphic to a closed 2-dimensional disc and containing the base point x – so that $\pi = \pi_1(\Sigma, X)$. Also, X being contractible allows one to fix a trivialization of the thickening of Σ over X: this gives meaning to the locally *over* and *under* branches when a knot diagram has a real crossing in X.

Construction of Φ. Pick a knot diagram $D \in \Sigma$ and assume that every real crossing of D lies over X. Then D defines a Gauss diagram on π, denoted by $\varphi(D)$: the signs of the arrows are given by the writhes (Definition 2.2.3), their orientation is defined by the trivialization of $M \to \Sigma$ over X, and each edge is decorated by the class in π of the corresponding arc in D. This defines $\varphi(D)$ without ambiguity if D has at least one real crossing. If it does not, then define $\varphi(D)$ as a Gauss diagram without arrows, decorated with the conjugacy class corresponding to the free homotopy class of D. Finally, put

$$\Phi(D) := [\varphi(D)] \text{ mod R-moves and } w\text{-moves.}$$

Invariance of Φ under diagram isotopy and detour moves. It is clear from the definitions that $\varphi(D)$ is strictly unchanged under detour moves on D. Now assume that D_1 and D_2 are equivalent under *usual* diagram isotopy – that is, diagram isotopy that may take real crossings out of X for some time. By Corollary 2.2.9, it is enough to understand what happens for a diagram isotopy along which only one crossing goes out of X. In that case, $\varphi(D)$ is changed by a w-move performed on the arrow corresponding to that crossing, where the conjugating element g is the loop followed by the crossing along the isotopy. Indeed, since the first Stiefel-Whitney class of the thickening of Σ coincides with that of its tangent bundle, it follows that:

1. The orientation of the fibre (and thus the notions of "over" and "under") is reversed along g if and only if $w(g) = -1$, which actually corresponds to the rule for arrow orientations in a w-move.
2. The orientation of the fibre over the crossing is reversed along g if and only if a given local orientation of Σ is reversed along g, so that the writhe of the crossing never changes.

Invariance of Φ under Reidemeister moves. Up to conjugacy by a diagram isotopy, it can always be assumed that a Reidemeister move happens inside X. In that case, at the level of $\varphi(D)$, it clearly corresponds to an R-move as described in Definition 2.3.1.

So far, Φ is a well-defined map from the set of virtual knot types on Σ to the set of virtual knot types on (π, w).

Construction of an inverse map Ψ. If G is a Gauss diagram without arrows, then define $\psi(G)$ as the totally virtual knot with free homotopy class equal to the marking of G – it is well-defined up to detour moves. If G has arrows, then for each of them draw a crossing inside X with the required writhe, and then join these

by totally virtual arcs with the required homotopy classes. The resulting diagram $\psi(G)$ is well-defined up to diagram isotopy and detour moves by this construction. In both cases, put

$$\Psi(D) := \text{virtual knot type of } \psi(D).$$

Let us prove that φ and ψ are inverse maps, so that Ψ will be the inverse of Φ as soon as it is invariant under R-moves and w-moves.

It is clear from the definitions that $\varphi \circ \psi$ coincides with the identity. It is also clear that $\psi \circ \varphi$ is the identity, up to detour moves, for *totally virtual* knot diagrams.

Now fix a knot diagram D with at least one real crossing (and all real crossings inside X). Recall that $\psi \circ \varphi(D)$ is defined up to diagram isotopy and detour moves, so fix a diagram D' in that class. There is a natural correspondence between the set of real crossings of D and those of D', due to the fact that both identify by construction with the set of arrows of $\varphi(D)$. Pick a diagram isotopy h that takes each real crossing of D to meet its match in D', *without leaving* X. Then clearly $\varphi(h(D)) = \varphi(D)$, and because $\varphi \circ \psi$ is the identity, one gets

$$\varphi(h(D)) = \varphi(D'). \tag{2.1}$$

The choice of h ensures that $h(D)$ and D' differ only by totally virtual arcs, and (2.1) implies that each of these, in $h(D)$, has the same class in $\pi_1(\Sigma, X)$ as its match in D', which means by definition that $h(D)$ and D' are equivalent up to detour moves. Thus $\psi \circ \varphi$ is the identity up to diagram isotopy and detour moves.

Invariance of Ψ under R-moves. Let us treat only the case of R_2-moves, which contains all the ideas. Let G_1 and G_2 differ by an R_2-move, and assume that G_1 is the one with more arrows. By appropriate diagram isotopy and detour moves *inside* X, performed on $\psi(G_1)$, it is possible to make the two concerned crossings "face" each other, as in Fig.2.11 (left). The paths α_1 and α_2 from this picture are totally virtual and trivial in $\pi_1(\Sigma, X)$, thus $\psi(G_1)$ is equivalent to the second diagram of Fig.2.11 up to detour moves. The fact that at this point, an R-II move is actually possible is a consequence of (in fact equivalent to) the combinatorial conditions defining the R-moves. Denote by D the third diagram of the picture. The "merge $\rightsquigarrow$ multiply" principle that rules R_2-moves implies that $\varphi(D) = G_2$, so that

$$\psi(G_1) \sim D \sim \psi \circ \varphi(D) = \psi(G_2), \tag{2.2}$$

where $\sim$ is the equivalence under diagram isotopy, detour moves and Reidemeister moves. It follows that $\psi(G_1)$ and $\psi(G_2)$ have the same knot type.

Invariance of Ψ under w-moves. Let G_1 and G_2 differ by a w-move on $g \in \pi$. Call c the corresponding crossing on the diagram $\psi(G_1)$. Then, pick two little arcs right before c, one on each branch, and make them follow g by a detour move. At the end, one shall see a totally virtual 4-lane railway as pictured on Fig.2.12 (middle): the strands are made parallel, *i.e.* any (virtual) crossing met by either of them is part of a larger picture as indicated by the zoom. This ensures that, using the mixed version of Reidemeister III moves, one can slide the real crossing all along the red part of the railway, ending with the diagram on the right of the picture – let us call

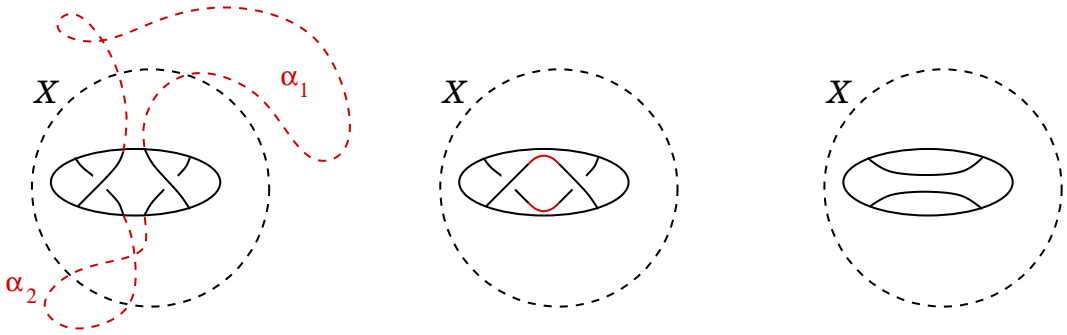

Figure 2.11: R_2-moves actually correspond to Reidemeister moves

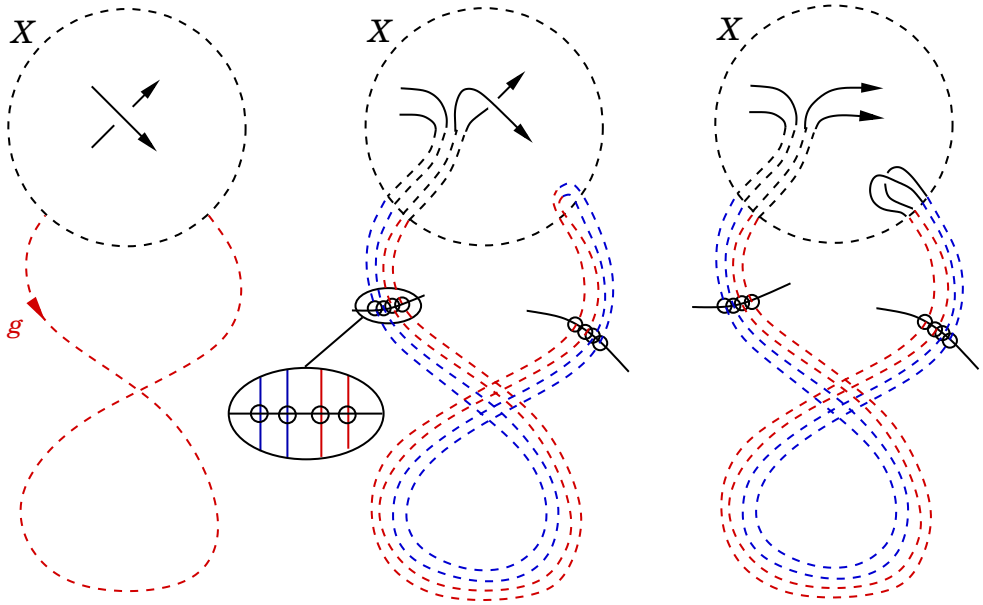

Figure 2.12: Performing a w-move – the railway trick

it D. The conclusion is identical to that for R-moves: again $\varphi(D) = G_2$ and (2.2) holds, whence $\psi(G_1)$ and $\psi(G_2)$ have the same knot type.

□

About the orbits of w-moves

It could feel natural to try to get rid of w-moves by understanding their orbits in a synthetic combinatorial way. This is what is done in Section 2.3.2 in the particular case of an abelian group π endowed with the trivial homomorphism $\pi \to \mathbb{F}_2$.

In general, for a Gauss diagram on π, G, denote by $h_1(G)$ the *set* of free homotopy classes of loops in the underlying topological space of G (it is the set of conjugacy classes in a free group on $deg(G) + 1$ generators). Also, denote by $h_1(\pi)$ the set of conjugacy classes in π. Then the π-markings of G define a map

$$F_G : h_1(G) \to h_1(\pi).$$

Observe that the map $G \mapsto F_G$ is invariant under w-moves. This raises a number of

questions that amout to technical group theoretic problems, and which will not be answered here (G^w denotes the orbit of G under w-moves):

1. Is the map $G^w \mapsto F_G$ injective?
2. If the answer to 1. is yes, then is G^w determined by a finite number of values of F_G, for instance its values on the free homotopy classes of *simple loops*?
3. Is it possible to detect in a simple manner what maps $h_1(G) \to h_1(\pi)$ lie in the image of $G^w \mapsto F_G$?

Remark 2.3.4. Gauss diagrams with decorations in $h_1(\Sigma)$ can be met for example in [15], where they are used to construct knot invariants in a thickened oriented surface Σ – see Section 3.4. If the answer to Question 1. above is no, then such invariants, which factor through F_G, stand no chance to be complete.

Remark 2.3.5. Even for diagrams with only one arrow, it still does not seem easy to answer the "simple loop" version of Question 2. Given x, y, h, k in a finite type free group, is it true that

$$hxh^{-1}kyk^{-1} = xy \implies \exists l, \begin{cases} hxh^{-1} = lxl^{-1} \\ kyk^{-1} = lyl^{-1} \end{cases} ?$$

Let us end with an example that shows that the values of F_G on the (finite) set of simple loops running along at most one arrow is not enough (cf. Question 2.). Fig.2.13 shows a Gauss diagram with such decorations – $\{a, b\}$ is a set of generators for the free group $\pi_1(\Sigma) \simeq \mathbb{F}(a, b)$, where Σ is a 2-punctured disc. These particular values of F_G do not determine the free homotopy class of the red loop γ, as it is shown in Fig.2.14.

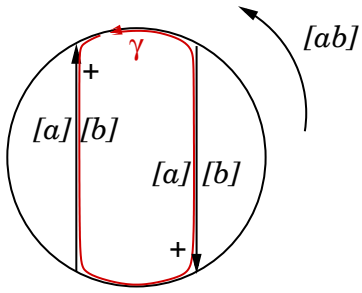

Figure 2.13: A Gauss diagram that does not define a unique virtual knot

In fact, these two virtual knots are even distinguished by Vassiliev-Grishanov's planar chain invariants, which means they represent different virtual knot types.

2.3.2 Abelian Gauss diagrams

In this subsection, π is assumed to be abelian, and w_0 denotes the trivial homomorphism $\pi \to \mathbb{F}_2$. We describe a version of Gauss diagrams that carries as much information as the previously introduced virtual knot types on (π, w_0), with two improvements:

→ The diagrams are made of less data than in the general version.

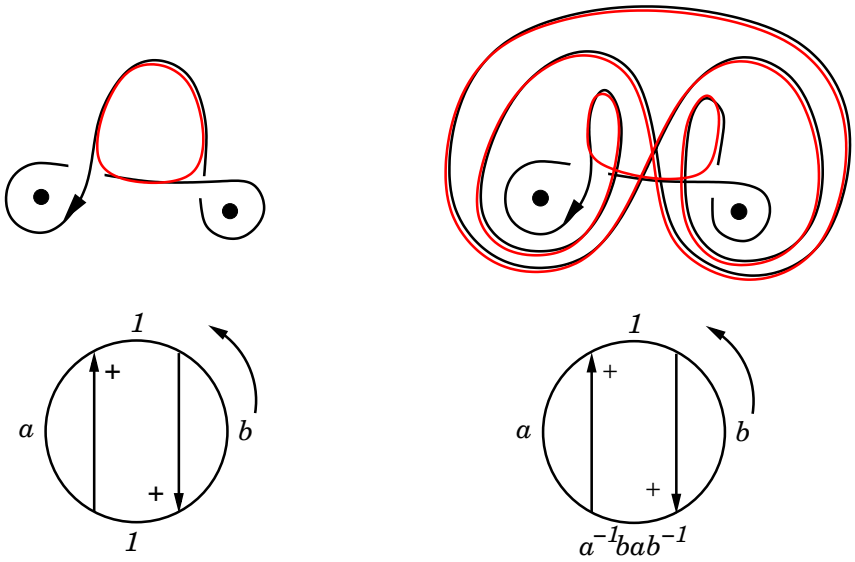

Figure 2.14: One red loop is trivial, while the other is a commutator

→ This version is free from conjugacy moves.

It is inspired from the decorated diagrams introduced by T. Fiedler to study combinatorial invariants for knots in thickened surfaces (see [9, 10]).

We use the same notation G for a Gauss diagram and its underlying topological space, that is a 1-dimensional complex with edges and arrows as oriented 1-cells. $H_1(G)$ denotes its first integral homology group.

Definition-Lemma 2.3.6 (fundamental loops)**.** *Let G be a classical Gauss diagram of degree n. There are exactly $n+1$ simple loops in G respecting the local orientations of edges and arrows, and going along at most one arrow. They are called the fundamental loops of G and their homology classes form a basis of $H_1(G)$.*

Definition 2.3.7 (abelian Gauss diagram)**.** Let π be an abelian group. An *abelian Gauss diagram on π* is a classical Gauss diagram G decorated with a group homomorphism $\mu : H_1(G) \to \pi$. It is usually represented by its values on the basis of fundamental loops, that is, one decoration in π for each arrow, and one for the base circle – that last one is called the *global marking of G*.

A Gauss diagram on π determines an abelian Gauss diagram as follows:

→ The underlying classical Gauss diagram is the same.

→ Each fundamental loop is decorated by the sum of the markings of the edges that it meets (see Fig 2.15).

This defines an *abelianization map* ab.

Proposition 2.3.8. *The map* ab *induces a natural $1-1$ correspondence between abelian Gauss diagrams on π and equivalence classes of Gauss diagrams on π up to w_0-moves. Moreover, if $\pi = \pi_1(\Sigma)$ is the fundamental group of a surface, then these sets are in $1-1$ correspondence with the set of virtual knot diagrams on Σ up to diagram isotopy and detour moves.*

Proof. The proof of the last statement is contained in that of Theorem 2.3.3 – through the facts that ϕ and ψ are inverse maps up to detour moves and diagram

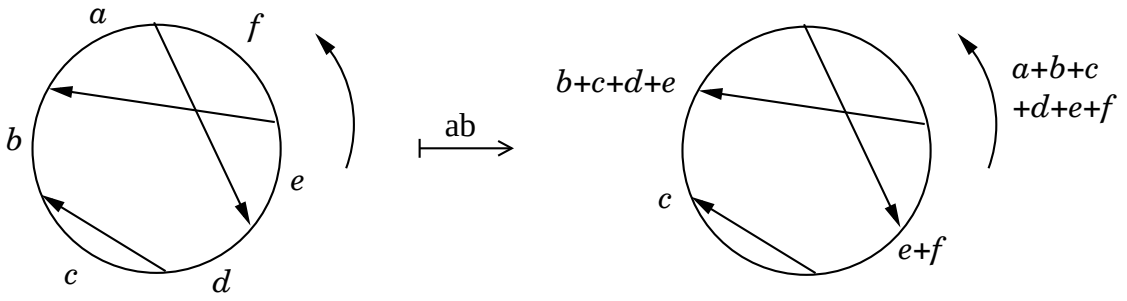

Figure 2.15: Abelianizing a Gauss diagram on an abelian group

isotopy, and that w-moves at the level of knot diagrams can be performed using only detour moves and diagram isotopies, by the railway trick (Fig.2.12).

As for the first statement, one easily sees that ab is invariant under w_0-moves. We have to show that conversely, if $\mathrm{ab}(G_1) = \mathrm{ab}(G_2)$, then G_1 and G_2 are equivalent under w_0-moves.

This is clear if G_1 has no arrows, since then $\mathrm{ab}(G_1) = G_1$. Now proceed by induction. Since G_1 and G_2 have the same abelianization, they have in particular the same underlying classical Gauss diagram, and there is a natural correspondence between their arrows.

Case 1: No two arrows in G_1 cross each other. Then at least one arrow surrounds a single isolated edge on one side (as in an R_1-move). Choose such an arrow α and remove it, as well as its match in G_2. By induction, there is a sequence of w_0-moves on the resulting diagram G_1' that turns it into G_2'. Since the arrows of G_1' have a natural match in G_1, those w_0-moves make sense there, and take every marking of G_1 to be equal to its match in G_2, except for those in the neighborhood of α. So we may assume that G_1 and G_2 only differ near α as in Fig.2.16. Since all the unseen markings coincide in G_1 and G_2, and since $\mathrm{ab}(G_1)$ and $\mathrm{ab}(G_2)$ have the same global marking, it follows that

$$a + b + c = a' + b' + c'.$$

Thus a w_0-move on α with conjugating element $g = a' - a$ turns G_1 into G_2.

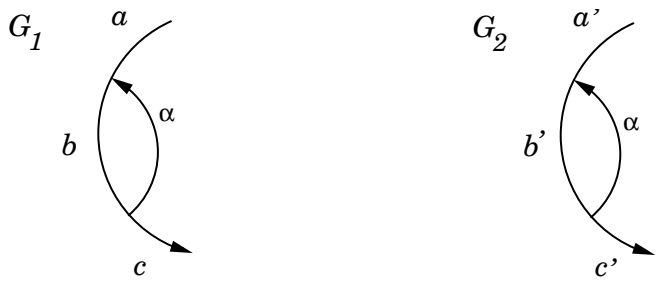

Figure 2.16: Notations for case 1

Case 2: There is at least one arrow α in G_1 that intersects another arrow. By the same process as in case 1, one may assume that G_1 and G_2 only differ near α – see Fig.2.17, where a, b, c and d actually correspond to pairwise distinct edges since α intersects an arrow. Again, since all the unseen markings coincide in G_1 and G_2,

one obtains

$$a + d = a' + d',$$

and

$$b + c = b' + c',$$

by considering the global marking, and the marking of α, in $\mathrm{ab}(G_1)$ and $\mathrm{ab}(G_2)$. Moreover, there is at least one arrow intersecting α: considering the marking of that arrow gives

$$a + b = a' + b'.$$

The last three equations may be written as

$$a' - a = b - b' = c' - c = d - d',$$

so that, again, a w_0-move on α with conjugating element $g = a' - a$ turns G_1 into G_2.

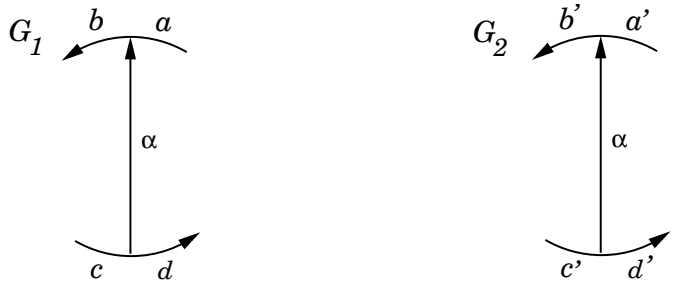

Figure 2.17: Notations for case 2

□

Remark 2.3.9. Another proof of this proposition was given in a draft paper, in the special case $\pi = \mathbb{Z}$ ([21], Proposition 2.2). As an exercise, one can show that this proof extends to the case of an arbitrary abelian group.

To make the picture complete, it only remains to understand R-moves in this context.

Definition 2.3.10 (obstruction loops)**.** Within any local Reidemeister picture like those shown on Fig.2.4 featuring at least one arrow, there is exactly one (unoriented) simple loop. We call it the *obstruction loop*. Fig.2.18 shows typical examples.

Definition 2.3.11 (R-moves)**.** A move from Fig.2.4 is likely to define an R-move only if the obstruction loop lies in the kernel of the decorating map $H_1(G) \to \pi$ (which makes sense even though the loop is unoriented). Under that assumption, the *R-moves for abelian Gauss diagrams* are defined by the usual conditions:

- $i = 1$. No additional condition.
- $i = 2$. The arrows head to the same edge, and have opposite signs.
- $i = 3$. The value of $\mathrm{w}(e)\varepsilon(e)$ is the same for all three visible edges e, and the values of $\uparrow(e)$ are pairwise different (see Definition 2.1.3).

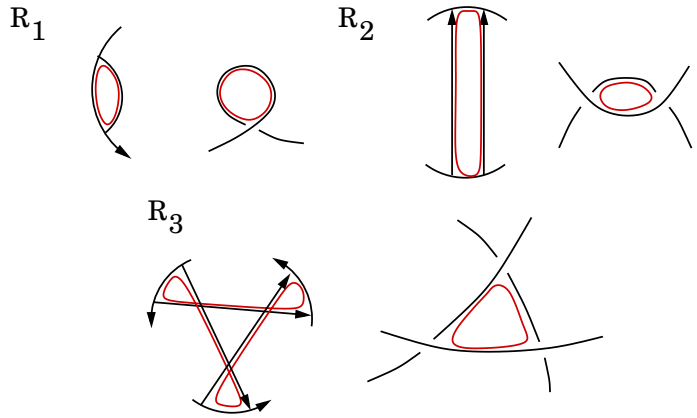

Figure 2.18: Homological obstruction to R-moves

Theorem 2.3.12. *The map* ab *induces a natural* $1-1$ *correspondence between equivalence classes of abelian Gauss diagrams on* π *up to R-moves and virtual knot types on* (π, w_0).

Proof. ab clearly maps an R-move in the non commutative sense to an R-move in the abelian sense. Conversely, if $\mathrm{ab}(G_1)$ and $\mathrm{ab}(G_2)$ differ from an (abelian) R-move, then the vanishing homological obstruction implies that G_1 and G_2 are in a position to perform a "generalized R-move" like the examples pictured on Fig.2.10. □

Theorems 2.3.3 and 2.3.12 together imply the following

Corollary 2.3.13. *If* Σ *is an orientable surface with abelian fundamental group, then there is a* $1-1$ *correspondence between abelian Gauss diagrams on* $\pi_1(\Sigma)$ *up to R-moves, and virtual knot types on* Σ.

2.3.3 Homological formulas

It may seem not easy to compute an arbitrary value of the linear map decorating an abelian Gauss diagram, given only its values on the fundamental loops. To end this section, we give two formulas to fill this gap, by understanding the coordinates of an arbitrary loop in the basis of fundamental loops.

The energy formula

Fix an abelian Gauss diagram G. Observe that as a cellular complex, G has no 2-cells, thus every 1-homology class has a unique set of "coordinates" along the family of edges and arrows. For each 1-cell c (which may be an arrow or an edge), we denote by $\langle \cdot, c \rangle : H_1(G) \to \mathbb{Z}$ the coordinate function along c. It is a group homomorphism.

Let us denote by $[A] \in H_1(G)$ the class of the fundamental loop associated with an arrow A (Fig.2.19 left).

Definition-Lemma 2.3.14 (Energy of a loop)**.** *Fix an edge e in G, and a class $\gamma \in H_1(G)$. The value of*

$$E_e(\gamma) = \langle \gamma, e \rangle - \sum_{\langle [A], e \rangle = 1} \langle \gamma, A \rangle \tag{2.3}$$

is independent of e. This defines a group homomorphism $E : H_1(G) \to \mathbb{Z}$.

Proof. Let us compare the values of $E.(\gamma)$ for an edge e and the edge e' right after it. e and e' are separated by a vertex P, which is the endpoint of an arrow A. There are two possible situations (Fig.2.19):

1. P is the tail of A. Then $\langle [A], e \rangle = 1$ and $\langle [A], e' \rangle = 0$, so that
$$E_e(\gamma) - E_{e'}(\gamma) = \langle \gamma, e \rangle - \langle \gamma, A \rangle - \langle \gamma, e' \rangle .$$
2. P is the head of A. Then $\langle [A], e \rangle = 0$ and $\langle [A], e' \rangle = 1$, so that
$$E_e(\gamma) - E_{e'}(\gamma) = \langle \gamma, e \rangle + \langle \gamma, A \rangle - \langle \gamma, e' \rangle .$$

In both cases, $E_e(\gamma) - E_{e'}(\gamma)$ is equal to $\langle \partial\gamma, P \rangle$, which is 0 since γ is a cycle. □

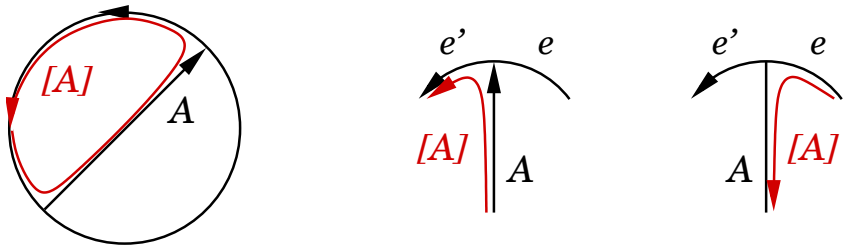

Figure 2.19: The fundamental loop of an arrow and the two cases in the proof of Lemma 2.3.14

Theorem 2.3.15. *For any $\gamma \in H_1(G)$, one has the decomposition*

$$\gamma = \sum_A \langle \gamma, A \rangle [A] + E(\gamma) [K] . \tag{2.4}$$

Proof. This formula is an identity between two group homomorphisms, so it suffices to check it on the basis of fundamental loops, which is immediate. □

Remark 2.3.16. The existence of a map E such that Theorem 2.3.15 holds was clear, since for each arrow A considered as a 1-cell, $[A]$ is the only fundamental loop that involves A. With that in mind, one may read into (2.3) as follows: $E(\gamma)$ counts the (algebraic) number of times that γ goes through an edge, minus the number of those times that are already taken care of by the fundamental loops of the arrows. This number has to be the same for all edges, so that one recovers a multiple of $[K]$.

The torsion formula

Looking at (2.4) and Fig.2.19, one may feel that it would be more natural to have $[K] - [A]$ involved in the formula, instead of $[A]$, for all arrows A such that $\langle \gamma, A \rangle$ is negative – that is, when γ runs along A with the wrong orientation more often than not. The formula then becomes

$$\gamma = \sum_{\langle \gamma, A \rangle > 0} \langle \gamma, A \rangle \, [A] + \sum_{\langle \gamma, A \rangle < 0} \langle \gamma, A \rangle \, ([A] - [K]) \, - \mathcal{T}(\gamma) \, [K] \, , \tag{2.5}$$

where

$$- \mathcal{T}(\gamma) = E(\gamma) + \sum_{\langle \gamma, A \rangle < 0} \langle \gamma, A \rangle \, . \tag{2.6}$$

Definition 2.3.17. $\mathcal{T}(\gamma)$ is called the *torsion* of γ.

How is (2.5) different from (2.4)?
$\ominus$ On the negative side, unlike the energy, $\mathcal{T}$ is not a group homomorphism. But it actually behaves almost like one:

Lemma 2.3.18. *Let γ_1 and γ_2 be two homology classes such that*

$$\forall A, \ \langle \gamma_1, A \rangle \, \langle \gamma_2, A \rangle \geq 0.$$

Then

$$\mathcal{T}(\gamma_1 + \gamma_2) = \mathcal{T}(\gamma_1) + \mathcal{T}(\gamma_2).$$

Proof. It follows from the definition and the fact that $E(\gamma)$ is a homomorphism. □

$\oplus$ On the positive side:

Lemma 2.3.19. *The torsion of a loop in a Gauss diagram G does not depend on the orientations of the arrows of G.*

Proof. By expanding the defining formula,

$$\mathcal{T}(\gamma) = - \langle \gamma, e \rangle \quad + \sum_{\substack{\langle \gamma, A \rangle < 0 \\ \langle [A], e \rangle = 0}} \langle \gamma, A \rangle \quad - \sum_{\substack{\langle \gamma, A \rangle > 0 \\ \langle [A], e \rangle = 1}} \langle \gamma, A \rangle \, ,$$

one sees that reversing an arrow makes its contribution (if non zero) switch from one sum to the other, while $\langle \gamma, A \rangle$ also changes signs. □

This lemma allows one to expect that $\mathcal{T}(\gamma)$ should admit a very simple combinatorial interpretation. It actually does, but only for a certain family of loops – the ERS loops defined below. Fortunately enough, this family will happen to positively generate $H_1(G)$, which allows one to compute the torsion of any loop by using Lemma 2.3.18.

Definition 2.3.20. The notation γ is used for loops as well as 1-homology classes. A homology class $\gamma \in H_1(G)$ is said to be

→ *ER* (for "edge-respecting"), if for every edge e, $\langle \gamma, e \rangle \geq 0$.
→ *simple* if it is the class of a simple (injective) loop, that is, $|\langle \gamma, c \rangle| \leq 1$ for every 1-cell c (edge or arrow).
→ *ERS* if it is ER and simple.
→ *proper* if it runs along at least one arrow.

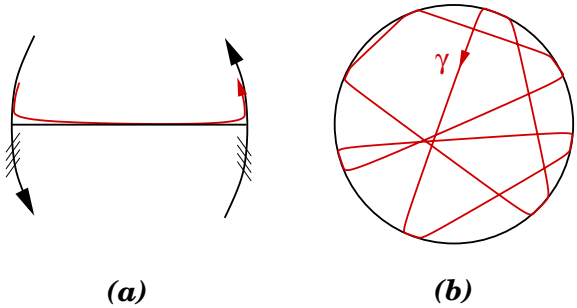

Figure 2.20: The local and global look of a proper ERS loop

Consider a permutation $\sigma \in \mathfrak{S}([\![1, n]\!])$, and set

$$\nearrow(\sigma) := \sharp \{ i \in [\![1, n]\!] \mid \sigma(i) > i \} .$$

It is easy to check that if σ_0 is the circular permutation $(1\,2\,\ldots\,n)$, then

$$\forall \sigma \in \mathfrak{S},\ \nearrow(\sigma) = \nearrow(\sigma_0 \sigma \sigma_0^{-1}).$$

Definition 2.3.21. The invariance property from above means that $\mathcal{T}$ is well-defined for permutations of a set of n points lying in an abstract oriented circle. We still denote this function by $\mathcal{T}$, and call it the *torsion* of a permutation.

Let γ be a proper simple loop, then the set of edges e such that $\langle \gamma, e \rangle \neq 0$ can be naturally assimiliated to a finite subset of an oriented circle, and γ induces a permutation of this set. Let us denote it by σ_γ.

Theorem 2.3.22. *For all proper ERS loops γ,*

$$\mathcal{T}(\gamma) = \nearrow(\sigma_\gamma).$$

Proof. One may assume that for every arrow A, $\langle \gamma, A \rangle = 1$. Indeed, deleting an arrow avoided by γ, or reversing the orientation of an arrow that γ runs in the wrong direction, have no effect on either side of the formula (notably because of Lemma 2.3.19). Under this assumption, half of the edges of G are run by γ: call them the *red edges of* G, while the other half are called the *blue edges*. Red and blue edges alternate along the orientation of the circle.

If e is any (red or blue) edge, we define:

$$\lambda(e) := \sum_A \langle [A], e \rangle .$$

Lemma 2.3.23. *Under the assumption that $\langle \gamma, A \rangle = 1$ for all A, the value of $\lambda(e)$ only depends on the color of the edge e. Moreover,*

$$\lambda(blue) = \lambda(red) - 1 = \nearrow(\sigma_\gamma).$$

Let us temporarily admit this result. By the definition of λ,

$$\begin{array}{rcl} \sum_A [A] & = & \sum \text{arrows} + \lambda(\text{red}) \sum(\text{red edges}) + \lambda(\text{blue}) \sum(\text{blue edges}) \\ & \underset{\text{Lemma 2.3.23}}{=} & \sum \text{arrows} + \sum (\text{red edges}) + \lambda(\text{blue}) \sum (\text{red and blue edges}) \\ & = & \gamma + \lambda(\text{blue})[K] \\ & \underset{\text{Lemma 2.3.23}}{=} & \gamma + \nearrow(\sigma_\gamma)[K]. \end{array}$$

Since it was assumed that $\langle \gamma, A \rangle = 1$ for every arrow, the definition of $\mathcal{T}$ (2.5) reads

$$\gamma = \sum_A [A] - \mathcal{T}(\gamma)[K],$$

which terminates the proof of the theorem, up to Lemma 2.3.23.

□

Proof of Lemma 2.3.23. In the case of $\sigma_0 = (1\,2\,\ldots\,n)$ depicted on Fig.2.21, it is easy to see that $\lambda(red) = n$ and $\lambda(blue) = n-1$, while $\nearrow(\sigma_0) = n-1$. The lemma being true for one diagram, let us show that it survives elementary changes that cover all the diagrams.

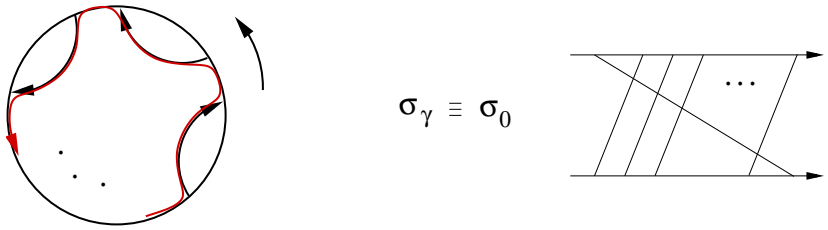

Figure 2.21: Braid-like representations of permutations are to be read from bottom to top

Notice that for every proper ERS loop γ, σ_γ is a *cycle*, and conversely a permutation that is a cycle uniquely defines an undecorated Gauss diagram *and* a proper ERS loop γ such that for every arrow A, $\langle \gamma, A \rangle = 1$. Thus, covering all possible permutations implies covering all possible diagrams and proper ERS loops. So all we have to check is that the formula survives an operation on σ_γ, of the form:

$$(\ldots i\, j \ldots) \longrightarrow (\ldots j\, i \ldots)$$

The corresponding move at the level of Gauss diagrams may be of six different types, grouped in three pairs of reverse operations (Fig.2.22).

On each diagram in Fig.2.22, the three moving arrows split the base circle into six regions. One computes the variation of λ separately for each of these regions, and sees that it is the same for each of them. The results are gathered in the following table, proving the lemma.

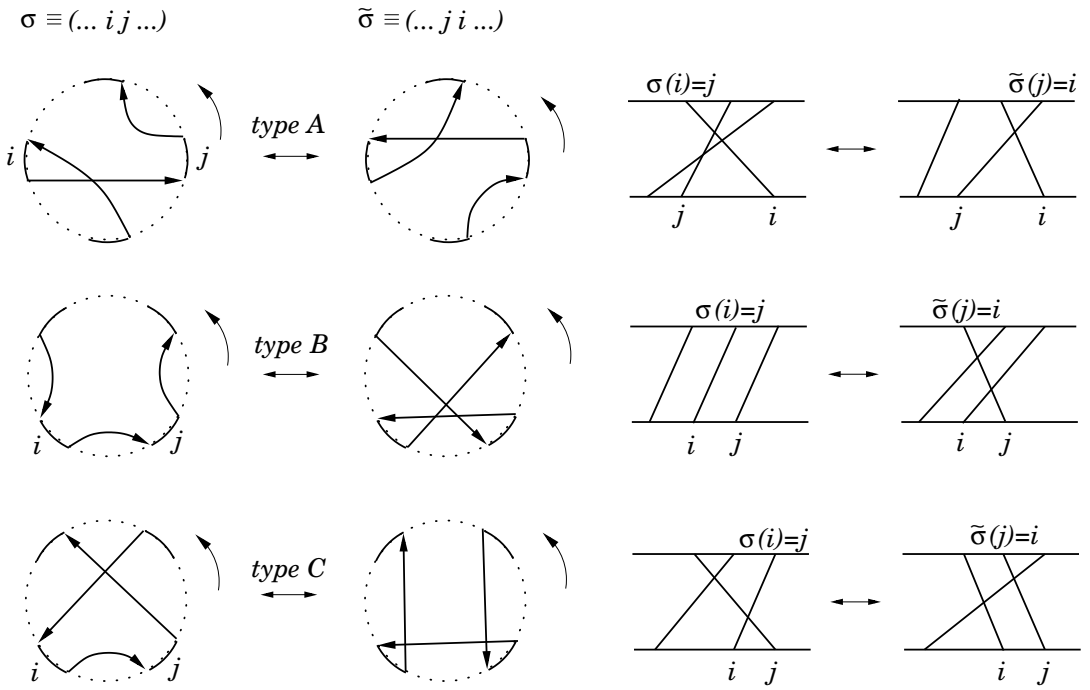

Figure 2.22: Twist moves on Gauss diagrams

type of move	variation of λ	variation of $\mathcal{T}(\gamma)$
A	unchanged	unchanged
B (from left to right)	decreases by 1	decreases by 1
C (from left to right)	decreases by 1	decreases by 1

□

Theorem 2.3.22 can be useful in practice, since the torsion of a permutation can be computed at a glance on the braid-like presentation. Observe that

1. Every non proper loop is homologous to a multiple of $[K]$, easy to determine.
2. For every proper loop γ, there is an integer n such that $\tilde{\gamma} = \gamma + n[K]$ is proper, ER, and has zero coordinate along at least one edge. Namely, $n = -\min_e \langle \gamma, e \rangle$.
3. Every class $\tilde{\gamma}$ as above decomposes as a sum $\tilde{\gamma} = \sum_i \gamma_i$ such that
   → all the γ_i's are proper and ERS
   → $\forall i, j, A, \langle \gamma_i, A \rangle \langle \gamma_j, A \rangle \geq 0$
4. By Lemma 2.3.18, $\mathcal{T}(\tilde{\gamma}) = \sum_i \mathcal{T}(\gamma_i)$, and the $\mathcal{T}(\gamma_i)$'s are given by Theorem 2.3.22.

This shows that it is possible to compute any homology class by using the torsion formula. Whether it is more interesting than the energy formula depends on the context.

Chapter 3

Arrow diagram formulas for virtual knots

In [30] and [31], Vassiliev studies the space of all knots by considering it a stratified space, where finite codimensional strata consist of *singular* knot types. The level 0 of the resulting cohomology theory consists of the so-called *finite-type knot invariants*. It is possible to understand these invariants separately from the general theory, in a more basic fashion – a point of view that first appeared in [2] and is the most frequently referred to. We recall it in section 3.1 (for a comprehensive introduction to the subject, see [1]).

It happens that the theory of finite-type invariants and that of Gauss diagrams are intimately related. A Gauss diagram can be regarded as a *function on the space of Gauss diagrams* (see [27] and [9]). The linear combinations of such functions that define invariants are called *formulas*. It was shown by M.Goussarov [13, 29] that Gauss diagram formulas exactly coincide with Vassiliev's finite type invariants in the classical case of knots in $\mathbb{S}^3$.

As functions, these invariants are defined on the set of all Gauss diagrams. Hence it is natural to wonder which of them are also invariants of *virtual knots*. This is what is done in [14], which (re)introduces the Polyak algebra (see also [25]), providing a handy set of equations defining virtual Gauss diagram formulas. This virtual aspect is the one investigated here. The constructions from [14] are extended to the most general case of Gauss diagrams on an arbitrary group.

In Subsection 3.2.2 is introduced a machinery to compare different kinds of Gauss diagrams from the viewpoint of invariants, via *symmetry-preserving maps*. Then we focus on *homogeneous* invariants and show (Theorem 3.2.24) that they exactly coincide with the *arrow diagram invariants* introduced in [27]. The main result is that these are the kernel of an easily computable linear map (Theorem 3.3.9), as predicted by a conjecture of M.Polyak [24]. Section 3.3.4 contains an alternative topological point of view on this map, which is more likely to allow generalizations to higher dimensions – a few steps are made in that direction. The last section contains examples, notably an alternative proof and a generalization of Grishanov-Vassiliev's theorem on planar chain invariants from [15] (Theorem 3.4.3).

In all the chapter, we fix an arbitrary group π and a homomorphism $w : \pi \to \mathbb{F}_2$. Unless otherwise specified, a Gauss diagram denotes a Gauss diagram on π, and a

virtual knot invariant is a map defined on Gauss diagrams, that is invariant under R-moves and w-moves. If π is abelian and if w is the trivial homomorphism, then every definition or assertion in this chapter has a matching version using abelian Gauss diagrams.

3.1 Finite-type invariants

Vassiliev and Vassiliev-Kauffman invariants

Let M be a smooth oriented 3-manifold and let us call a *k-singular knot* in M a smooth oriented immersion $\mathbb{S}^1 \to M$ with k ordinary double points – that is, points in M with exactly two preimages, at which the differentials of the immersion are linearly independent.

Let p be a double point of a singular knot. A *desingularization of p* is the process of pushing one branch of the knot near p so that it does not intersect the other branch any more. Up to local isotopy, there are exactly two ways to do this, distinguished by a sign (the *local writhe*) defined as follows.

Definition 3.1.1. With the above notations, number arbitrarily 1 and 2 the branches of the knot near p. By definition the tangent directions (v_1, v_2) to the branches span a plane inside T_pM. Pick a complementary direction v_3 (such that $v_1 \oplus v_2 \oplus v_3 = T_pM$), and push the branch 1 in the direction of v_3. The desingularization is said to have *positive writhe* if the triple (v_1, v_2, v_3) is consistent with the orientation of M, *negative* otherwise. Through a generic chart of M near p, one recovers the pictures at the left of Fig.2.2.

Let $K \subset M$ be a k-singular knot with double points numbered from 1 to k. Then any map $\sigma : \{1, \dots, k\} \to \{\pm 1\}$ defines a regular knot K^σ. A knot invariant with values in an abelian group induces an invariant of k-singular knots by the formula

$$d^k\nu(K) = \sum_{i=1}^{k} \mathrm{sign}(\sigma)\nu(K^\sigma),$$

where $\mathrm{sign}(\sigma)$ is the product of all $\sigma(i)$'s. By symmetry, this does not depend on the numbering of the crossings.

Definition 3.1.2 (Vassiliev's finite-type invariants)**.** A classical knot invariant ν with values in an abelian group is said to be of *finite type in the sense of Vassiliev* if there is an integer $k \in \mathbb{N}$ such that $d^k\nu$ identically vanishes. The *degree* of ν is the highest value of k such that $d^k\nu$ is non trivial.

From now on M denotes the total space of a thickened surface $M \to \Sigma$, and the knots considered are always assumed to be in generic position with respect to the bundle projection – though isotopies may cross non generic strata, as usual, when a Reidemeister move happens.

By expanding the alternate sum $d^k\nu(K)$, one sees that being a finite-type invariant is actually a purely combinatorial property and can be defined on Gauss diagrams. This observation appeared first in [17] and directly extends to Gauss

diagrams on a weighted group. Indeed, pick any k arrows in a Gauss diagram G and number them from 1 to k. Then with every map $\sigma \in \{\pm 1\}^k$, associate the diagram G_σ obtained from G by reversing the orientation and writhe of the i-th arrow for every i such that $\sigma(i) = -1$ (leaving all π-markings unchanged).

Definition 3.1.3 (Vassiliev-Kauffman's finite-type invariants of virtual knots)**.** A virtual knot invariant with values in an abelian group is said to be of finite type of degree at most k in the sense of Vassiliev-Kauffman if it satisfies the equation

$$\sum_{\sigma \in \{\pm 1\}^{k+1}} \operatorname{sign}(\sigma) \nu(G_\sigma) = 0, \tag{3.1}$$

for any choice of a Gauss diagram G and a set of $k+1$ arrows in it.

Remark 3.1.4. When (π, w) is the weighted fundamental group of a surface (Definition 2.2.2), then by adding the constraint that G must be represented by a *real* knot, one recovers the classical notion of Vassiliev's finite-type invariants of knots in a thickened surface.

Remark 3.1.5. It is also possible to define finite-type invariants of *abelian Gauss diagrams* (Definition 2.3.7) by the same equation. But in that case, one should be careful that reversing the orientation of an arrow implies "reversing" its π-marking, from p to $\mu(K) - p$, since the associated fundamental loop is changed.

Finite type invariants of semi-virtual knots

Another notion of "finite type" exists for virtual knot invariants, and was introduced in [14]. It is designed to axiomatize those virtual knot invariants that can be presented by Gauss diagrams (the meaning and the necessity of this will be explained in the next section).

As before, pick any k numbered arrows in a Gauss diagram G. For a map $\sigma \in \{\pm 1\}^k$, $G_{(\sigma)}$ is the subdiagram of G obtained by *deleting* the i-th arrow for every i such that $\sigma(i) = -1$ (recall that a deletion consists in a virtualization from the knot diagram viewpoint).

Definition 3.1.6 (Goussarov-Polyak-Viro's finite type invariants of semi-virtual knots)**.** A virtual knot invariant with values in an abelian group is said to be of finite type of degree at most k in the sense of GPV if it satisfies the equation

$$\sum_{\sigma \in \{\pm 1\}^{k+1}} \operatorname{sign}(\sigma) \nu(G_{(\sigma)}) = 0, \tag{3.2}$$

for any choice of a Gauss diagram G and a set of $k+1$ arrows in it.

The terminology "semi-virtual" was coined in [14] and explained as follows. Just like the alternating sum

$$\sum_{\sigma \in \{\pm 1\}^{k+1}} \operatorname{sign}(\sigma) G_\sigma$$

in the Vassiliev settings may be formally assimilated with a unique knot diagram with $k+1$ "singular" crossings subject to the formal relation "*singular* = *positive*

$-$ *negative*", the sum in (3.2) may be interpreted as the value of ν on a unique knot diagram with $k+1$ "semi-virtual" signed crossings, subject to (defined by) the formal relations

$$\begin{cases} \text{semi-positive} &= \text{positive} - \text{virtual} \\ \text{semi-negative} &= \text{negative} - \text{virtual} \end{cases}.$$

So one should understand via this terminology that the invariants have a finite-type property with respect to these semi-virtual arrows, but as maps they remain invariants of Gauss diagrams in the usual sense.

Notice that one has the formal relation *"singular = semi-positive − semi-negative"*, from which finite type invariants in the sense of GPV are necessarily of finite type in the sense of Vassiliev-Kauffman. The converse is not true (see [17],[6] and the next section).

3.2 Gauss diagram invariants

3.2.1 General algebraic settings

We denote by $\mathfrak{G}_n$ (*resp.* $\mathfrak{G}_{\leq n}$) the $\mathbb{Q}$-vector space freely generated by Gauss diagrams on π of degree n (*resp.* $\leq n$), and set $\mathfrak{G} = \varinjlim \mathfrak{G}_{\leq n}$. Unless π is a finite group, these spaces are not finitely generated, and we define their hat versions $\widehat{\mathfrak{G}}_n$ (*resp.* $\widehat{\mathfrak{G}}_{\leq n}$) as the $\mathbb{Q}$-spaces of formal series of Gauss diagrams of degree n (*resp.* $\leq n$). Finally, set $\widehat{\mathfrak{G}} = \varinjlim \widehat{\mathfrak{G}}_{\leq n}$. An arbitrary element of $\widehat{\mathfrak{G}}$ is usually denoted by $\mathcal{G}$ and called a *Gauss series*, of degree n if it is represented in $\widehat{\mathfrak{G}}_{\leq n}$ but not in $\widehat{\mathfrak{G}}_{\leq n-1}$. The notation G is saved for single Gauss diagrams. A Gauss diagram G of degree n has a *group of symmetries* $\mathrm{Aut}(G)$, which is a subgroup of $\mathbb{Z}/2n$, made of the rotations of the circle that leave unchanged a given representative of G (see Subsection 3.2.2).

By quotienting the space $\mathfrak{G}$ by the subspace spanned by the Reidemeister relators and w-moves relators, one obtains the $\mathbb{Q}$-space freely generated by virtual knot types. On Fig.3.1 is reminded a reduced generating set of Reidemeister relators, coming from [26] (Theorem 1.1). Notice that the proof in [26] is given for real knots in $\mathbb{S}^3$, but since it is local, it works as well for Gauss diagrams on a group.

There is a linear isomorphism $I : \mathfrak{G}_{\leq n} \to \mathfrak{G}_{\leq n}$, the keystone to the theory, which maps a Gauss diagram of degree n to the formal sum of its 2^n subdiagrams:

$$I(G) = \sum_{\sigma \in \{\pm 1\}^n} G_{(\sigma)}, \tag{3.3}$$

where $G_{(\sigma)}$ is G deprived from the arrows that σ maps to -1 (see Definition2.3.1 for subdiagrams). The inverse map of I is given by

$$I^{-1}(G) = \sum_{\sigma \in \{\pm 1\}^n} \mathrm{sign}(\sigma) G_{(\sigma)}. \tag{3.4}$$

Definition 3.2.1. A *Gauss diagram formula* is a virtual knot invariant of the form

$$\nu_{\mathcal{G}} : G \mapsto v(\mathcal{G}, I(G)), \tag{3.5}$$

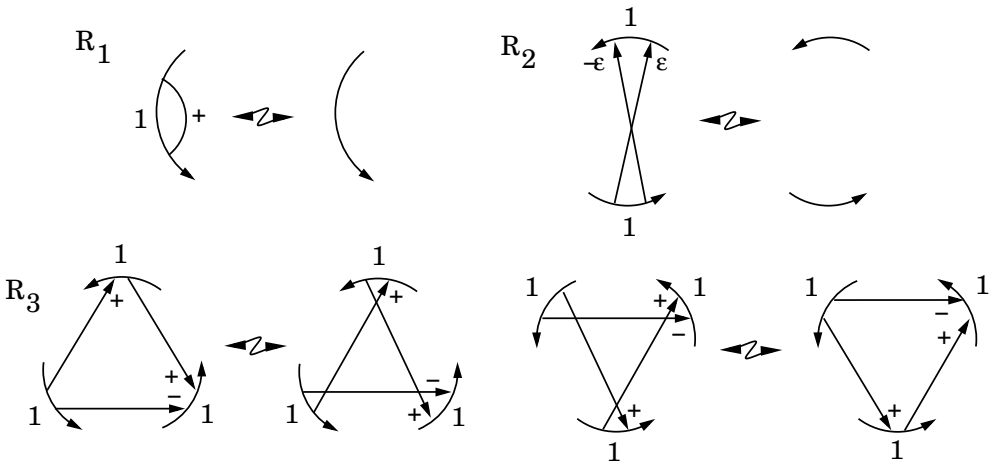

Figure 3.1: A reduced set of R-moves – see Definition 2.3.1 for the rules on π-markings.

where $\mathcal{G} \in \widehat{\mathfrak{G}}$ and v is an orthogonal scalar product on $\mathfrak{G}$ with respect to the basis given by Gauss diagrams. Such a formula "counts" the subdiagrams of G, with weights given by the coefficients of $\mathcal{G}$. Notice that only one of the two arguments of v needs to be a finite sum for the expression to make sense. We do not make a distinction between a virtual knot invariant and the linear form induced on $\mathfrak{G}$.

Since this theory was born, mainly two scalar products have been used, namely:
→ The *orthonormal* scalar product, which shall be denoted here by $(,)$.
→ Its normalized version $\langle , \rangle$, defined by

$$\langle G, G' \rangle := |\mathrm{Aut}(G)|(G, G'). \tag{3.6}$$

Roughly speaking, $\langle , \rangle$ counts parametrized configurations of arrows, while $(,)$ counts unordered sets of arrows. Notice that $\langle , \rangle$ is still symmetric (hence a scalar product).

The orthonormal version is used notably in [14] and [9]. The normalized version was already defined in [27] (though their Theorem 2 is stated in terms of $(,)$), but it was O.P.Östlund who first formally stated that $\langle , \rangle$ is more convenient to get nice properties when dealing with Gauss diagrams with symmetries ([23], Sections 2.2 and 2.4). The main results of the present chapter will confirm this fact. The pairing $\langle , \rangle$ is also used in [15], and implicitly in [31].

Proposition 3.2.2 ([27],[14])**.** *For all $\mathcal{G} \in \widehat{\mathfrak{G}}$, the map $\nu_{\mathcal{G}}$ defined by* (3.5) *satisfies equations* (3.1) *and* (3.2) *with $k = \deg(\mathcal{G})$. Consequently, any Gauss diagram formula $\mathcal{G}$ is a finite-type invariant in both senses of Vassiliev-Kauffman and GPV, of degree no greater than* $\deg(\mathcal{G})$.

The converse of this statement in the sense of GPV is true, and follows from (3.2) and (3.4) (it is contained in the first lines of Section 3 of [14]). It is precisely the raison d'être of GPV's semi-virtual theory.

The converse in the sense of Vassiliev-Kauffman is false in general, but it is true if one restricts to real knots in $\mathbb{S}^3$ – it is a result of Goussarov. The precise statement, however, needs one to introduce the theory of *long knots*. Before we

describe it, let us mention why Goussarov's theorem does *not* imply a similar statement for virtual knots. Indeed, a virtual knot invariant of finite-type in the sense of Vassiliev-Kauffman induces a classical Vassiliev invariant. By Goussarov's theorem the induced invariant can be represented by a Gauss diagram formula *in the sense of real knots*. But even though that formula defined a function on all Gauss diagrams, there is no reason for it to coincide with the invariant we started from. There is even no reason for which it would define a virtual knot invariant at all. The first example of a Vassiliev-Kauffman invariant that is not GPV can be found in [17]; M.Chrisman [6, 5] describes an infinite family of such invariants.

Long knots and Goussarov's theorem

Definition 3.2.3. A *long knot* is a smooth embedding $\mathbb{R} \to \mathbb{R}^3$ that coincides with the embedding $t \mapsto (t, 0, 0)$ outside the segment $[-1, 1]$. By Alexandroff compactification, a long knot closes into a classical knot in $\mathbb{S}^3$.

Proposition 3.2.4. *Two long knots with isotopic closures are isotopic.*

Sketch of the proof. By assumption there is a positive diffeomorphism h of $\mathbb{S}^3$ taking the closure of one knot to the other. It can clearly be assumed that h coincides with the identity on a close contractible neighborhood of the infinity, containing the image of $\mathbb{R} \setminus [-1, 1]$. Now for any close contractible subset $X \subset \mathbb{S}^3$ the space $\mathrm{Diff}^+(\mathbb{S}^3, X)$ is path-connected. Hence there is an isotopy from h to the identity, that induces a long knot isotopy. □

Long knots come with their Gauss diagram theory, obtained from the classical one by adding a base point to Gauss diagrams, which must be away from the arrows and from the local Reidemeister pictures (if the obstruction loop defined on Fig.2.18 contains the base point, then the move is forbidden). Finite-type invariants and Gauss diagram formulas are defined by the same equations as before, respectively (3.1) and (3.5) – note that in this framework, the pairings $(,)$ and $\langle , \rangle$ coincide, since a based diagram cannot have symmetries.

Theorem 3.2.5 (Goussarov [13], see also [29])**.** *Let ν be a finite-type $\mathbb{Z}$-valued invariant of (real) long knots in $\mathbb{R}^3$, of degree n. Then there is a linear combination with integer coefficients $\mathcal{G}$ of based Gauss diagrams of degree at most n, such that $\nu = \nu_{\mathcal{G}}$.*

It is clear that a Vassiliev invariant of classical knots induces a Vassiliev invariant of long knots, and the converse holds by Proposition 3.2.4. Hence Goussarov's theorem fully describes Vassiliev invariants of classical knots (that is, actual knots in the sphere).

The proof given by Goussarov strongly makes uses of the *order* on the crossings, induced by the base point. Unfortunately, there is no satisfying long knot theory in more complicated 3-manifolds, which is the main reason why the representability of Vassiliev invariants by Gauss diagram formulas is still open for arbitrary thickened surfaces.

The Polyak algebra

A Gauss series $\mathcal{G} \in \widehat{\mathfrak{G}}$ defines a virtual knot invariant if and only if the function $\langle \mathcal{G}, I(.) \rangle$ is zero on the subspace spanned by R-moves and w-moves relators. Hence it is interesting to understand the image of that subspace under I with a simple family of generators. This is the idea of the construction of the Polyak algebra ([25, 14]).

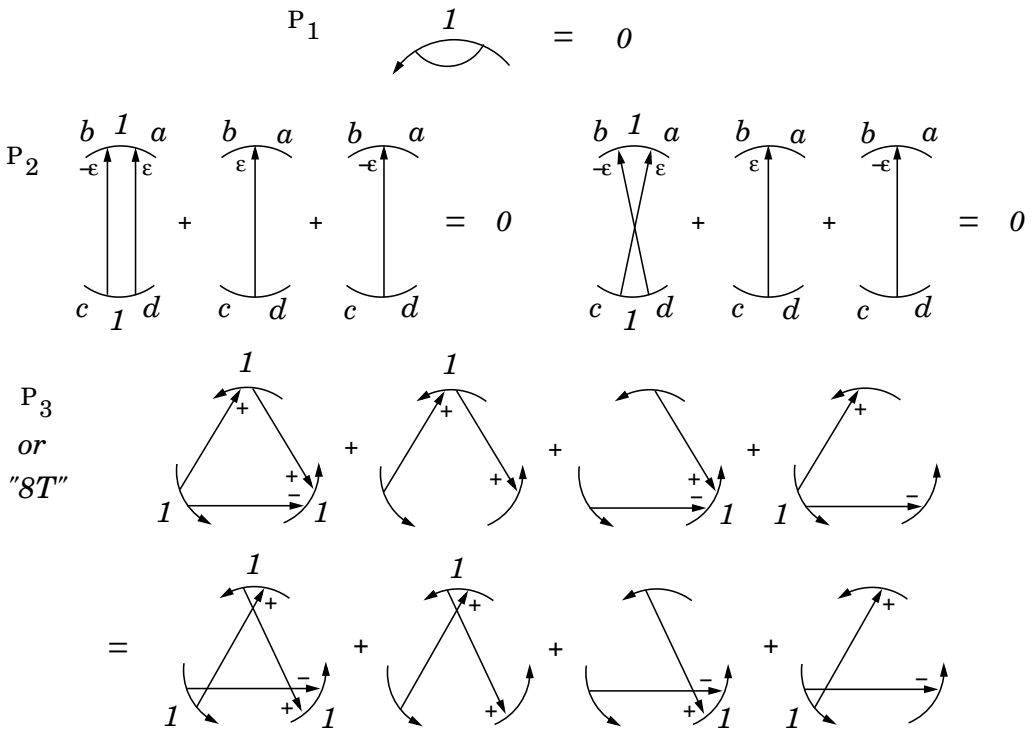

Figure 3.2: The three kinds of Polyak relations – only one P_3 relation is shown, there is a second one obtained by reversing all the arrow orientations.

In the present case, $\mathcal{P}$ is defined as the quotient of $\mathfrak{G}$ by

→ the relations shown in Fig.3.2, which we call P_1, P_2, P_3 (or $8T$ *relation*),

→ the W relation, which is simply the linear match of w-moves (*i.e.* just replace the "$\rightsquigarrow$" with a "=" in all the relations from Fig.2.9).

Be careful that unlike R_1-moves, where an isolated arrow surrounding an edge marked with 1 simply disappears, in a P_1-move the presence of such an arrow completely kills the diagram. Fig.3.2 does not feature the π-markings for P_3 to lighten the picture, but they have to follow the usual "merge $\rightsquigarrow$ multiply" rule (see Definition 2.3.1).

The following proposition extends Theorem 2.D from [14].

Proposition 3.2.6. *The map I induces an isomorphism $\mathfrak{G}/_{\mathrm{R,W}} \to \mathfrak{G}/_{\mathrm{P,W}} =: \mathcal{P}$. More precisely, I induces an isomorphism between* $\mathrm{Span}(\mathrm{R}_i)$ *and* $\mathrm{Span}(\mathrm{P}_i)$*, for $i = 1, 2, 3$, and between* $\mathrm{Span}(\mathrm{W})$ *and itself. It follows that the map $G \to I(G) \in \mathcal{P}$ defines a complete invariant for virtual knots.*

A word about invariants of real knots

As one can see from the definitions, it is *a priori* easier for a Gauss series to define a real knot invariant than to define a virtual knot invariant – there are less relations to satisfy. But describing in pure combinatorial terms which of the virtual relations a real knot invariant need not satisfy is far from easy. There is no "real" Polyak algebra. Consider for instance the formula for the invariant v_3 given by [27] (Theorem 2): it is reproduced here with on Fig.3.3 (the meaning of those diagrams without signs is given in Subsection 3.2.3). On the same picture is shown a couple of virtual knots of the same virtual type, on which v_3 takes different values. This implies that Polyak-Viro's formula does not define a virtual invariant – and as an empiric corollary, that it should be difficult to prove that it is actually an invariant for real knots.

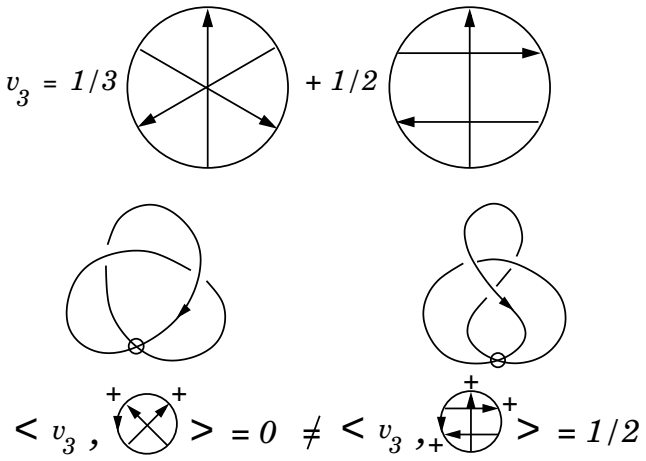

Figure 3.3: Polyak-Viro's formula for v_3 is not a virtual invariant

O.P.Östlund ([23], Section 8) developed a language that allowed him to prove Polyak-Viro's formula (Proposition 9.4). But the proof relies on the fortuitous fact that we know an identity of Gauss diagram functions on real links (two ways to compute the linking number). To detect systematically arrow diagram formulas for real knots, one should be able to describe the set of arrow diagram functions that are identically 0 on real links.

In the present chapter, only invariants of virtual knots are considered – partially because there is no notion of "real" Gauss diagrams on an arbitrary group. It is not hopeless that a nice characterization of Gauss diagrams of real knots can be found (it is done in the classical case, see [17], Section 3.3), as well as their specific Gauss diagram invariants, that will formally become a definition of "realness" in the present settings.

3.2.2 The symmetry-preserving injections

Depending on the context, one may have to consider simultaneously different types of Gauss diagrams, with more or less decorations. This subsection presents a natural way to do it, convenient from the viewpoint of Gauss diagram invariants.

The construction requires one to choose a kind of combinatorial objects that is the "father" of all other kinds, in the sense of quotienting. We present the construction by taking as the father type that of Gauss diagrams on a group.

In first place, we do not regard Gauss diagrams up to homeomorphisms of the circle: the base circle is assumed to be the unit circle in $\mathbb{C}$, the endpoints of the arrows are assumed to be located at the $2n$-th roots of unity, and the arrows are straight line segments. Such a diagram is called *rigid*.

By a "type of rigid Gauss diagrams" we mean an equivalence relation on the set of rigid Gauss diagrams on π, which is required to satisfy two properties:
1. (Degree property) All diagrams in a given equivalence class shall have the same degree.
2. (Stability property) The action of $\mathbb{Z}/2n$ on the set of Gauss diagrams of degree n shall induce an action on the set of degree n equivalence classes.

Since every construction in this subsection is therefore destined to be homogeneous, the degree of all Gauss diagrams is once and for all set equal to n. A *rigid Gauss diagram of type* $\sim$ is an equivalence class under the relation $\sim$. A *Gauss diagram (of type* $\sim$*)* is the orbit of a rigid diagram of type $\sim$ under the action of $\mathbb{Z}/2n$. The corresponding $\mathbb{Q}$-spaces are respectively denoted by $\mathfrak{G}_{\sim}^{\text{rigid}}$ and $\mathfrak{G}_{\sim}$.

Since $\mathbb{Z}/2n$ is abelian, two elements from the same orbit have the same stabilizer, hence a Gauss diagram G has a well-defined *group of symmetries* $\mathrm{Aut}(G)$, which is the stabilizer of any of its rigid representatives under the action of $\mathbb{Z}/2n$. Consequently, the space $\mathfrak{G}_{\sim}$ is endowed with a pairing $\langle , \rangle$ defined by (3.6).

Now consider two types of rigid Gauss diagrams, say 1 and 2, such that relation 1 is finer than relation 2 ("$1 \prec 2$").

Definition 3.2.7 (Forgetful projections)**.** A 1-rigid diagram G_1 determines a unique 2-rigid diagram whose $\mathbb{Z}/2n$-orbit only depends on that of G_1. This induces a natural surjective map at the level of Gauss diagram spaces, denoted by

$$\mathrm{T}_2^1 : \mathfrak{G}_{(1)} \twoheadrightarrow \mathfrak{G}_{(2)}.$$

Note that this map may be not well-defined on the spaces of formal series of Gauss diagrams, if some 2-equivalence class contains infinitely many 1-classes.

Example: the abelianization map ab (Definition 2.3.7) induces by linearity a forgetful projection from Gauss diagrams on π to abelian diagrams on π, when π is abelian.

Definition 3.2.8 (Symmetry-preserving injections)**.** In the opposite way, there is a map $\mathfrak{G}_{(2)}^{\text{rigid}} \to \mathfrak{G}_{(1)}^{\text{rigid}}$ that sends a 2-rigid diagram G_2 to the formal sum of all 1-classes that it contains. When this sum is pushed in $\mathfrak{G}_{(1)}$, the result

- → is well-defined: a 2-rigid diagram cannot contain infinitely many rigid representatives of a given Gauss diagram of type 1, since the orbits are finite ($\mathbb{Z}/2n$ is finite).
- → only depends on the $\mathbb{Z}/2n$-orbit of G_2.

This induces an injective *symmetry-preserving map* at the level of formal series,

$$\mathrm{S}_2^1 : \widehat{\mathfrak{G}_{(2)}} \hookrightarrow \widehat{\mathfrak{G}_{(1)}}.$$

S_2^1 is well-defined, componentwise, since 2-rigid diagrams from different $\mathbb{Z}/2n$-orbits contain 1-rigid diagrams from disjoint sets of $\mathbb{Z}/2n$-orbits (the images of two different Gauss diagrams do not overlap). It is injective for the same reason.

The terminology is explained by the following fundamental formula:

Lemma 3.2.9. *With notations as above, for any Gauss diagram G_2 of type 2,*

$$\mathrm{S}_2^1(G_2) = \sum_{\mathrm{T}_2^1(G_1)=G_2} \frac{|\mathrm{Aut}(G_2)|}{|\mathrm{Aut}(G_1)|} G_1. \tag{3.7}$$

Informally, the weight given to a preimage of G_2 under T_2^1 is the amount of symmetry that it has lost by the gain of more information. Note that the weights are integers, since $\mathrm{Aut}(G_1)$ identifies with a subgroup of $\mathrm{Aut}(G_2)$.

Proof. Fix a representative G_2^{rigid} of G_2. By the stability property, $\mathrm{Aut}(G_2)$ acts on the set of 1-classes contained in G_2^{rigid}. Moreover, by definition of $\mathrm{Aut}(G_2)$, two different orbits under that action still lie in different orbits under the action of $\mathbb{Z}/2n$ itself. Therefore there is a $1-1$ correspondence between the $\mathrm{Aut}(G_2)$-orbits and the Gauss diagrams that happen in the sum $\mathrm{S}_2^1(G_2)$. The stabilizer of a given 1-class G_1^{rigid} is by definition $\mathrm{Aut}(G_1)$, whence the cardinality of the corresponding orbit, which is also the coefficient of G_1 in $\mathrm{S}_2^1(G_2)$, is $\frac{|\mathrm{Aut}(G_2)|}{|\mathrm{Aut}(G_1)|}$. □

Proposition 3.2.10.

1. *For any three relations such that $1 \prec 2 \prec 3$, the following diagrams commute:*

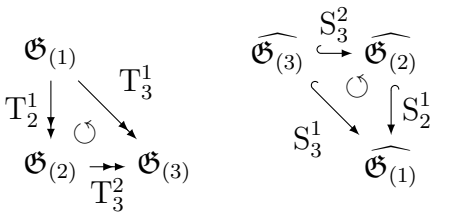

2. *Injections and projections are pairwise $\langle , \rangle$-adjoint, in the sense that*

$$\forall\ \mathcal{G}_1 \in \mathfrak{G}_{(1)},\ \mathcal{G}_2 \in \widehat{\mathfrak{G}_{(2)}},\quad \left\langle \mathrm{S}_2^1(\mathcal{G}_2), \mathcal{G}_1 \right\rangle = \left\langle \mathcal{G}_2, \mathrm{T}_2^1(\mathcal{G}_1) \right\rangle.$$

3. $\mathrm{Im}\,\mathrm{S}_2^1 = \mathrm{Ker}^{\perp}\,\mathrm{T}_2^1$.

Proof. 1. The first diagram commutes directly from the definition of the maps T_i^j. As for the maps S_i^j, since they are defined componentwise it is enough to check it for a single diagram G_3. In that case, it is a consequence of Lemma 3.2.9 and the relation $\mathrm{T}_3^1 = \mathrm{T}_3^2 \circ \mathrm{T}_2^1$.

2. In both sides, it is clear that only a finite number of terms in $\mathcal{G}_2$ are relevant, namely those that are projections of some terms of $\mathcal{G}_1$ under T_2^1. Thus, by bilinearity, it is enough to consider single diagrams G_1 and G_2. If $G_2 \neq \mathrm{T}_2^1(G_1)$, then both sides are 0. If $G_2 = \mathrm{T}_2^1(G_1)$, then

$$\begin{aligned} \left\langle \mathrm{S}_2^1(G_2), G_1 \right\rangle &= \left\langle \tfrac{|\mathrm{Aut}(G_2)|}{|\mathrm{Aut}(G_1)|} G_1, G_1 \right\rangle \\ &= |\mathrm{Aut}(G_2)|, \end{aligned}$$

while

$$\begin{aligned}\left\langle G_2, \mathrm{T}_2^1(G_1)\right\rangle &= \langle G_2, G_2\rangle \\ &= |\mathrm{Aut}(G_2)|.\end{aligned}$$

3. The inclusion $\mathrm{Im}\,\mathrm{S}_2^1 \subset \mathrm{Ker}^\perp \mathrm{T}_2^1$ follows immediately from 2. For the converse, pick a Gauss diagram series $\mathcal{G}_1$ in $\mathrm{Ker}^\perp \mathrm{T}_2^1$. For any two 2-related Gauss diagrams of type 1, G_1 and G_1', one has

$$\langle \mathcal{G}_1, G_1 - G_1' \rangle = 0.$$

Thus, if G_2 is a Gauss diagram of type 2, one can define $\phi(G_2)$ to be the value of $\langle \mathcal{G}_1, G_1\rangle$ for any preimage G_1 of G_2 under T_2^1, and set

$$\mathcal{G}_2 = \sum \frac{\phi(G_2)}{|\mathrm{Aut}(G_2)|} G_2,$$

where the sum runs over all Gauss diagrams of type 2. Finally,

$$\begin{aligned}\mathrm{S}_2^1(\mathcal{G}_2) &= \sum \tfrac{|\mathrm{Aut}(\mathrm{T}_2^1(G_1))|}{|\mathrm{Aut}(G_1)|} \tfrac{\phi(\mathrm{T}_2^1(G_1))}{|\mathrm{Aut}(\mathrm{T}_2^1(G_1))|} G_1 \\ &= \sum \tfrac{\langle \mathcal{G}_1, G_1\rangle}{|\mathrm{Aut}(G_1)|} G_1 \\ &= \mathcal{G}_1\end{aligned}.$$

□

In practice, point 3 is useful in both directions: whether one needs a characterization of the series that lie in the image of some map S (Lemma 3.2.19), or of the series that define invariants under some kind of moves (Propoosition 3.3.4). Point 2 states that symmetry-preserving maps are the good dictionary to understand invariants that were defined via forgetful projections.

Remark 3.2.11. Every construction and result in this subsection can be extended by replacing the set of rigid Gauss diagrams of degree n with any set endowed with the action of an abelian finite group.

3.2.3 Arrow diagrams and homogeneous invariants

Definition 3.2.12. An *arrow diagram (on π)* is a Gauss diagram G (on π) of which the signs decorating the arrows have been forgotten. As usual, it is considered up to homeomorphisms of the circle.

This notion is originally due to M.Polyak ([25, 27]). Beware that the terminology in [14] is different: arrows in arrow diagrams *have* signs).

Arrow diagram spaces $\mathfrak{A}_n$, $\mathfrak{A}_{\leq n}$, $\mathfrak{A}$, the hat versions, and the pairings $(,)$ and $\langle,\rangle$ are defined similarly to their signed versions (Subsection 3.2.1). We use notations A for an arrow diagram and $\mathcal{A}$ for an *arrow diagram series – i.e.* an element of $\widehat{\mathfrak{A}}$.

Arrow diagram formulas

In the language of Subsection 3.2.2, arrow diagrams are a kind of Gauss diagrams satisfying the degree and stability properties – the equivalence relation on rigid Gauss diagrams is given by $G \sim G' \Leftrightarrow$ one may pass from G to G' by writhe changes. Therefore, an arrow diagram A has a well-defined symmetry group $\mathrm{Aut}(A)$, and there are a symmetry-preserving map $\mathrm{S}_a : \widehat{\mathfrak{A}} \hookrightarrow \widehat{\mathfrak{G}}$ and a projection $\mathrm{T}_a : \mathfrak{G} \twoheadrightarrow \mathfrak{A}$. However, for the purpose of defining arrow diagram invariants, we are going to twist these maps a little, by pushing an additional sign into the weights:

Definition 3.2.13. Define the linear maps $S : \widehat{\mathfrak{A}} \to \widehat{\mathfrak{G}}$ and $T : \mathfrak{G} \to \mathfrak{A}$ componentwise by

$$S(A) := \sum_{\mathrm{T}_a(G)=A} \mathrm{sign}(G) \frac{\mathrm{Aut}(A)}{\mathrm{Aut}(G)} G \tag{3.8}$$

$$T(G) := \mathrm{sign}(G)\, \mathrm{T}_a(G) \tag{3.9}$$

Proposition 3.2.14.

1. *S and T are $\langle , \rangle$-adjoint, in the sense that*

$$\forall\, \mathcal{G} \in \mathfrak{G},\, \mathcal{A} \in \widehat{\mathfrak{A}}, \quad \langle S(\mathcal{A}), \mathcal{G} \rangle = \langle \mathcal{A}, T(\mathcal{G}) \rangle .$$

2. $\mathrm{Im}\, S = \mathrm{Ker}^{\perp} T$.

The proof is completely similar to that of Proposition 3.2.10.

Definition 3.2.15. A Gauss diagram formula that lies in the image of the map S is called an *arrow diagram formula*.

Very roughly, such an invariant counts subdiagrams with weights given by the product of the writhes of the arrows involved. A lot of the explicit formulas that have been found so far are actually arrow diagram formulas – for non trivial thickened surfaces as well as the sphere $\mathbb{S}^3$. It is historically the first kind of Gauss diagram invariants that were ever defined ([27]).

Remark 3.2.16. One can define brackets $(\!(A, G)\!)$ and $\langle\!\langle A, G \rangle\!\rangle$ in the following way: for every subdiagram of G that becomes A after one forgets its signs, form the product of these signs. Sum up all these products, and call the result $(\!(A, G)\!)$. On the other hand, put $\langle\!\langle A, G \rangle\!\rangle := |\mathrm{Aut}(A)|(\!(A, G)\!)$ – this is what is called $\langle A, G \rangle$ in [23] (section 2.2). Then for every arrow diagram A and every Gauss diagram G, the following equality holds:

$$\langle\!\langle A, G \rangle\!\rangle = \langle S(A), I(G) \rangle .$$

The equality

$$(\!(A, G)\!) = (S(A), I(G))$$

holds for all G if and only if A has no symmetries other than the identity.

Proof. By definition of S,

$$\begin{aligned}\langle S(A), I(G)\rangle &= \textstyle\sum_{\mathrm{T}_a(H)=A} \mathrm{sign}(H)\frac{|\mathrm{Aut}(A)|}{|\mathrm{Aut}(H)|}\langle H, I(G)\rangle \\ &= |\mathrm{Aut}(A)| \textstyle\sum_{\mathrm{T}_a(H)=A} \mathrm{sign}(H)(H, I(G)) \\ &= \langle\!\langle A, G\rangle\!\rangle\,.\end{aligned}$$

This proves the first equality as well as the "if" part of the last statement. For the "only if" part, set G to be any preimage of A under T_a. Then:

$$\begin{aligned}(S(A), I(G)) &= \textstyle\sum_{\mathrm{T}_a(H)=A} \mathrm{sign}(H)\frac{|\mathrm{Aut}(A)|}{|\mathrm{Aut}(H)|}(H, I(G)) \\ &= \mathrm{sign}(G)\frac{|\mathrm{Aut}(A)|}{|\mathrm{Aut}(G)|},\end{aligned}$$

while

$$(\!(A, G)\!) = \mathrm{sign}(G).$$

So one must have $|\mathrm{Aut}(A)| = |\mathrm{Aut}(G)|$ for all G such that $\mathrm{T}_a(G) = A$, which can be true only if $|\mathrm{Aut}(A)| = 1$. Indeed, if $\rho \in \mathrm{Aut}(A) \setminus \{\mathrm{Id}\}$, pick an arrow α of A such that $\rho(\alpha) \neq \alpha$ and construct G by adding signs to A in such a way that $\mathrm{sign}(\alpha) = 1$ and $\mathrm{sign}(\rho(\alpha)) = -1$. Necessarily $\rho \notin \mathrm{Aut}(A^\sigma)$, so that $|\mathrm{Aut}(A^\sigma)| < |\mathrm{Aut}(A)|$. □

Homogeneous invariants

Definition 3.2.17. For each $n \in \mathbb{N}$, there is an orthogonal projection $p_n : \widehat{\mathfrak{G}} \to \widehat{\mathfrak{G}}_n$ with respect to the scalar product $\langle , \rangle$. For $\mathcal{G} \in \widehat{\mathfrak{G}}$, the *principal part* of $\mathcal{G}$ is defined by $p_n(\mathcal{G})$, with $n = \deg(G)$. $\mathcal{G}$ is called *homogeneous* if it is equal to its principal part.

Let $\mathcal{G}$ be a homogeneous Gauss series. Then $\mathcal{G}$ satisfies the P_2 and P_3 relations (*i.e.* $\langle \mathcal{G}, \mathrm{P}_i\rangle = 0$ for $i = 2, 3$) if and only if it satisfies the *homogeneous* relations $\langle \mathcal{G}, p_k(\mathrm{P}_i)\rangle = 0$ for all k. These are denoted by $\mathrm{P}_2^{(n-1),1}$, $\mathrm{P}_2^{(n-2),2}$, $\mathrm{P}_3^{(n-2),2}$ (or $G6T$) and $\mathrm{P}_3^{(n-3),3}$ (or $G2T$). The parenthesized numbers in exponent indicate in each case how many arrows are unseen. P_1 and W relations are already homogeneous and do not get a new name. Some examples are shown on Fig.3.4; for a full list, just consider the projections of the relations of Fig.3.2.

Homogeneous relations are also defined for arrow diagram spaces, denoted by AP_1, $\mathrm{AP}_2^{(n-2),2}$, $\mathrm{AP}_3^{(n-2),2}$ (or $A6T$), $\mathrm{AP}_3^{(n-3),3}$ (or $A2T$) and AW (Lemma 3.2.19 below explains why $\mathrm{AP}_2^{(n-1),1}$ is useless: it reads $0 = 0$). They are the images under T (3.9) of the homogeneous relations for Gauss diagrams – in particular one should be especially careful to the signs in the $A6T$ relations. A full list is presented in Fig.3.5.

Lemma 3.2.18. *Let* $\mathcal{A} \in \widehat{\mathfrak{A}}$ *and let* X *be a name among* P_1, $\mathrm{P}_2^{(n-2),2}$, $\mathrm{P}_3^{(n-2),2}$, $\mathrm{P}_3^{(n-3),3}$, W. *Then*

$$\mathcal{A} \in \mathrm{Span}^\perp(\mathrm{AX}) \Longleftrightarrow S(\mathcal{A}) \in \mathrm{Span}^\perp(\mathrm{X}).$$

where orthogonality is as usual in the sense of $\langle , \rangle$.

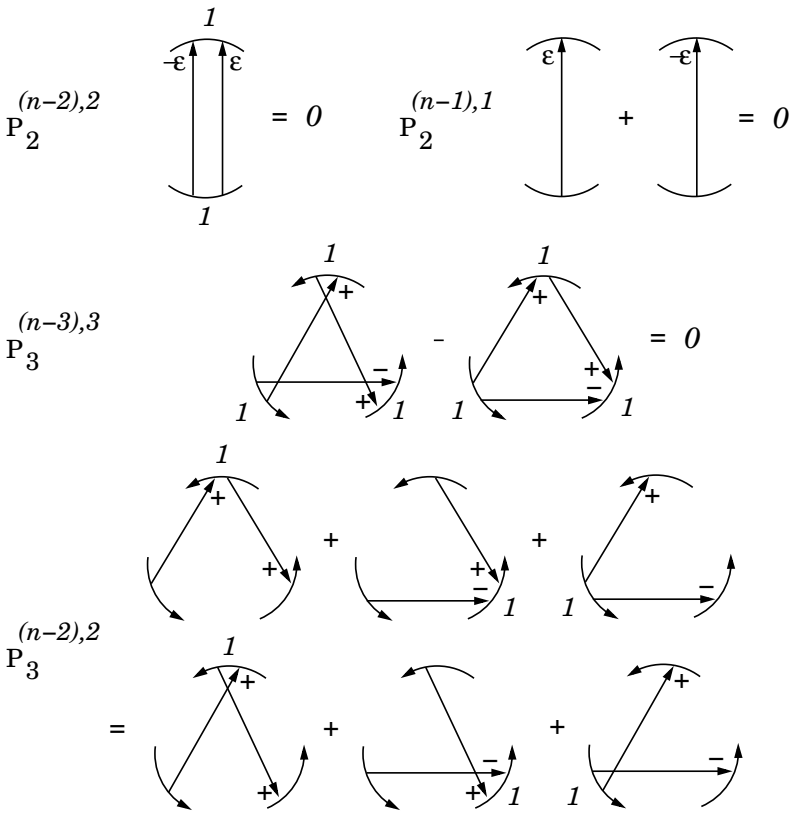

Figure 3.4: Some homogeneous Polyak relations

Proof. It is a direct consequence of part 1. of Proposition 3.2.14. □

Lemma 3.2.19. *Let $\mathcal{G} \in \widehat{\mathfrak{G}}$. Then $\mathcal{G}$ lies in the image of the map $S : \widehat{\mathfrak{A}} \to \widehat{\mathfrak{G}}$ if and only if $\mathcal{G}$ satisfies all the homogeneous relations $\left\langle \mathcal{G}, \mathrm{P}_2^{(n-1),1} \right\rangle = 0$.*

Proof. Notice that the $\mathrm{P}_2^{(n-1),1}$ relators span the kernel of the map T. Hence the result follows from point 2. of Proposition 3.2.14. □

Corollary 3.2.20. *Let $\mathcal{G} \in \widehat{\mathfrak{G}}$ be a Gauss diagram formula. Then its principal part lies in the image of the map S, i.e. can be represented by a (homogeneous) arrow diagram series.*

Remark 3.2.21. This statement in the context of knot theory in the sphere is contained in the lines of [14], Section 3.1.

Proof. Let $\mathcal{G}_d$ be the principal part of $\mathcal{G}$. Since $\mathcal{G}$ is a Gauss diagram formula it must satisfy the P_2 relations (Proposition 3.2.6), which implies, because $\mathcal{G}$ does not have summands of degree higher than d, that $\mathcal{G}_d$ must satisfy the $P_2^{(n-1),1}$ relations. Lemma 3.2.19 concludes the proof. □

One has the immediate corollary:

Corollary 3.2.22. *Any homogeneous Gauss diagram formula for virtual knots is an arrow diagram formula.*

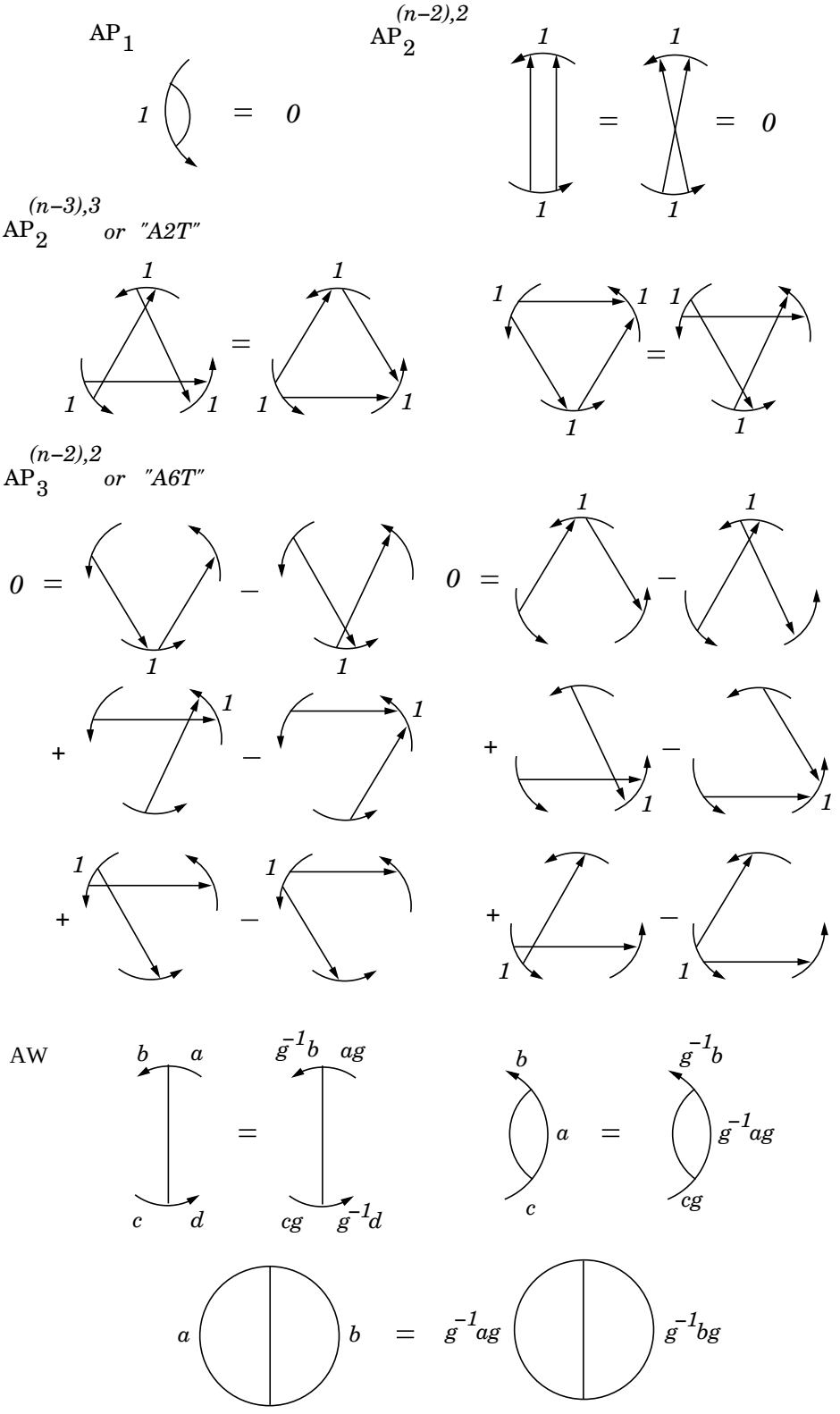

Figure 3.5: The homogeneous arrow relations – as usual, in AW the orientation of an arrow is reversed if and only if $w(g) = -1$.

We will prove that the converse is true in some sense (Theorem 3.2.24). It requires the following inclusion, which is a crucial point in all main results in this chapter.

Lemma 3.2.23. *For all $n \geq 3$:*

$$\mathrm{Span}(A2T) \subseteq \mathrm{Span}(A6T) \oplus \mathrm{Span}(\mathrm{AP}_2^{(n-2),2}).$$

Proof. Figs.3.6 and 3.7 show eight $A6T$ relations, where it is assumed that the unseen parts are identical in all 48 diagrams, and that every totally visible edge (there are three on each diagram) is decorated by 1. Some arrows are dashed, only for the sake of clarity. Up to $\mathrm{AP}_2^{(n-2),2}$, the combination

$$(1) + (2) + \frac{1}{2}\left[(3) + (4) - (5) - (6) - (7) - (8)\right]$$

gives the left one of the two $A2T$ relations shown on Fig.3.5. To get the other half of $\mathrm{Span}(A2T)$, just reverse the arrows in the previous equation. □

Theorem 3.2.24. *Any homogeneous part of an arrow diagram formula is itself an arrow diagram formula.*

Proof. Let $\mathcal{A} \in \widehat{\mathfrak{A}}$ be an arrow diagram formula. It suffices to prove that the principal part of $\mathcal{A}$, say $\mathcal{A}_d$, is an arrow diagram formula. By Proposition 3.2.6, $\langle S(\mathcal{A}), \mathrm{P}_i\rangle = 0$ for $i = 1, 2, 3$. Let us show that the same goes for $\mathcal{A}_d$.

1. P_1 and S are homogeneous, so $\langle S(\mathcal{A}_d), \mathrm{P}_1\rangle = 0$.

2. By Lemma 3.2.19

$$\left\langle S(\mathcal{A}_{d-1}), P_2^{(d-2),1}\right\rangle = 0, \qquad \text{and} \tag{3.10}$$

$$\left\langle S(\mathcal{A}_d), P_2^{(d-1),1}\right\rangle = 0. \tag{3.11}$$

The equations $\langle S(\mathcal{A}), \mathrm{P}_2\rangle = 0$ together with (3.10) imply that

$$\left\langle S(\mathcal{A}_d), \mathrm{P}_2^{(d-2),2}\right\rangle = 0. \tag{3.12}$$

Finally, (3.11) and (3.12) yield $\langle S(\mathcal{A}_d), \mathrm{P}_2\rangle = 0$.

3. The last and crucial point:

$$\begin{aligned}
\langle S(\mathcal{A}), \mathrm{P}_3\rangle = 0 \implies & \left\langle S(\mathcal{A}_d), \mathrm{P}_3^{(d-2),2}\right\rangle = 0 \\
\overset{(3.12)\,+\,\text{Lemma } 3.2.18}{\implies} & \left\langle \mathcal{A}_d, \mathrm{AP}_3^{(d-2),2}\right\rangle = 0 \text{ and } \left\langle \mathcal{A}_d, \mathrm{AP}_2^{(d-2),2}\right\rangle = 0 \\
\overset{\text{Lemma } 3.2.23}{\implies} & \left\langle \mathcal{A}_d, \mathrm{AP}_3^{(d-2),2}\right\rangle = 0 \text{ and } \left\langle \mathcal{A}_d, \mathrm{AP}_3^{(d-3),3}\right\rangle = 0 \\
\overset{\text{Lemma } 3.2.18}{\implies} & \left\langle S(\mathcal{A}_d), \mathrm{P}_3^{(d-2),2}\right\rangle = 0 \text{ and } \left\langle S(\mathcal{A}_d), \mathrm{P}_3^{(d-3),3}\right\rangle = 0 \\
\implies & \langle S(\mathcal{A}_d), \mathrm{P}_3\rangle = 0.
\end{aligned}$$

□

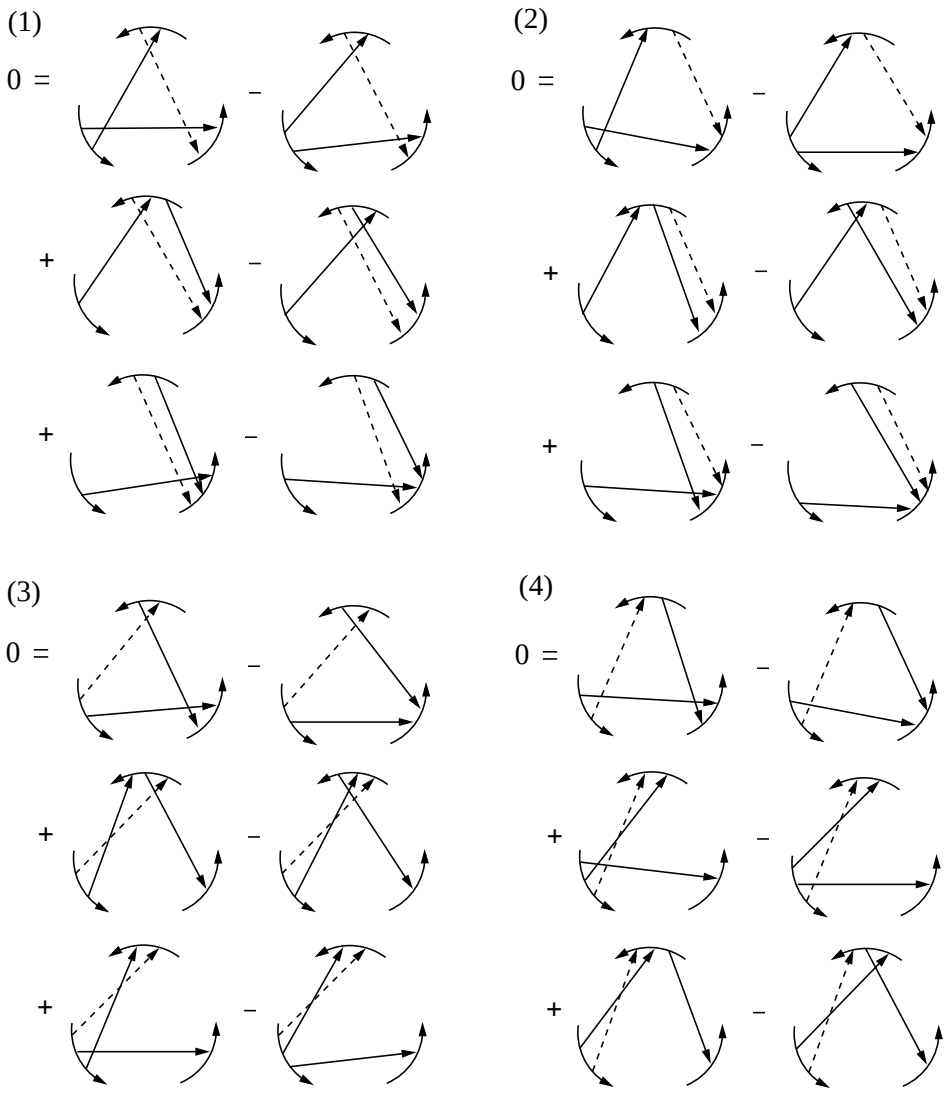

Figure 3.6: Proof of Lemma 3.2.23 – part 1

3.3 Polyak's conjecture

During Swiss Knots conference in 2011, Michael Polyak gave a talk in which he conjectured that Gauss diagram formulas for knots in $\mathbb{S}^3$ were the kernel of a linear map with values in some space of *degenerate diagrams* – defined below. We shall not give a formal statement of the conjecture here, since it was never written by its author, but there is a video of the talk available online ([24]). It happens that the map d suggested as a candidate has the property of being homogeneous:

$$\forall \mathcal{G} \in \mathfrak{G}, [d(\mathcal{G}) = 0 \iff \forall n \in \mathbb{N}, d(p_n(\mathcal{G})) = 0] .$$

It follows from Subsection 3.2.3 that, in the virtual settings, the best that one may expect from such a map is to detect *arrow diagram formulas*. So we restrict our attention to this kind of invariants, and give two independent proofs that such a map exists to detect Reidemeister III invariance – while R-I and R-II are extremely easy to check.

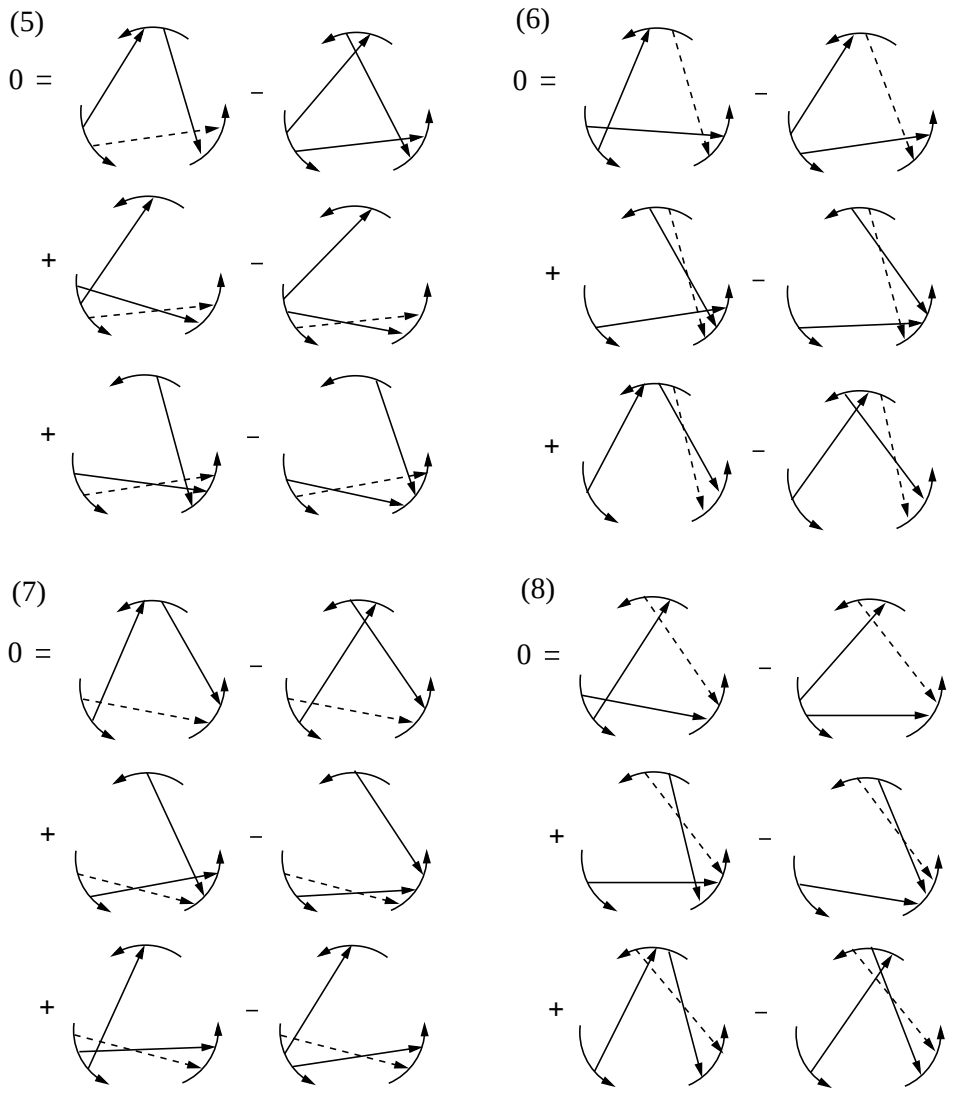

Figure 3.7: Proof of Lemma 3.2.23 – part 2

3.3.1 Based and degenerate diagrams

Definition 3.3.1. A *based* Gauss diagram is a Gauss diagram together with a distinguished (*base*) edge. Based arrow diagrams are defined similarly. The corresponding spaces are denoted by $\mathfrak{G}_\bullet$ and $\mathfrak{A}_\bullet$, in reference to the dot that we use in practice to pinpoint the distinguished edge.

A *degenerate Gauss diagram (with one degeneracy)* is a Gauss diagram in which one edge, whose endpoints belonged to two different arrows, has been shrunk to a point. The spaces of degenerate diagrams are denoted by $\mathfrak{DG}$ and $\mathfrak{DA}$ respectively.

Even though they would encode long knots in the classical theory (see Definition 3.2.3), based diagrams only have a combinatorial interest here. On the other hand, degenerate diagrams have a natural topological interpretation that will be explained in Subsection 3.3.4.

The space of degenerate arrow diagrams is meant to be quotiented by the so-called *triangle relations*, shown in Fig.3.8. The quotient space is denoted by $\mathfrak{DA}/_\nabla$.

These relations originated in the early work of M.Polyak on arrow diagrams ([25]).

From the knot diagram viewpoint, one sees that two coinciding arrowheads is a Reidemeister III move with an indeterminacy: the branch of the knot corresponding to the degenerate point is known to be "above" the two other branches, but nothing is known about the relative position of these two. It is natural to set this indeterminate position to be equal to the formal sum of the two possible resolutions of the indeterminacy.

Yet another interpretation arises from the reading of [28]: one sees that while a Reidemeister III move should be 1 codimensional, it is actually 3 codimensional from the Gauss diagram viewpoint (three arrows meet in a triangle). This is too much concentrated information. By expanding artificially the stratum, one gets a cell – called $\mathcal{C}_Y$ in [28] – whose boundary is essentially a triangle relator.

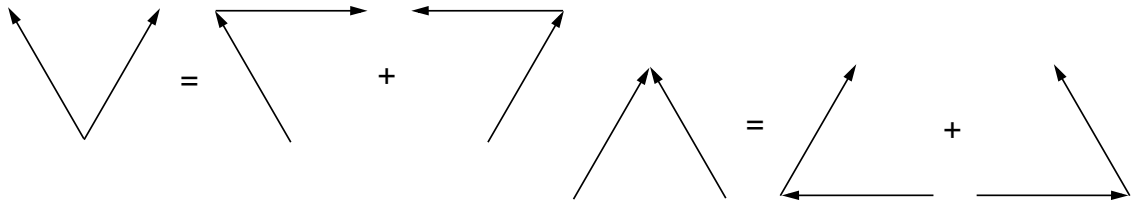

Figure 3.8: The triangle relations

Definition 3.3.2. Call a degenerate diagram *monotonic* if an arrowhead and an arrowtail meet at the degenerate point.

Lemma 3.3.3. $\widehat{\mathfrak{DA}/_{\nabla}}$ *is naturally isomorphic with the* $\mathbb{Q}$*-space of formal series of monotonic arrow diagrams.*

Proof. It suffices to show that the set of monotonic diagrams forms a basis of $\mathfrak{DA}/_{\nabla}$. It is clearly a generating set thanks to the ∇ relations, and it is free because every non monotonic diagram happens in exactly one relation, and every relation contains exactly one of them. □

3.3.2 Detecting arrow diagram formulas

In this subsection we describe a handy set of necessary and sufficient conditions for $\mathcal{A} \in \widehat{\mathfrak{A}}$ to define an arrow diagram formula. Invariance under w, R_1, R_2 and R_3-moves are studied separately. While the first three conditions require little work, the last one is the heart of our understanding of Polyak's conjecture.

w-invariance

Proposition 3.3.4. *There is an injective "symmetry-preserving" map* $\mathrm{S}^a_{aw} : \widehat{\mathfrak{A}/_{\mathrm{AW}}} \hookrightarrow \widehat{\mathfrak{A}}$ *defined componentwise by the formula*

$$\alpha \mapsto \sum_{A \in \alpha} \frac{|\mathrm{Aut}(\alpha)|}{|\mathrm{Aut}(A)|} A.$$

If $\mathcal{A} \in \widehat{\mathfrak{A}}$*, then the map* $G \mapsto \langle\langle \mathcal{A}, G \rangle\rangle = \langle S(\mathcal{A}), I(G) \rangle$ *is invariant under* w*-moves if and only if* $\mathcal{A}$ *lies in the image of* S^a_{aw}*.*

Proof. The equivalence relation defined by AW-moves and writhe changes on the set of rigid Gauss diagrams on π satisfies the degree and stability properties from Subsection 3.2.2. Hence one may apply the results of that section to get the existence and elementary properties of S^a_{aw}. The last assertion follows from sucessive application of the W part of Lemma 3.2.18 and point 3 of Proposition 3.2.10. □

This means that an arrow diagram formula must be represented by a series of w-orbits of arrow diagrams. In practice, this condition is most of time satisfied by construction. An important example is the sum of all elements contained in a set that is stable under w-moves.

R_1 and R_2 invariance

Proposition 3.3.5. *Let $\mathcal{A} \in \widehat{\mathfrak{A}}$. Then the function $G \mapsto \langle S(\mathcal{A}), I(G)\rangle$ is invariant under R_1 (resp. R_2) moves if and only if $\mathcal{A}$ satisfies all AP_1 (resp. $\mathrm{AP}_2^{(n-2),2}$) relations.*

Proof. By Proposition 3.2.6, the R_1 and R_2 invariance are equivalent to the relations $\langle S(\mathcal{A}), \mathrm{P}_1\rangle = 0$ and $\langle S(\mathcal{A}), \mathrm{P}_2\rangle = 0$ being satisfied. Lemma 3.2.19 implies that the second of these relations is actually equivalent to $\langle S(\mathcal{A}), \mathrm{AP}_2^{(n-2),2}\rangle = 0$. Lemma 3.2.18 concludes the proof. □

In practice, these conditions are easy to check naked-eye.

R_3 invariance

Definition 3.3.6. Say that a based diagram $A_\bullet$ is *nice* if its base edge
→ is decorated by 1,
→ is bounded by the endpoints of two different arrows.

Lemma 3.3.7. *Nice based diagrams have a sign ε induced by Definition 2.1.3.*

Proof. The sign ε from Definition 2.1.3 takes as an argument the edge of a Gauss diagram. Since it does not depend on the writhes of the arrows, it is well-defined for arrow diagrams with a preferred edge. □

Definition 3.3.8. Let $A_\bullet$ be a based arrow diagram. If $A_\bullet$ is not nice, then put $\delta(A_\bullet) = 0$. If $A_\bullet$ is nice, then

1. Shrink the base edge to a point.
2. Multiply the resulting degenerate diagram by $\varepsilon(A_\bullet)$, and call the result $\delta(A_\bullet)$.

This process defines a map $\delta : \widehat{\mathfrak{A}_\bullet} \to \widehat{\mathfrak{D}\mathfrak{A}}$ – well defined since any monotonic diagram has finitely many preimages. Now let A be an arrow diagram, and denote by $\bullet(A) \in \mathfrak{A}_\bullet$ the sum of all based diagrams that one can form by choosing a base edge in A. Finally, define

$$\begin{array}{rccc} d: & \widehat{\mathfrak{A}} & \to & \widehat{\mathfrak{D}\mathfrak{A}} \\ & \mathcal{A} & \mapsto & \delta(\bullet(\mathcal{A})) \end{array}.$$

Theorem 3.3.9. *Let $\mathcal{A} \in \widehat{\mathfrak{A}}$ satisfy the R_2 invariance condition from Proposition 3.3.5. Then the following are equivalent:*

→ *The map* $G \mapsto \langle S(\mathcal{A}), I(G)\rangle$ *is invariant under* R_3*-moves.*
→ $d(\mathcal{A}) = 0$ *modulo the triangle relations.*
→ $\mathcal{A} \in \mathrm{Span}^{\perp}(A6T)$.

This theorem gives a formal proof to the fact that the $\langle , \rangle$ pairing enables a uniformization of the formulas that depend on parameters: we shall see for instance that the degenerate cases of Grishanov-Vassiliev's invariants need not be treated separately. See also Proposition 2 from [10], where points (i) and (ii) are actually the same formula, or the special case $2a = K$ in Theorem 3.4.9 below.

Remark 3.3.10. Unlike Polyak's conjecture initially predicted, this map d encodes Reidemeister III invariance only assuming that Reidemeister II invariance is already satisfied. For one thing, in practice this is not a problem, since checking R_1 and R_2 invariance is already as easy as one can hope. Besides, it is actually possible to define a map $\tilde{d}$ such that $(d \oplus \tilde{d})(\mathcal{A}) = 0$ if and only if $\mathcal{A}$ is an arrow diagram formula, with no previous conditions on $\mathcal{A}$. By this way, one gets a statement exactly similar to the initial conjecture, except that it deals with virtual knot invariants. This map $\tilde{d}$ has also a nice topological interpretation, but in practice it looks like an artefact to encode the conditions of Proposition 3.3.5 (*i.e.* AP_1 and $\mathrm{AP}_2^{(n-2),2}$ relations), and it does not make the detection of invariants easier.

Remark 3.3.11. Based on our understanding of the conjecture, it seems not to hold for invariants of usual knots: the "boundary" of the formula for v_3 (Fig.3.3 here) is not zero, even mod 2. The virtual statement presented here seems to be the best one can get.

Proof. The proof will consist in defining and explaining the following chain of equivalences.

$$d(\mathcal{A}) = 0 \bmod \nabla \Leftrightarrow (\bullet(\mathcal{A}), A6T_\bullet) = 0 \Leftrightarrow \ \langle \mathcal{A}, A6T\rangle = 0 \Leftrightarrow \ \langle S(\mathcal{A}), I(\mathrm{R}_3)\rangle = 0$$

Notice that both extremities of this chain are *homogeneous* conditions (for the right one, it follows from the proof of Theorem 3.2.24). So we can assume that $\mathcal{A}$ is homogeneous.

1. $d(\mathcal{A}) = 0 \bmod \nabla \Leftrightarrow (\bullet(\mathcal{A}), A6T_\bullet) = 0$.
$\mathfrak{DA}/\nabla$ is endowed with the orthonormal scalar product $(,)$ with respect to the basis of monotonic diagrams (Definition 3.3.2). We simply compute the coordinates of $d(\mathcal{A})$ in this basis. Note that the pairing $(,)$ is still defined for any couple of series in $\widehat{\mathfrak{DA}/\nabla}$ one of which is finite.

Let D be a monotonic degenerate diagram and $A_\bullet$ a based diagram. The coordinate of $\delta(A_\bullet)$ along D is given by

$$(\delta(A_\bullet), D) = (A_\bullet, A6T_\bullet(D)),$$

where $A6T_\bullet(D)$ is what we call the *based* 6-term relation associated with D (see an example on Fig.3.9). It is a consequence of the fact that the sign of a diagram in a based $A6T$-relation is equal to the ε sign of that diagram. The equivalence follows.

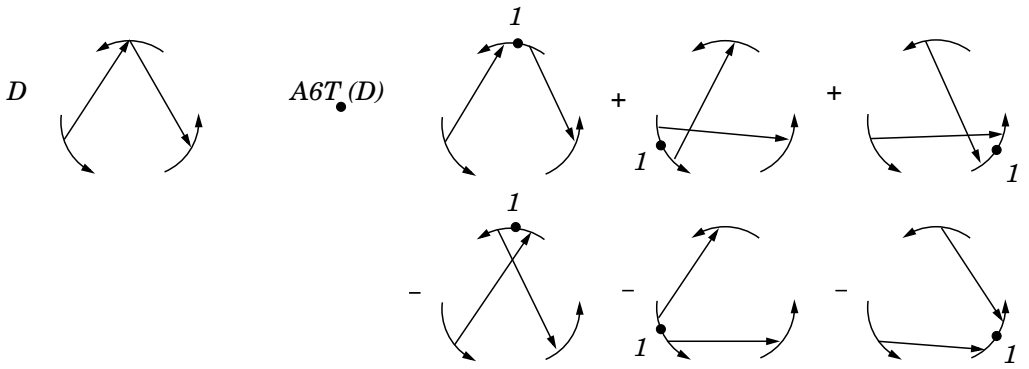

Figure 3.9: The based 6-term relation associated with a degenerate diagram

2. Notice that in the language of Subsection 3.2.2, the map $\bullet(\cdot)$ is nothing but the symmetry-preserving map from $\mathfrak{A}$ to $\mathfrak{A}_\bullet$ (all based diagrams have a trivial symmetry group). The result follows then from point 2. of Proposition 3.2.10.

3. $\langle \mathcal{A}, A6T\rangle = 0 \Leftrightarrow \ \langle S(\mathcal{A}), I(\mathrm{R}_3)\rangle = 0$

By Proposition 3.2.6, $\langle S(\mathcal{A}), I(.)\rangle$ being invariant under R_3 moves is equivalent to $S(\mathcal{A})$ satisfying every P_3 relation. Since by hypothesis $\mathcal{A}$ is homogeneous (say of degree n), this is equivalent to $S(\mathcal{A})$ actually satisfying separately the $G6T$ and $G2T$ relations. By Lemma 3.2.18, this is again equivalent to $\mathcal{A}$ satisfying the $A6T$ and $A2T$ relations. Finally, Lemma 3.2.23 implies that under the current assumption that $\langle \mathcal{A}, \mathrm{AP}_2^{(n-2),2}\rangle = 0$, satisfying $A6T$ and $A2T$ relations is actually equivalent to satisfying $A6T$ relations alone.

□

3.3.3 Invariance criterion for w-orbits

As we have seen, an arrow diagram series defines an invariant only if it has a preimage in $\widehat{\mathfrak{A}/_{\mathrm{AW}}}$. The above criteria for invariance under R-moves nicely extend in terms of that preimage. This is especially interesting when w-orbits are well understood, for instance if π is abelian and w is trivial (Proposition 2.3.8).

w-moves for based and degenerate diagrams

These moves are defined similarly to the regular version (Fig.2.9, top-left and top-right), with additional moves in the degenerate case, that modify the neighborhood of the arrows meeting at the degenerate point (Fig.3.10 shows the extreme cases – there are obvious intermediate ones, when only one or two of the unseen arcs is empty). The arrows both change orientations if $w(g) = -1$, and keep the same otherwise.

Definition 3.3.12. Pick a based arrow diagram $A_\bullet$. If its base edge is bounded by twice the same arrow, then set $\delta_w([A_\bullet]) = 0$. If it is bounded by two different arrows, then

1. pick a nice diagram $A_\bullet^{(1)}$ AW-equivalent to $A_\bullet$,

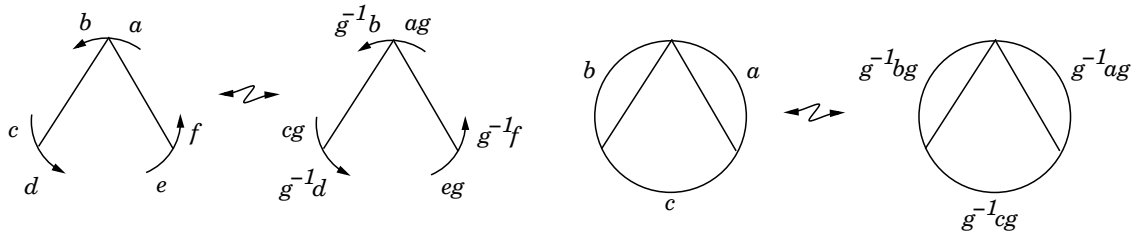

Figure 3.10: The "degenerate" w-move – the most general and the most exceptional cases. The two arrows change orientations if and only if $w(g) = -1$.

2. set $\delta_w([A_\bullet]) = \left[\delta(A_\bullet^{(1)})\right]$.

Finally, set

$$d_w([A]) = \delta_w([\bullet(A)]).$$

As usual, δ_w and d_w are defined componentwise on formal series of w-orbits.

Consistency of the definition. Observe that when the endpoints of an edge belong to two different arrows, then any value can be given to its marking by using the appropriate w-move. This proves that step 1 is always possible – though not in a unique way.

For step 2, first notice that two w-moves performed on different arrows from an arrow diagram commute, so that any finite sequence of w-moves amounts to a sequence made of one move for each arrow. If such a sequence leaves the marking of the base edge unchanged (and equal to 1), then the moves on the two adjacent arrows must involve the same conjugating element g. It follows that whenever $A_\bullet$ and $A'_\bullet$ are nice and lie in the same w-orbit,

- $\to$ $\varepsilon(A_\bullet) = \varepsilon(A'_\bullet)$,
- $\to$ the degenerate diagrams obtained by shrinking their bases also lie in the same orbit.

Hence δ_w is well-defined. □

How to handle the quotients by ∇ relations

Note that the quotient of $\mathfrak{DA}$ by the ∇ relations does not fit in the general framework in which symmetry preserving maps were introduced: indeed, it does not come from an equivalence relation at the level of the *set* of diagrams.

However, the set of classes of monotonic diagrams forms a basis of $\mathfrak{DA}/_\nabla$. This induces an injective section i of the projection $s : \mathfrak{DA} \twoheadrightarrow \mathfrak{DA}/_\nabla$. Both s and i extend componentwise to formal series of w-orbits.

The same phenomenon happens between $\widehat{\mathfrak{DA}/_{\mathrm{AW}}}$ and $\widehat{\mathfrak{DA}/_{\mathrm{AW},\nabla}}$, because w-moves never change the status of a degenerate diagram – monotonic or not – and the set of monotonic w-orbits still forms a basis of $\mathfrak{DA}/_{\mathrm{AW},\nabla}$. Again there are maps s_w and i_w such that $s_w \circ i_w = \mathrm{Id}$, at the level of formal series.

Finally, this allows us to construct a symmetry-preserving map $\mathrm{S}^\nabla_{w\nabla} : \widehat{\mathfrak{DA}/_{\mathrm{AW},\nabla}} \to \widehat{\mathfrak{DA}/_\nabla}$, by regarding the restriction of $\mathrm{S}^d_{dw} : \widehat{\mathfrak{DA}/_{\mathrm{AW}}} \to \widehat{\mathfrak{DA}}$ to the subspaces of monotonic diagrams.

Summary

In the following diagram, the two squares and the two triangles on the left are commutative, as well as the internal and external squares on the right. Except for $\mathrm{S}^{\nabla}_{w\nabla}$, all vertical arrows are symmetry-preserving injections in the usual sense.

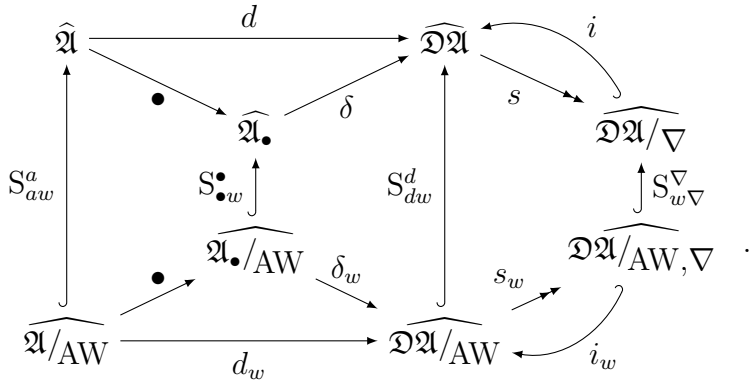

Theorem 3.3.13. *An arrow diagram series $\mathcal{A}$ is an arrow diagram formula if and only if each of the following holds:*

1. *$\mathcal{A}$ has a preimage $\mathcal{A}_w$ by S^a_{aw}.*
2. *$\mathcal{A}_w$ is mapped to 0 in $\widehat{\mathfrak{D}\mathfrak{A}/_{\mathrm{AW},\nabla}}$.*
3. *$\mathcal{A}_w$ satisfies the equations*

$$\langle \mathcal{A}_w, \mathrm{T}^a_{aw}(\mathrm{AP}_1)\rangle = 0 \quad \textit{and} \quad \left\langle \mathcal{A}_w, \mathrm{T}^a_{aw}(\mathrm{AP}_2^{(\mathrm{n}-2),2})\right\rangle = 0 \ .$$

Proof. 1 is necessary because of Proposition 3.3.4, and 3 because of Proposition 3.3.5 and point 2 of Proposition 3.2.10. If 1 and 3 are satisfied, then Theorem 3.3.9 implies that $\mathcal{A}$ defines an arrow diagram formula if and only if $s(d(\mathcal{A})) = 0$. This is equivalent to $\mathrm{S}^{\nabla}_{w\nabla}(s_w(d_w(\mathcal{A}_w))) = 0$ since the diagram commutes, and to $s_w(d_w(\mathcal{A}_w))) = 0$ since $\mathrm{S}^{\nabla}_{w\nabla}$ is injective. □

Remark 3.3.14. To apply the above theorem to an element of $\widehat{\mathfrak{A}/_{\mathrm{AW}}}$, one never needs to push it through symmetry-preserving maps (in the upper half of the diargam). Hence the checkings are done using the most compact expressions. Also, Point 3 can be checked separately on each w-orbit that happens in $\mathcal{A}_w$, and for each of them it can be checked on any representative diagram by a simple criterion.
For AP_1 relations to hold, the situation at the left of Fig.3.11 simply must never happen (the 1-marking is invariant under w-moves).
For $\mathrm{AP}_2^{(\mathrm{n}-2),2}$, the situations at the middle and at the right of the picture are forbidden:

1. if $w(g) = 1$ and the arrows have "the same" orientation (in the sense of the picture),
2. if $w(g) \neq 1$ and the arrows have "different" orientations.

Again these conditions are stable by w-moves.

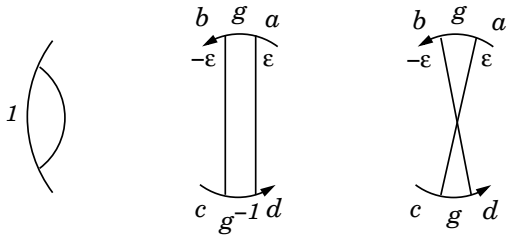

Figure 3.11: Forbidden situations – the rules for the arrow orientations are explained above.

3.3.4 The topological viewpoint

The notion of degenerate Gauss diagrams much resembles the "J-blocks" encountered in the work of V.A.Vassiliev that gave birth to the theory of finite type invariants ([30]; they are called "pure J-blocks" in [31]). In that case, higher order differentials were natural to define, for the whole theory is inspired from simplicial topology.

In this subsection, we define a framework in which the map d can be understood as a direct summand of a 0-coboundary map inspired from simplicial topology. This map d^0 satisfies Theorem 3.3.9 without the R_2-invariance assumption. Then it is shown how the space of values of d^0 can be thought of as a space of 1-cochains in this new framework. Hopefully this will lead to a full theory computing the "finite-type cohomology" of the space of all diagrams of a given knot type.

Notations and basic notions

Recall that $\mathfrak{G}$ denotes the $\mathbb{Q}$-space freely generated by all Gauss diagrams on a fixed group π. Here, it is to be thought of as a space of 0-chains.

A *full degenerate diagram* is the result of adding an arrow to a degenerate diagram with one degeneracy (Definition 3.3.1) to complete its two meeting arrows into a triangle. The resulting triangle should be oriented as one of the two examples from Fig.3.12. There is no constraint on the sign of the additional arrow.

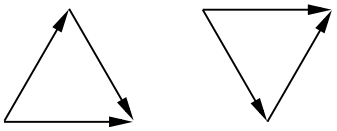

Figure 3.12: Admissible triangles in a degenerate diagram

Definition 3.3.15 (germs)**.** Let (G^-, Δ, G^+) be a triple where G^- and G^+ are two Gauss diagrams that differ only from an R_3 move, and Δ is the degenerate diagram obtained from any of G^- and G^+ by shrinking each of the three concerned edges to a point. Such a triple is called a *(full) germ*. Forgetting the signs of all the arrows in all three diagrams, one obtains an *arrow germ*.

A *partial germ* is a triple $(G^-_\bullet, \Lambda, G^+_\bullet)$ where $G^\pm_\bullet$ are based arrow diagrams that differ only by a switch of the two arrow ends near the base edge, and Λ is the

degenerate diagram that results from shrinking to a point the base edge of either $G^-_\bullet$ or $G^+_\bullet$. *Partial arrow germs* are defined similarly.

Subgerms are defined similarly to subdiagrams, with three requirements:

- → The π-markings have to follow the "merge $\rightsquigarrow$ multiply" rule (see Definition 2.3.1).
- → If one forgets an arrow in one of the three diagrams, then one must forget the matching arrows in both of the other.
- → One may forget at most one arrow from the triangle of Δ, in which case the only remaining unit-marked edge from the R_3 pictures is chosen as a base edge.

The $\mathbb{Q}$-spaces generated by full, partial, arrow and partial arrow germs are submitted to the relations $(x, y, z) + (z, y, x) = 0$, and denoted respectively by $\Gamma_\Delta\mathfrak{G}$, $\Gamma_\Lambda\mathfrak{G}$, $\Gamma^\Delta\mathcal{A}$ and $\Gamma^\Lambda\mathcal{A}$.

The space $\Gamma^\Lambda\mathfrak{A}$ is meant to be modded out by the *triangle relations*, that can be of two types. One of them is shown on Fig.3.13, the other is obtained by reversing all the arrows in the picture. The quotient is denoted by $\Gamma^\Lambda\mathfrak{A}/_\nabla$.

Finally, set

$$\Gamma^1\mathfrak{A} = \Gamma^\Lambda\mathfrak{A}/_\nabla \oplus \Gamma^\Delta\mathfrak{A}.$$

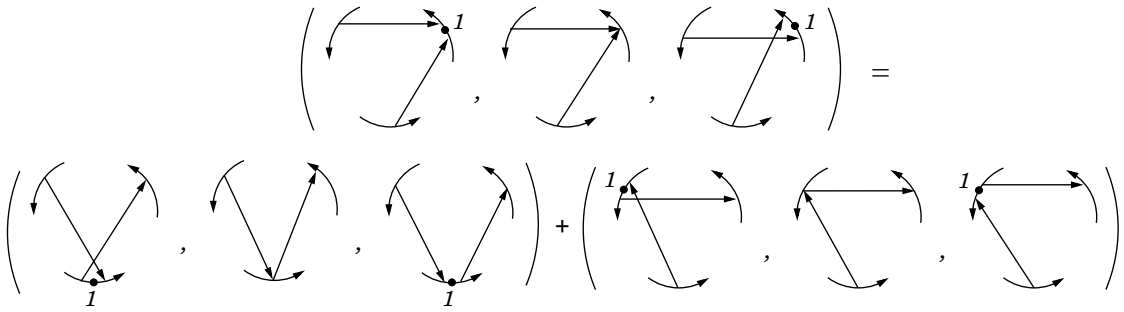

Figure 3.13: The triangle relation for partial germs

The coboundary d^0

Definition 3.3.16. Let A be an arrow diagram. Set $d^0(A)$ to be the formal sum of all arrow germs (A^-, Δ, A^+) and partial arrow germs $(A^-_\bullet, \Lambda, A^+_\bullet)$ such that A^+ (with its base edge forgotten in the second case) is equal to A. This defines componentwise a linear map

$$d^0 : \widehat{\mathfrak{A}} \to \widehat{\Gamma^1\mathfrak{A}},$$

that splits into $d^\Lambda \oplus d^\Delta$.

The following theorem translates Theorem 3.3.9 in the language of the present settings. Points 3. and 4. tell that we actually go a bit further here, since the R_2 invariance assumed in the previous theorem is here gotten rid of. We keep the notation d for the map $d : \widehat{\mathfrak{A}} \to \widehat{\mathfrak{D}\mathfrak{A}/_\nabla}$ from Subsection 3.3.2.

Theorem 3.3.17.

1. *There is an isomorphism* $\Phi : \widehat{\Gamma^{\Lambda}\mathfrak{A}} \xrightarrow{\simeq} \widehat{\mathfrak{D}\mathfrak{A}}$ *that induces an isomorphism* $\tilde{\Phi} : \widehat{\Gamma^{\Lambda}\mathfrak{A}/_{\nabla}} \xrightarrow{\simeq} \widehat{\mathfrak{D}\mathfrak{A}/_{\nabla}}$*, such that*
$$d = \tilde{\Phi} \circ d^{\Lambda}.$$
2. *For any* $A \in \widehat{\mathfrak{A}}$ $d^{\Lambda}(\mathcal{A}) = 0$ *if and only if* $\mathcal{A}$ *satisfies all the* $A6T$ *relations.*
3. *For any* $\mathcal{A} \in \widehat{\mathfrak{A}}$*,* $d^{\Delta}(\mathcal{A}) = 0$ *if and only if* $\mathcal{A}$ *satisfies all the* $A2T$ *relations.*
4. $\mathrm{Ker}(d^0)$ *is the space of arrow diagram series* $\mathcal{A}$ *such that* $\langle S(\mathcal{A}), I(\cdot)\rangle$ *is invariant under* R_3*-moves.*

Remark 3.3.18. Compare the definitions of d and d^{Λ}: even though they are isomorphic, the latter seems to be free from the sign ε (Definition 2.1.3). In the topological framework, this sign is actually hidden inside the algebraic structure, via the triangle relations.

Proof. 1. Let $\lambda = (A^-_\bullet, \Lambda, A^+_\bullet)$ be a partial arrow germ. Notice that $A^+_\bullet$ is necessarily *nice* (Definition 3.3.6), so that we can set $\varepsilon(\lambda) := \varepsilon(A^+_\bullet)$ (see Lemma 3.3.7). Now put
$$\Phi(\lambda) = \varepsilon(\lambda)\Lambda.$$
This is a definition, since the relator $(A^-_\bullet, \Lambda, A^+_\bullet) + (A^+_\bullet, \Lambda, A^-_\bullet)$ is mapped to 0, and it extends componentwise to formal series spaces, since a given Λ happens only in a finite number (2) of partial arrow germs.

On the other hand, if Λ is a degenerate arrow diagram with one degeneracy, Λ has two resolutions that are non degenerate diagrams with a base edge marked with 1 and with opposite ε signs: call them $A^+_\bullet$ and $A^-_\bullet$ so that $\varepsilon(A^+_\bullet) = +1$. Then set
$$\Psi(\Lambda) = (A^-_\bullet, \Lambda, A^+_\bullet).$$

It is immediate to check that Ψ and Φ are inverse maps sending triangle relations to triangle relations, and that
$$d = \Phi \circ d^{\Lambda}.$$

2. In the proof of Theorem 3.3.9, it is shown that $\mathrm{Ker}(d)$ is the space of arrow diagrams satisfying $A6T$ relations (the hypothesis of the theorem does not serve for that). Thus 2. follows from 1.

3. There is a basis of $\Gamma^{\Delta}\mathfrak{A}$ whose every element is an arrow germ, for example the set of arrow germs such that in the first diagram of the triple, the two arrowheads that are meant to exchange their positions belong to arrows that cross each other. One readily sees that the set of coordinates of $d^{\Delta}(\mathcal{A})$ in that basis is exactly the set of relators $\langle \mathcal{A}, A2T\rangle$.

4. By definition,
$$\mathrm{Ker}(d^0) = \mathrm{Ker}(d^{\Lambda}) \cap \mathrm{Ker}(d^{\Delta}).$$
Hence the result follows from 2. and 3. □

Remark 3.3.19. One should think of Λ as a part of a 1-codimensional stratum in a stratified topological space. The ε signs of the two based arrow diagrams adjacent to Λ give a co-orientation. From that point of view, the isomorphism Φ is assimilated with a map that sends a simplex to its dual in a dual simplicial decomposition, and the map $\Lambda \mapsto \langle \Psi(\Lambda), \cdot \rangle$ is the Poincaré duality at the level of chains and cochains.

$\Gamma^1\mathfrak{A}$ is a space of 1-cochains

The space $\Gamma_\Delta\mathfrak{G}$ should be thought of as a space of 1-chains (that would encode generic paths in the space of virtual knot diagrams, though R_1 and R_2 moves are neglected). In particular, there is a linear *boundary map* defined on the generators by

$$\begin{array}{rccc} \partial: & \Gamma_\Delta\mathfrak{G} & \to & \mathfrak{G} \\ & (G^-, \Delta, G^+) & \mapsto & G^+ - G^- \end{array}.$$

We want to see $\Gamma^1\mathfrak{A}$ as a space of functions on $\Gamma_\Delta\mathfrak{G}$, in such a way that there is a Stokes formula between d^0 and ∂. As usual, we seek help from symmetry-preserving maps, and we use twisted versions as in the non-degenerate case (Definition 3.2.13) in order to recover the Stokes formula.

Pick a (partial or full) arrow germ γ of degree n an number the arrows of its three diagrams from 1 to n, consistently. Then every map $\sigma : \{1, \dots, n\} \to \{\pm 1\}$ defines a full germ γ^σ. Let $\mathrm{sign}(\sigma)$ be the product of all the $\sigma(i)$'s. We define the map S componentwise by the formula

$$\begin{array}{rccc} S: & \Gamma^\Lambda\widehat{\mathfrak{A} \oplus \Gamma}^\Delta\mathfrak{A} & \to & \Gamma_\Lambda\widehat{\mathfrak{G} \oplus \Gamma}_\Delta\mathfrak{G} \\ & \gamma & \mapsto & \sum_{\sigma \in \{\pm 1\}^n} \mathrm{sign}(\sigma)\gamma^\sigma \end{array}$$

On the other hand, there is a linear map

$$I : \Gamma_\Delta\mathfrak{G} \to \Gamma_\Lambda\mathfrak{G} \oplus \Gamma_\Delta\mathfrak{G}$$

that sends a germ $\delta = (G^-, \Delta, G^+)$ to the formal sum of its subgerms. As usual, $\Gamma_\Lambda\mathfrak{G} \oplus \Gamma_\Delta\mathfrak{G}$ is endowed with a pairing $\langle , \rangle$ defined by (3.6), which is nothing but the orthonormal scalar product with respect to the basis of germs and partial germs since these never have non trivial symmetries – for germs, it follows from the orientation constraint, see Fig.3.12).

Definition 3.3.20. For $\gamma \in \Gamma^\Lambda\widehat{\mathfrak{A} \oplus \Gamma}^\Delta\mathfrak{A}$ and $\delta \in \Gamma_\Delta\mathfrak{G}$, set

$$\langle\!\langle \gamma, \delta \rangle\!\rangle = \langle S(\gamma), I(\delta) \rangle \,.$$

Recall the double bracket for usual diagrams from Remark 3.2.16:

$$\langle\!\langle \mathcal{A}, G \rangle\!\rangle = \langle S(\mathcal{A}), I(G) \rangle \,.$$

Lemma 3.3.21. *The value of the bracket $\langle\!\langle \gamma, \delta \rangle\!\rangle$ only depends on the class of γ in $\Gamma^1(\mathfrak{A})$.*

This is a consequence of a deeper fact: let $\gamma = (A^-, \Delta, A^+)$ denote an arrow germ. Assigning writhe decorations to the arrows as usual with a map $\sigma : \{1, \dots, |\Delta|\} \to \{\pm 1\}$, consistently for all three diagrams, one obtains a *formal full germ* γ^σ, which may or may not actually be an R_3 move. It happens that the triangle relations detect that:

Lemma 3.3.22. *With the above notations, γ^σ is an R_3-move if and only if for every triangle relator ∇,*

$$\langle\langle \nabla, \gamma^\sigma \rangle\rangle = 0.$$

Proof. The terms in the sum $I(\gamma^\sigma)$ that contain a full triangle can be forgotten, they clearly do not take part in the computation. The remaining terms can be grouped by triples, in which any two partial germs differ only by the arrow that they miss from the triangle (see an example on Fig. 3.14).

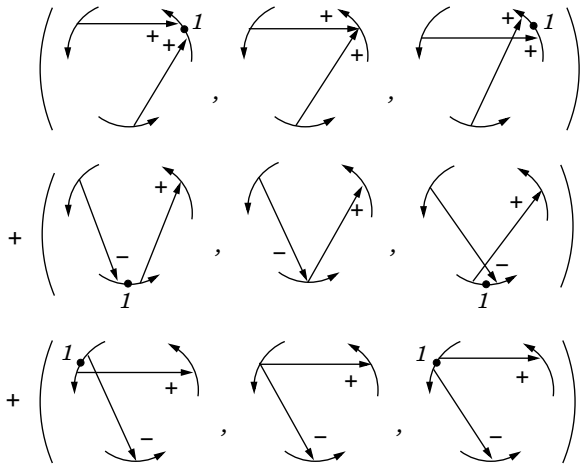

Figure 3.14: One possible triple in the sum $I(\gamma)$

Pick such a triple, say λ. First we diminish the number of terms in $\langle S(\nabla), \lambda \rangle$ by using a forgetful projection T that keeps track of the product of the signs that it forgets – it works exactly as in Proposition 3.2.14. Now in $\langle \nabla, T(\lambda) \rangle$, there are $3 * 3 = 9$ terms, and it is easy to see that either they are all zero, or two of them are non zero. Moreover, in the last case, one of these two must involve the partial germ of ∇ whose degenerate diagram is not monotonic (the one at the left (top)-hand side in the example of Fig. 3.13). The other one depends on the type of the triangle in γ (see Fig. 3.12). In any case, the crucial reason for these two to cancel is that

1. The map T has put in front of each diagram the product of the signs it has forgotten – the product of the signs of the unseen arrows on Fig. 3.14 is the same for both diagrams, so we may divide and keep only the product of the two present arrows.

2. The ε sign of each partial germ from Fig. 3.13 is equal to $+1$.

Thus $\langle \nabla, T(\lambda) \rangle$ is zero if and only if computing ε times the product of signs of the visible arrows gives the same result for both relevant diagrams in λ, which is precisely a consequence of the fact that λ comes from an R_3 move (Lemma 2.1.4). This proves the "only if" part.

For the converse, pick a ∇ relation of degree two (*i.e.* without unseen arrows in Fig. 3.13). Then the only relevant terms in the sum $I(\gamma)$ are those obtained by forgetting all arrows but two from the triangle. There are only three such partial germs. The computation is the same as before, and the assumption that the bracket is zero allows one to apply Lemma 2.1.4 the other way, and conclude.

□

Theorem 3.3.23 (Stokes Formula)**.** *For all* $\mathcal{A} \in \widehat{\mathfrak{A}}$ *and* $\gamma \in \Gamma_\Delta \mathfrak{G}$*,*

$$\langle\langle d^0\mathcal{A}, \gamma\rangle\rangle = \langle\langle \mathcal{A}, \partial\gamma\rangle\rangle.$$

Remark 3.3.24. Note that this gives a new proof to point 4. of Theorem 3.3.17, that is independent from Subsection 3.3.2 and the knowledge of the Polyak algebra. Informally, it can be stated as: $d^0(\mathcal{A})$ contains (is) the information of how the function $\langle\langle \mathcal{A}, \cdot\rangle\rangle$ changes under all possible R_3 moves.

Remark 3.3.25. It is likely that one can define a combinatorial encoding of codimension 2 strata in the space of virtual knot diagrams (hence a notion of 1-cocycles), and with the same ideas as in this subsection find a map d^1 whose kernel is the subspace of elements $x \in \widehat{\Gamma^1\mathfrak{A}}$ for whom $\langle\langle x, \cdot\rangle\rangle$ is a 1-cocycle. If one can do that, then by the Stokes formula $d^1 \circ d^0$ will automatically be zero. This speaks largely in favor of our definitions.

Proof. By bilinearity it is enough to prove the formula for an arrow diagram A and a germ γ. Choose a map σ that adds a sign to each arrow of A, and (consistently) to each arrow in each diagram in the sum d^0A – for this consistency to make sense, we use the initial definition of d^0A as a representative modulo the triangle relations.

If $\tilde{\gamma} = (\tilde{\gamma}^-, \tilde{\gamma}^\Lambda, \tilde{\gamma}^+)$ is a partial subgerm of γ, then:

$$\left\langle \left(d^0A\right)^\sigma, \tilde{\gamma} \right\rangle = \left\langle \left(d^\Lambda A\right)^\sigma, \tilde{\gamma} \right\rangle = \left\langle A^\sigma, \tilde{\gamma}^+ - \tilde{\gamma}^- \right\rangle. \tag{3.13}$$

Indeed, the first equality is obvious, and as for the second,

1. If A^σ is different from both $\tilde{\gamma}^+$ and $\tilde{\gamma}^-$, then both sides of the equality are zero.
2. Otherwise, $\langle (d^\Lambda A)^\sigma, \tilde{\gamma}\rangle$ counts the unit-marked edges of A^σ that, when shrunk to a point, turn A^σ into $\tilde{\gamma}^\Lambda$. There are exactly $|\mathrm{Aut}\,(A^\sigma)|$ of them, and each counts for $+1$ (*resp.* -1) if $A^\sigma = \gamma^+$ (*resp.* $A^\sigma = \gamma^-$).

The equality follows then from the definition of the bracket:

$$\left\langle A^\sigma, \tilde{\gamma}^+ - \tilde{\gamma}^- \right\rangle = |\mathrm{Aut}\,(A^\sigma)| \left(A^\sigma, \tilde{\gamma}^+ - \tilde{\gamma}^-\right).$$

Similarly, if $\tilde{\gamma} = \left(\tilde{\gamma}^-, \tilde{\gamma}^\Delta, \tilde{\gamma}^+\right)$ is a full subgerm of γ, then:

$$\left\langle \left(d^0A\right)^\sigma, \tilde{\gamma} \right\rangle = \left\langle \left(d^\Delta A\right)^\sigma, \tilde{\gamma} \right\rangle = \left\langle A^\sigma, \tilde{\gamma}^+ - \tilde{\gamma}^- \right\rangle. \tag{3.14}$$

Finally, notice that if G is a subdiagram of γ^+ in which less than two arrows are involved in the R_3 move, then G is a subdiagram of γ^- as well and the contribution of these to $\langle A, \partial\gamma\rangle$ is 0. By definition of a subgerm, one never erases more than

one arrow from the triangle, so these diagrams do not contribute either on the left-hand-side.

It follows that the Stokes formula is the sum of the equations (3.13) and (3.14) (with both sides multiplied by sign(σ)) over all possible choices of σ and $\tilde{\gamma}$.

□

3.4 Examples and applications

3.4.1 Grishanov-Vassiliev's planar chain invariants

In [15], S.A.Grishanov and V.A.Vassiliev define an infinite family of arrow diagram formulas for real knots in $\Sigma \times \mathbb{R}$, for an arbitrary orientable surface Σ. We repeat their construction and generalize their result to the present settings. Recall that $h_1(\Sigma)$ denotes the set of conjugacy classes in $\pi_1(\Sigma)$.

Definition 3.4.1. A *naked arrow diagram* is an arrow diagram with every decoration forgotten except for the local orientations. It is called *planar* if no two of its arrows intersect – thus one may regard it as a part of the plane, up to isotopy.

A *chain presentation* of such a diagram with n arrows is a way to number its $n+1$ bounded complementary components in the plane from 1 to $n+1$, in such a way that the numbering increases when one goes from the left to the right of an arrow.

Let U_n be the sum of all planar isotopy equivalence classes of chain presentations of naked arrow diagrams with n arrows. U_n is called the *universal degree n planar chain* ([15], Definition 1).

Definition 3.4.2. An *h_1-decorated planar diagram* is the result of assigning an element of $h_1(\Sigma) \setminus \{1\}$ to each region in a planar naked arrow diagram.

We consider two ways to construct such diagrams:

1. From the datum of a chain presentation together with a system $\Gamma = \{\gamma_1, \ldots, \gamma_{n+1}\}$ – which yields the notion of Γ-decorated diagrams.
2. From a planar arrow diagram on $\pi = \pi_1(\Sigma)$: each region of the diagram receives the conjugacy class of the product of the π-markings at its boundary, in the order induced by the orientation of the circle (the product is not well-defined, but its conjugacy class is).

Call Φ_Γ the sum obtained by decorating every diagram in U_n with a fixed system Γ ([15], Definition 2). Note that some of the summands in U_n – namely those with non trivial symmetries – may lead to the same decorated diagram if some of the γ_i's are equal; unlike Grishanov-Vassiliev, we do not forbid that. Of course these summands happen with coefficients greater than 1 in Φ_Γ.

To understand Φ_Γ as an arrow diagram series, we apply the machinery of symmetry-preserving maps from Subsection 3.2.2. Even though it is absent from the notations, all considered diagrams are planar:

→ $\mathfrak{A}^\Gamma$ is the $\mathbb{Q}$-space generated by Γ-decorated planar diagrams (hence of degree n).

- $\mathfrak{A}^{\rightsquigarrow\Gamma}$ is the subspace of $\mathfrak{A}_n$ generated by planar arrow diagrams on $\pi_1(\Sigma)$ *that induce* Γ*-decorated diagrams.*
- $\mathfrak{A}_n^{1,2,\cdots}$ is the $\mathbb{Q}$-space generated by all chain presentations of planar naked arrow diagrams of degree n.

Note that $\mathfrak{A}_n^{1,2,\cdots}$ is not defined by an equivalence relation on rigid Gauss diagrams on $\pi_1(\Sigma)$. The father of all types of Gauss diagrams here is the type of planar Gauss diagrams on $\pi_1(\Sigma)$ endowed with a chain presentation, such that the chain presentation and the π-markings induce the same h_1-decorated diagram – it is the pullback of Diagram (3.15) below.

Let us denote by S_Γ^a the symmetry-preserving map $\widehat{\mathfrak{A}^\Gamma} \hookrightarrow \widehat{\mathfrak{A}_n}$, and set

$$\widetilde{\Phi}_\Gamma = \mathrm{S}_\Gamma^a(\Phi_\Gamma).$$

Theorem 3.4.3. *For any system of non-trivial conjugacy classes* $\Gamma = (\gamma_1, \ldots, \gamma_{n+1})$, $\widetilde{\Phi}_\Gamma$ *defines an arrow diagram formula for virtual knots.*

This improves Theorem 1 of [15], since we remove the assumption that Γ is unambiguous (*i.e.* any of the γ_i's may coincide) and show that $\widetilde{\Phi}_\Gamma$ is an invariant for virtual knots. The reason why $\widetilde{\Phi}_\Gamma$ coincides *as an invariant* with Grishanov-Vassiliev's Φ_Γ is Point 2 of Proposition 3.2.10.

Proof. 1. First, notice that an equivalence class of arrow diagrams under AW-moves determines an h_1-decorated diagram. Thus the map S_Γ^a factorizes through S_{aw}^a (by point 1. of Proposition 3.2.10), wherefrom Proposition 3.3.4 implies that $\widetilde{\Phi}_\Gamma$ defines an invariant under w-moves.

2. The fact that no γ_i may be trivial gives immediately the condition of R_1 and R_2 invariance from Proposition 3.3.5.

3. For R_3, the more convenient here is to check condition 3 of Theorem 3.3.9. In any *A6T* relation, only three diagrams possibly have pairwise non intersecting arrows, and either all three of them do, either no one does. This yields two kinds of reduced relations. Let us consider only that on Fig.3.15 (ignore the markings i, j, k for now), the other case is completely similar. Write the relator of the picture as $A_1 - A_2 - A_3$ in the order of reading. One has to prove that

$$\left\langle \widetilde{\Phi}_\Gamma, A_1 \right\rangle = \left\langle \widetilde{\Phi}_\Gamma, A_2 \right\rangle + \left\langle \widetilde{\Phi}_\Gamma, A_3 \right\rangle.$$

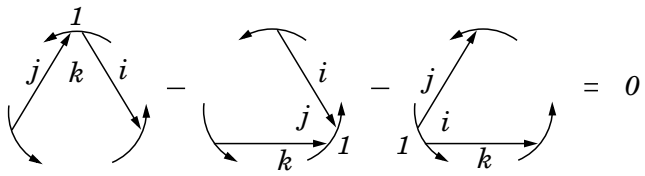

Figure 3.15: One of the two reduced 6-term relations for planar diagrams

The three spaces defined previously fit into the diagram

$$\begin{array}{ccccc} \mathfrak{A}^{\rightsquigarrow\Gamma} & & & & \mathfrak{A}_n^{1,2,\cdots} \\ & \searrow^{\mathrm{T}_\Gamma^a} & & \swarrow_{\mathrm{T}_\Gamma^{1,2,\cdots}} & \\ & & \mathfrak{A}^\Gamma & & \end{array} \quad . \tag{3.15}$$

Pick a planar arrow diagram A of degree n, and consider the set $\mathrm{Dec}(A)$ of all rigid representatives of all preimages of $\mathrm{T}^a_\Gamma(A)$ under the map $\mathrm{T}^{1,2,\cdots}_\Gamma$. By Definition 3.2.8, the cardinality of that set is the sum of all coefficients of $\mathrm{S}^{1,2,\cdots}_\Gamma(\mathrm{T}^a_\Gamma(A))$, which means, since the sum of all generators of $\mathfrak{A}^{1,2,\cdots}_n$ is U_n:

$$\sharp\,\mathrm{Dec}(A) = \left(U_n, \mathrm{S}^{1,2,\cdots}_\Gamma(\mathrm{T}^a_\Gamma(A))\right).$$

But no diagram decorated with a chain presentation admits non-trivial symmetries, whence, by successive applications of Proposition 3.2.10 2.,

$$\begin{aligned}\sharp\,\mathrm{Dec}(A) &= \left\langle U_n, \mathrm{S}^{1,2,\cdots}_\Gamma(\mathrm{T}^a_\Gamma(A))\right\rangle \\ &= \langle \Phi_\Gamma, \mathrm{T}^a_\Gamma(A)\rangle \\ &= \left\langle \widetilde{\Phi}_\Gamma, A\right\rangle.\end{aligned}$$

Now it remains to see that

$$\sharp\,\mathrm{Dec}(A_1) = \sharp\,\mathrm{Dec}(A_2) + \sharp\,\mathrm{Dec}(A_3).$$

Look at Fig.3.15 again, now considering the markings i, j, k. Each element of $\mathrm{Dec}(A_1)$ determines either an element of $\mathrm{Dec}(A_2)$, or an element of $\mathrm{Dec}(A_3)$, as indicated by the picture, depending on whether $i < j$ or $i > j$. This separates $\mathrm{Dec}(A_1)$ into two parts, respectively in bijection with $\mathrm{Dec}(A_2)$ and $\mathrm{Dec}(A_3)$, and terminates the proof.

□

3.4.2 There is a Whitney index for non nullhomotopic virtual knots

In the classical framework, the Whitney index is an invariant of regular plane curve homotopies which, together with the total writhe number, classifies the representatives of any given knot type up to regular isotopy. In other words, these invariants count the (algebraic) number of Reidemeister I moves that *have to* happen in a sequence of moves connecting two given diagrams. Here we describe such an invariant for *virtual* knot diagrams that are not homotopically trivial.

The classical Whitney index

Let $\delta : \mathbb{S}^1 \to \mathbb{R}^2$ be a smooth immersion (with non-vanishing differential). There is an associated Gauss map

$$\begin{array}{rccc}\Gamma: & \mathbb{S}^1 & \to & \mathbb{S}^1 \\ & p & \mapsto & u_p(\delta)\end{array},$$

where $u_p(\delta)$ is the unitary tangent vector to δ at the point p. It depends on a trivialization of the tangent space to $\mathbb{R}^2$.

Definition 3.4.4 (usual Whitney index)**.** The index of the above Gauss map only depends on the homotopy class of δ within the space of smooth immersions. It is called the *rotation number*, or *Whitney index*, of δ.

Given a projection $\mathbb{R}^3 \to \mathbb{R}^2$, a generic isotopy of a knot $\mathbb{S}^1 \to \mathbb{R}^3$ is called a *regular isotopy* if the corresponding sequence of Reidemeister moves does not involve R-I. Clearly, the Whitney index of planar loops induces an invariant of regular isotopy classes of knots. In practice, it can be easily computed by looking at the Seifert circles of the projection (each of them contributes by $+1$ or -1). The total writhe number of a classical knot projection is also an invariant of regular isotopy. These two invariants together satisfy the following

Lemma 3.4.5 (see [18])**.** *Two equivalent knot diagrams are regularly equivalent if and only if their projections have the same total writhe and the same Whitney index.*

Proof. There are four types of real Reidemeister I creating moves (and as many deleting ones), which can be sorted according to the change that they induce on the Whitney index and the total writhe of a diagram (see Fig.3.16). Two R-I moves of a given type (Fig.3.16) performed on a given knot diagram always produce regularly equivalent diagrams. Indeed, one can slide a loop all along the knot without using R-I moves. Moreover, the knot diagram version of the *Whitney trick* (see [18]) gives sequences of R-II and R-III moves that allow one to

- → Replace a couple of R-I births (or deaths) that together induce no writhe or Whitney index changes.
- → Replace an R-I birth (*resp.* death) with a death (*resp.* birth).

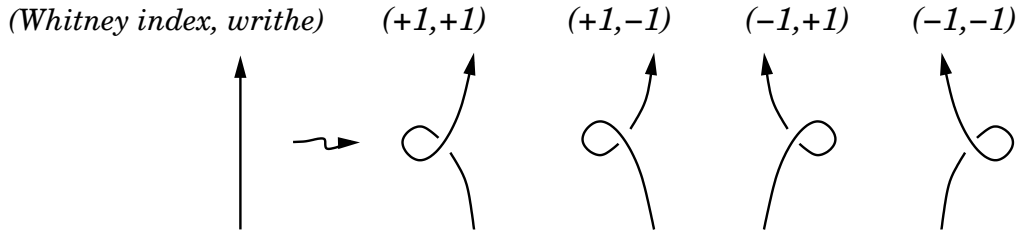

Figure 3.16: R-I moves sorted by their effect on the regular invariants

Now pick a sequence of Reidemeister moves connecting two diagrams that have the same regular invariants. Turn every R-I death into an R-I birth, and then make all R-I births of the sequence happen before every other move. When an R-I birth was meant to happen, just slide the little loop that was created at the beginning all along the knot, up to the right place. Finally, since all the R-I moves now at the beginning of the sequence imply no changes of regular invariants, it means that they can be replaced with R-II and R-III moves using the Whitney trick. □

The virtual framework

We want to define a Whitney index for virtual knots, that satisfies a version of Lemma 3.4.5.

Given the virtual Reidemeister I moves, it does not seem reasonable to hope for counting the degree of a Gauss map. Relatedly, the Seifert circles are not embedded any more, and they do not have a well-defined contribution (at least not in the previous sense). Even when one looks only at real knot diagrams, the Whitney index is no more invariant when virtual moves are allowed: see Fig.3.17. In other

words, though virtual moves do not connect knot diagrams that are not isotopic in the usual sense, they do add bridges between different regular isotopy classes.

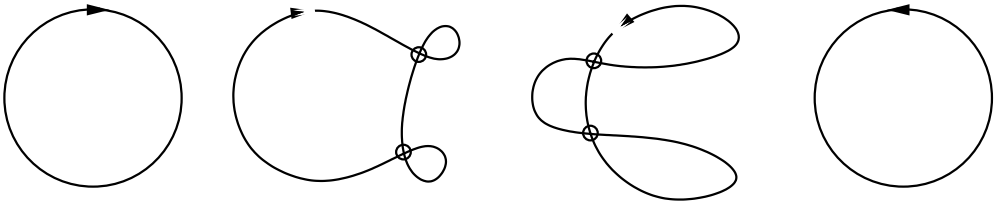

Figure 3.17: A "regular" sequence that changes the Whitney index

From now on, let Σ be an orientable surface with non trivial fundamental group.

Definition 3.4.6. Two virtual knot diagrams in Σ are called *regularly equivalent* if they are connected by a sequence of moves that does not involve the *real* Reidemeister I move.

In [17], regular equivalence is defined as equivalence under all moves but the real R-I *and* the virtual R-I too. Here, our goal is to define maps on the set of Gauss diagrams, so implicitly they must be invariant under all detour moves anyway.

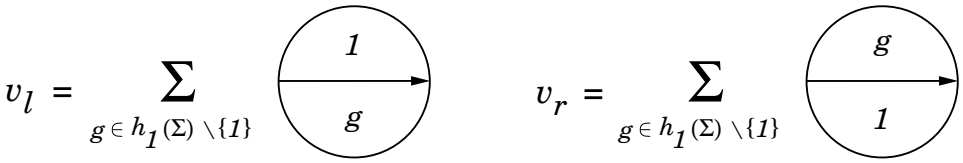

Figure 3.18: The regular invariants for non nullhomotopic virtual knots

Lemma 3.4.7. *The h_1-decorated diagram series v_l and v_r from Fig.3.18 define invariants of regular equivalence. Moreover, two virtual knot diagrams from the same knot type with non trivial homotopy class are regularly equivalent as soon as both v_l and v_r coincide on them.*

Proof. First assertion. First, notice that since Σ is orientable, $w = w_1(T\Sigma)$ is trivial and the w-moves never change the orientation of an arrow. Hence a w-orbit of planar Gauss diagrams on $\pi_1(\Sigma)$ determines an $h_1(\Sigma)$-decorated diagram (see Definition 3.4.2). In restriction to the diagrams that happen in v_l and v_r, this forgetful map is actually a $1-1$ correspondence. Hence v_l and v_r can be regarded as series of w-orbits of Gauss diagrams, so that they satisfy the w invariance criterion (Proposition 3.3.4). The invariance under R_2 and R_3 moves is clear from the criteria given in Subsection 3.3.2.

Second assertion. The proof is essentially the same as that of Lemma 3.4.5. A little loop can run along a knot diagram without using R-I moves even where there are virtual crossings. The table from Fig.3.16 becomes, respectively (for the couple (v_l, v_r)):

$$(0,+1) \quad (-1,0) \quad (+1,0) \quad (0,-1).$$

This is the essential reason for which one needs the assumption that the knot diagrams are not nullhomotopic: otherwise the increase would be $(0,0)$ for all R-I moves. □

Finally, looking at the above table, which details *how* v_l and v_r control the R-I moves, it appears that:

1. $v_r + v_l$ behaves like the total writhe number under Reidemeister moves: it has the same "derivative". It follows that these differ by a constant that depends only on the virtual knot type, *i.e.* a virtual knot invariant in the usual sense (see Fig.3.19).

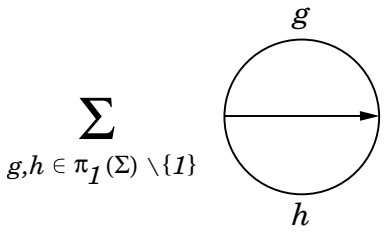

Figure 3.19: The difference between $v_r + v_l$ and the (usual) total writhe number

2. *In restriction to real knot diagrams,* $v_r - v_l$ has the same derivative as the Whitney index, with respect to Reidemeister moves. Hence there is an invariant of real knots c such that for every real knot diagram D, $v_r(D) - v_l(D) + c(D)$ is the usual Whitney index of D.

Question. Does c extend into a virtual knot invariant?
If it is true that real knot theory faithfully embeds into virtual knot theory (as it does when $\Sigma = \mathbb{R}^2$ by Kauffman's theorem [17]), then the answer to the above question is yes.

Definition-Lemma 3.4.8. *Call* $v_r - v_l$ *the* Whitney index *of non nullhomotopic virtual knot diagrams, and call* $v_r + v_l$ *their* writhe number*. These make Lemma 3.4.5 hold for non nullhomotopic virtual knot diagrams.*

Proof. It follows immediately from Lemma 3.4.7 and the above remarks. □

3.4.3 Some more computations

In practice, Theorem 3.3.13 gives a very easy means of checking that an arrow diagram series defines a virtual invariant. On another hand, finding virtual invariants when one has no clue of a potential formula demands to solve the system of equations $A6T$.

We wrote a program to do this for abelian Gauss diagrams, looking for invariants that vanish on all closed braids, and only a few results came, namely the Grishanov-Vassiliev's planar chain invariants, and the following:

Theorem 3.4.9. *Let* π *be an abelian group and let* a, K *be two elements in* π*, with* $a \neq 0$*. Then the sum* I_5 *of Fig.3.20, where the global markings of all five diagrams is* K*, is an arrow diagram formula for virtual knots on* (π, w_0)*.*

This seems to give a positive answer to T. Fiedler's question about the existence of N-invariants not contained in those from [10], Proposition 2.

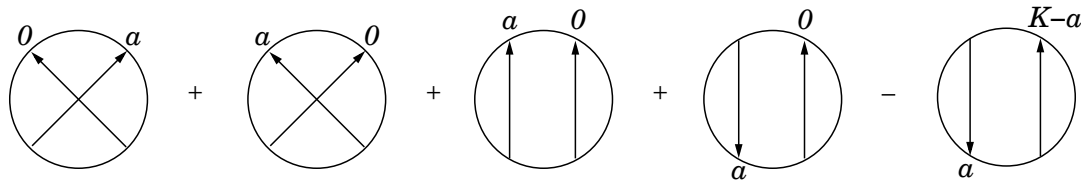

Figure 3.20: An invariant of finite length for virtual knots with global marking K – when $\pi = \mathbb{Z}$, it vanishes on closed braid diagrams in the annulus.

On the other hand, the sparse landscape of results leads to think that most arrow diagram invariants might have infinite algebraic length – which makes them difficult to find.

Notice that in case $a = K$, the formula has only 3 terms – but still defines an invariant. Let us compute it for the family of knots $\mathcal{K}_{2i+1}$ whose first terms are drawn in Fig.3.21. These knot diagrams are drawn in the annulus, whence $\pi = \pi_1(\mathbb{R} \times \mathbb{S}^1) \simeq \mathbb{Z}$. Here a and K are both set equal to 1.

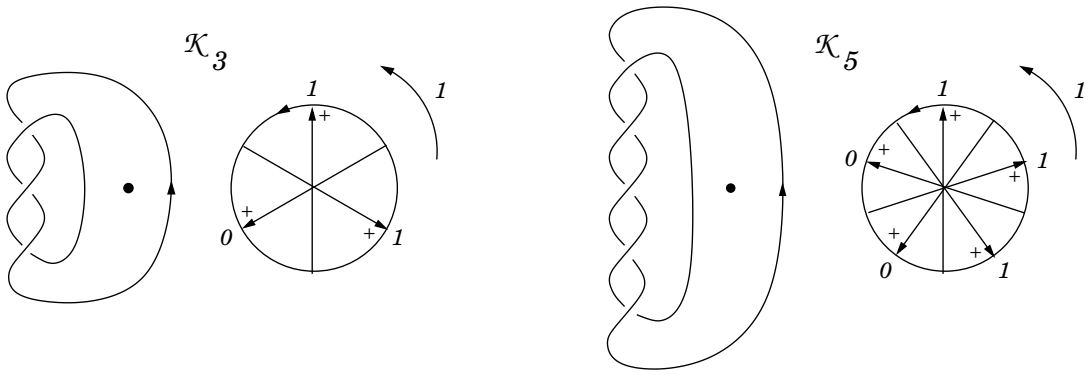

Figure 3.21: $\mathcal{K}_3$ and $\mathcal{K}_5$

No two arrows in the Gauss diagram of $\mathcal{K}_{2i+1}$ are parallel, so that only the first two arrow diagrams of Fig.3.4.9 are relevant. Any of the i arrows with $\mathbb{Z}$-marking 0 intersects every one of the $i + 1$ arrows marked with 1. Hence

$$I_5(\mathcal{K}_{2i+1}) = i(i + 1).$$

On the other hand, Vassiliev-Grishanov's invariants all vanish on these knots.

Chapter 4

Towards detection of closed braids

There are currently no known algorithms to decide whether a given (real) knot diagram in $\mathbb{R}\times\mathbb{S}^1$ is equivalent modulo Reidemeister moves to a *closed braid* diagram, *i.e.* a diagram on which the projection $\mathbb{R} \times \mathbb{S}^1 \to \mathbb{S}^1$ induces a covering map ([16], Section 2.2 and following). The question still makes sense in the virtual framework, and it is still non trivial. It is not known either whether a real knot that is equivalent to a virtual closed braid is always equivalent to a real closed braid.

In [10], T. Fiedler suggests an attempt to answer the first question by finding finite type invariants presented by Gauss diagram formulas that vanish on every closed braid. He conjectures that finite type invariants separate closed braids (which he calls *global knots*) from non global knots.

Here we attempt to detect closed braids by studying the set of loops respecting the orientation in a diagram, especially their homology classes in $H_1(\mathbb{R} \times \mathbb{S}^1)$. It produces a systematic way to detect diagrams that are in a closed braid position (Theorem 4.2.2, see Subsection 2.3.3). We conjecture that for knot diagrams with a minimal number of real crossings, not being in a closed braid position implies not being a closed braid at all (up to Reidemeister moves).

The last part is a draft study towards that conjecture, trying to understand how the above set of loops behaves under Reidemeister moves.

4.1 Tangles and T-diagrams

Looking at the construction of Gauss diagrams on a group π, one could wonder if it makes sense, from the topological viewpoint, to consider a particular presentation of π, and decorate the edges of Gauss diagrams with words in this presentation. The answer is yes, at least when the surface is obtained from a (maybe punctured) disc by some identifications on the boundary. In that case one can regard the "word-decorated" version as coming from a Gauss diagram theory for tangles. We only investigate the case of the annulus $\mathbb{R} \times \mathbb{S}^1$.

Definition 4.1.1. A *T-diagram* (on $\mathbb{Z}$) is a classical Gauss diagram with a finite number of points on its circle *marked* with $\oplus$ or $\ominus$. A T-diagram determines a Gauss diagram (on $\mathbb{Z}$), by decorating each edge with the sum of all markings it contains.

There are R-moves defined as usual (Definition 2.1.4), except that the edges on the local Reidemeister pictures shall not contain any markings. There are the usual "conjugacy moves" (Definition 2.3.1, where here w is the trivial homomorphism since the annulus is orientable), and finally there are "word moves", replacing a word with another according to a relation from the group presentation (here $\mathbb{Z}$) – see Fig. 4.1.

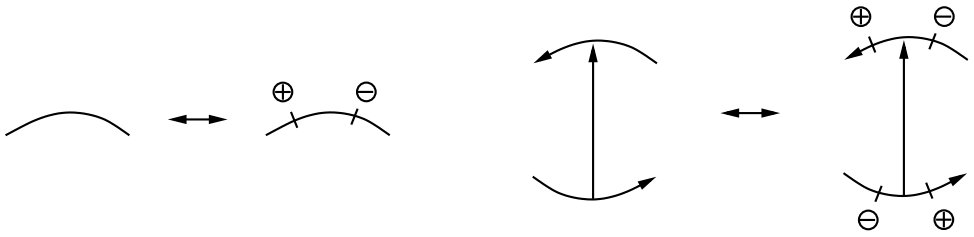

Figure 4.1: Examples of word and conjugacy moves – the orientation of an arrow never changes here.

Since the annulus is orientable with an abelian fundamental group, it also enjoys an Abelian Gauss diagram theory (see Subsection 2.3.2). Recall that a Gauss diagram determines a unique abelian diagram. A T-diagram whose underlying abelian diagram is G is called a *refinement* of G.

Definition 4.1.2. A *(virtual) tangle diagram* is an oriented uni- and tetra-valent graph embedded in $\mathbb{R} \times [0,1]$, such that each tetravalent vertex has been decorated as a real or virtual crossing, and such that the graph intersects $\mathbb{R} \times \{0,1\}$ exactly at the univalent vertices, one at each (i,j), $i = 1,\ldots,n$ and $j = 0,1$. Under the identification of $\mathbb{R} \times \{0\}$ with $\mathbb{R} \times \{1\}$, such a diagram becomes a link diagram in $\mathbb{R} \times \mathbb{S}^1$, and throughout this thesis we will always assume that *our tangles close into knots*.

Remark 4.1.3. This definition is equivalent to virtual knot diagrams in $\mathbb{R} \times \mathbb{S}^1$ that are transverse to some specified section $S = \mathbb{R} \times \{t\}$. We will refer to either point of view without distinction.

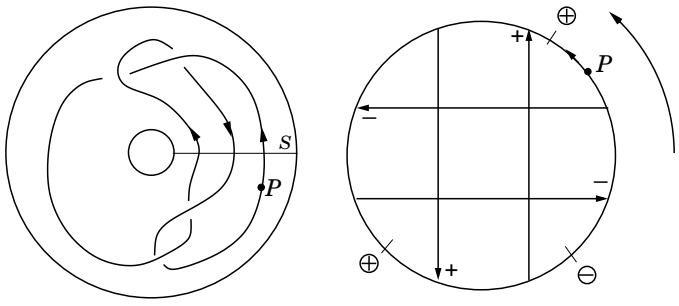

Figure 4.2: Associating a T-diagram with a knot and a section – P is here only for the sake of clarity.

It is straightforward to see that a tangle diagram determines a T-diagram, using algebraic intersection indices between the section and the knot as markings (see

Fig.4.2). Using the same kind of arguments as in the proof of Theorem 2.3.3, it is possible to prove

Theorem 4.1.4. *Every T-diagram is represented by a virtual tangle, which is unique up to diagram isotopy, detour moves and conjugacy by totally virtual braids. Moreover, two braids define the same virtual knot type in the annulus if and only if their T-diagrams are equivalent under* R *moves, word moves and conjugacy moves.*

4.1.1 T-diagrams of real knots

This is a parenthesis to show that unlike the Gauss diagram theories from Chapter 1, which are mostly useful for describing virtual knots, T-diagrams are also an effective tool for the study of real knots, because they stay closer to topology. We prove that a real knot diagram in the annulus is determined by its abelian Gauss diagram up to *mere diagram isotopy*, as soon as it cannot be isotoped into a little disc. This case one needs to avoid amounts to the classical theory, where such a result holds for diagrams in the sphere but not in the disc: one needs "arc slides over infinity" to be considered as diagram isotopies.

Definition 4.1.5. Say that a real knot diagram in the annulus is *full* if its complementary has two unbounded components – or, equivalently, if it can not be isotoped so as to be contained in a disc (by a *diagram* isotopy).

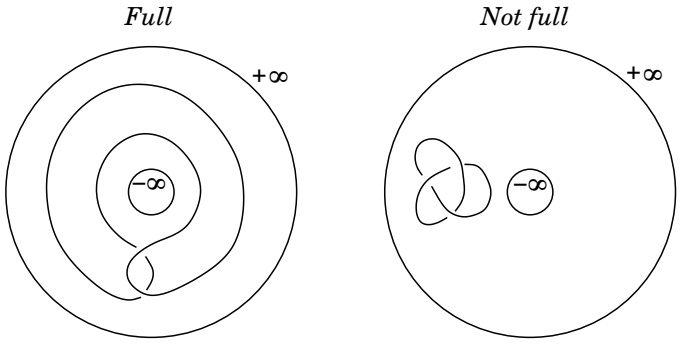

Figure 4.3: Fullness is not defined up to Reidemeister moves

Let D be a full diagram. Then its complementary in $\mathbb{R} \times \mathbb{S}^1$ has two connected components with the homotopy type of a circle, each of which is bounded by a simple loop in D with homology class 1, and every other component is homeomorphic to an open disc – bounded by a simple loop in D with homology class 0.

Definition 4.1.6. In a full knot diagram, the two loops with homology class 1 described above are called the *leftmost* and *rightmost* loops, according to whether they bound the $-\infty$ or $+\infty$ end of $\mathbb{R}\times\mathbb{S}^1 \setminus D$. The boundaries of the disc components are called the *internal loops* of D.

Lemma 4.1.7. *A real knot diagram is full if and only if its abelian Gauss diagram has at least one non trivial $\mathbb{Z}$-marking.*

Proof. Recall that the $\mathbb{Z}$-markings of an abelian Gauss diagram G are the images of a basis of $H_1(G)$ into $\mathbb{Z} \simeq H_1(\mathbb{R} \times \mathbb{S}^1)$. If D is not full then clearly every loop in its Gauss diagram has marking 0. Conversely, if D is full, then its leftmost loop has marking 1. Since by assumption D is real, this loop actually corresponds to a loop in G, because the two branches of any crossing are actually connected by an arrow. Since some loop has a nontrivial image, any basis must contain an element with a nontrivial image. □

Lemma 4.1.8. *Let D be a real knot diagram, and T a T-diagram whose underlying abelian Gauss diagram is that of D. Then there is a diagram T' obtained from T by removing some markings, a knot diagram D' isotopic to D and a section $S = \mathbb{R} \times \{t\}$, such that T' is the T-diagram of (D', S).*

Note that removing markings may be actually necessary – see Fig.4.4.

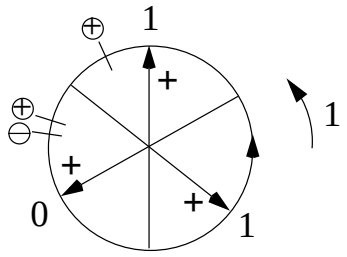

Figure 4.4: A non real refinement of a real abelian Gauss diagram

Proof. If D is isotopic to a knot diagram D' contained in a little disc, then put $T' = T$ with all the markings removed, and choose a section S that avoids D'.

Now assume that D is full. Draw the markings of T on D, then replace each of them by a little arrow transverse to the knot diagram, that indicates the way a section should locally behave so as to give the marking (step *a)* on Fig.4.5). We construct a path joining the two ends of $\mathbb{R} \times \mathbb{S}^1$, without self-intersection (so that some diagram isotopy can make it into a section $\mathbb{R} \times \{t\}$), and meeting D only at the places and with directions indicated by the arrows (T' being obtained by removing all the markings left away from that path).

Start drawing such a path γ from the end corresponding to $-\infty$. Recall that the sum of the markings met by a loop in T is equal to its $\mathbb{Z}$-marking in the underlying abelian diagram. Hence, since the leftmost loop of D has homology class 1, there is at least one little arrow indicating a "way to leave" the component, and as soon as we have left it, there will be as many ways to come back as to leave again.

Note. Here is the crucial point for D to be real: if it were not, then the boundary of its complementary components would be loops in D, but not in T, so that one would have no control on the markings they contain.

The internal loops have homology class 0, so that each time γ enters a component that is not the $+\infty$ end, the fact that it could come implies that there is necessarily a way to leave. So we are sure of eventually reaching $+\infty$ (step *b)* on Fig.4.5). Finally, if γ ever crosses itself, just forget what happened between the two times it were at that point (step *c)* on Fig.4.5). □

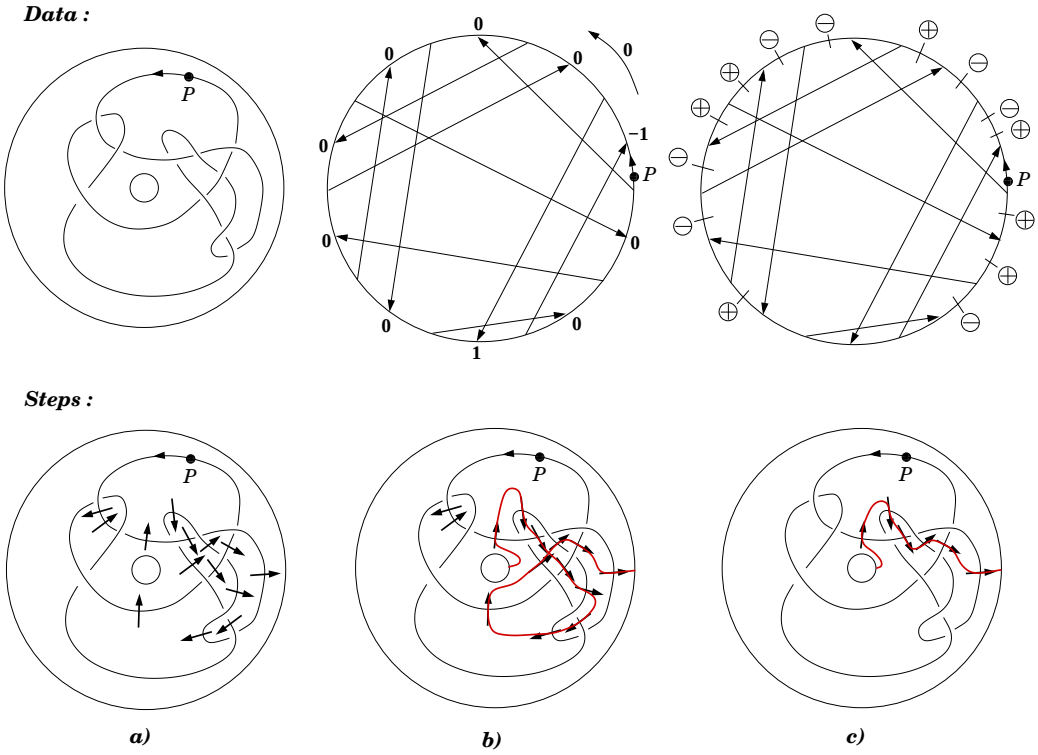

Figure 4.5: Steps of the proof of Lemma 4.1.8

Theorem 4.1.9. *Two full knot diagrams with the same abelian Gauss diagram are isotopic to each other.*

Proof. Let T be a refinement of the common abelian Gauss diagram G, with *minimal* number of markings – notice that this number must be positive by Lemma 4.1.7. Then by Lemma 4.1.8 both knot diagrams can be written as the closure of a tangle with T-diagram T. So all one needs to prove is that there is only one way to draw a real tangle diagram representing T under the previous conditions.

First let us show that the connected components of such a diagram are uniquely determined, so that the only possible choice left consists in their relative position in $\mathbb{R} \times [0, 1]$.

Pick a marking in T: it must correspond to the beginning of a strand. From there follow the orientation of T, collecting every piece of information and using them to draw, step by step, a neighborhood of the strand (see Fig.4.6).

▶ When one encounters the endpoint of an arrow, its direction and sign completely determine the local picture (step a).

▷ If the second endpoint of some arrow is met, it means one has to join a piece of diagram already in the picture, and there is at most one way to do it: indeed, the ends of every strand must stay in the unbounded region of the plane, so that at the end they can be glued to the boundary of $\mathbb{R} \times [0, 1]$ (step b). This point makes the crucial difference between Gauss diagram theories in $\mathbb{R}^2$ and $\mathbb{R} \times \mathbb{S}^1$.

▷ When one finally meets a marking again, it is the end of the strand and one stops here (step c).

▶ If there are any, pick an arrow that was already met at exactly one endpoint,

and start over from the other endpoint to extend the corresponding local incomplete picture (step d).

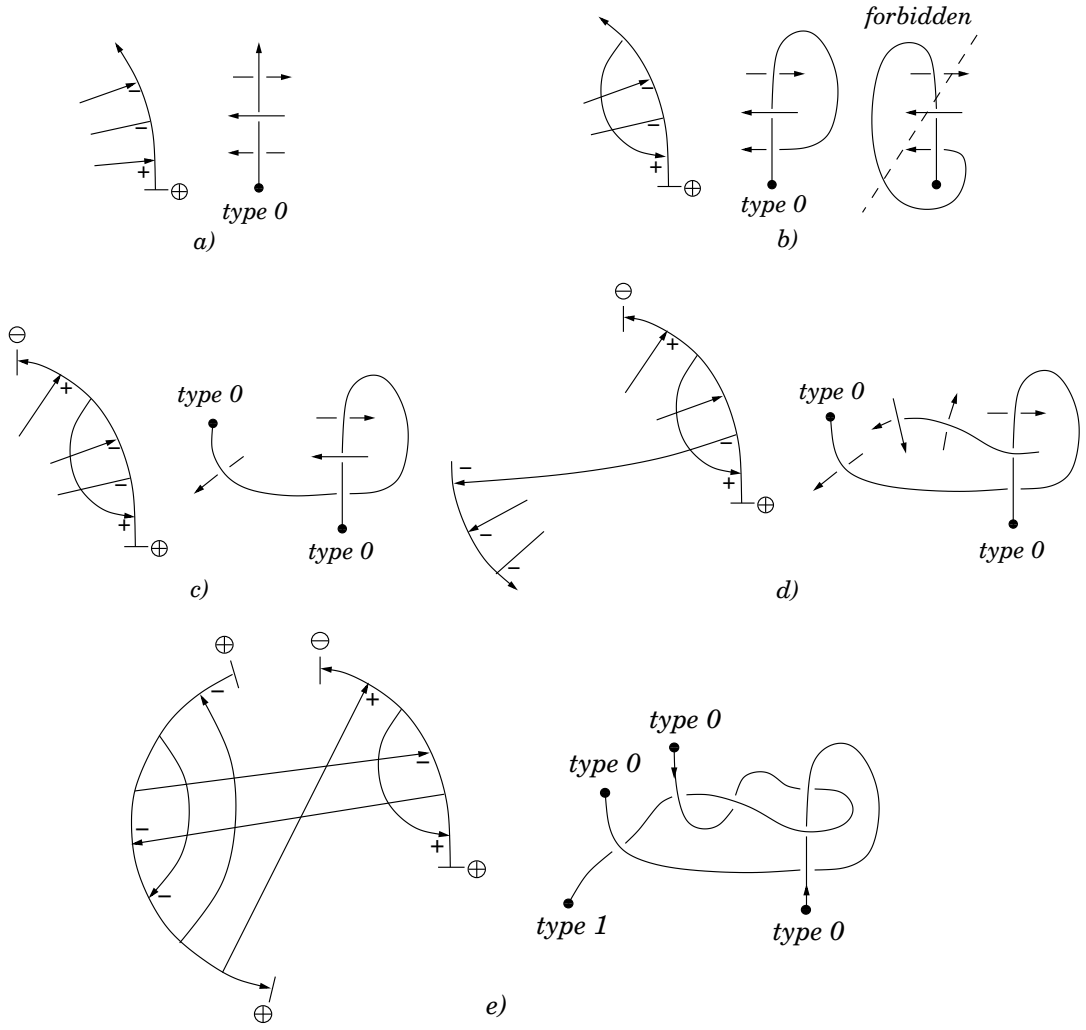

Figure 4.6: The connected components of a real tangle are uniquely determined

When this is all over, one has drawn what must be a connected component of any tangle representing T, without making any choice (step e).

Each univalent vertex of these components has a *type*, 0 or 1, according to whether it is meant to be glued to either of the two sides of $\mathbb{R} \times [0, 1]$. This side information is contained in T, through the orientation near the markings, and through their signs. Let us call *mates* two vertices that are meant to be identified when we finally close the tangle.

We claim that any of the components must contain both types of vertices. Otherwise, consider a tangle whose T-diagram is T (we know there is at least one), then S' on Fig.4.7 contradicts the minimality of T.

So our components look like bowels, as pictured in Fig.4.7, and it remains to show that one can read from T in what order they shall be.

First, the leftmost of them is uniquely determined by the property that its left "boundary path" joins two mates (it is meant to become the leftmost loop of the

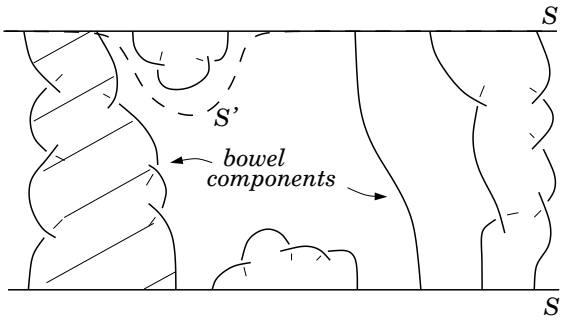

Figure 4.7: The connected components of a tangle

knot). Indeed, if there were two or more components with that property, the tangle would close into a disconnected diagram, and certainly not into a knot.

Now assume that one has been able to determine which are the k leftmost components in a unique way. Look at the bottom ends of the picture they form.

▷ Take the leftmost of them whose mate is not already in the picture: the component containing its mate is necessarily the next we should draw.

▷ If all bottom ends already have their mate, look at the upper ends and repeat the same procedure.

▷ If all upper ends also have their mate, then it means that the two rightmost ends in the picture are mates, and belong to one and the same component: this characterizes the rightmost loop of the knot, so the picture is actually complete.

□

4.2 A characterization of closed braid diagrams

In [10], T.Fiedler gives examples of arrow diagram formulas that are identically zero on closed braids – or more generally "global knots" – and the argument is that they are made of arrow diagrams that cannot be subdiagrams of a closed braid. The basic idea is that in a closed braid diagram, any nontrivial loop that respects the orientation (and sometimes turns at the crossings) must have positive homology class in $\mathbb{R} \times \mathbb{S}^1$. For example, it is shown that the configuration on Fig.4.8a may not happen in a closed braid diagram. Another proof of this fact consists in finding a refinement, as pictured on Fig.4.8b, to see that the red loop has marking 0 in $\mathbb{Z} \simeq H_1(\mathbb{R} \times \mathbb{S}^1)$ since it avoids all the markings, though it always respects the orientation of the circle. Yet another proof, the easiest in practice, is to apply one of the formulas from Subsection 2.3.3.

In this section we show that the rough idea above is actually a necessary and sufficient criterion to detect diagrams that may happen as subdiagrams of closed braids. Since deleting an arrow amounts to virtualizing a crossing, the question amouts to: which abelian Gauss diagrams represent virtual closed braids up to diagram isotopy and detour moves (see Proposition 2.3.8)?

Recall that topologically, a Gauss diagram G is a 1-dimensional complex whose oriented 1-cells are the edges and the arrows. A homology class $\gamma \in H_1(G)$ has a

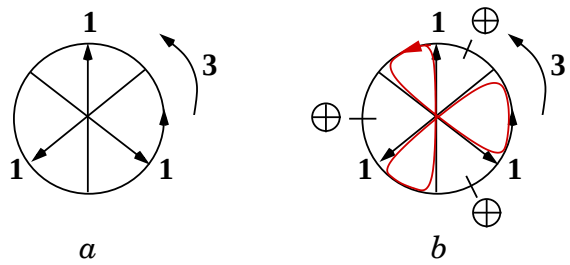

Figure 4.8: This configuration of abelian Gauss diagrams is not braid-admissible

unique set of "coordinates" along these cells. γ is called *edge-respecting* (ER) if for any edge e, the coordinate $\langle \gamma, e \rangle$ is non-negative (see Definition 2.3.20).

Definition 4.2.1. Let G be an abelian Gauss diagram on $\mathbb{Z}$. Then G is called *braid-admissible*, or simply *admissible* (*resp. weakly admissible*), if every non-trivial ER class in $H_1(G)$ has positive (*resp.* non-negative) $\mathbb{Z}$-marking.

A T-diagram is called (*resp.* weakly) admissible if its underlying abelian diagram is (*resp.* weakly) admissible.

Theorem 4.2.2. *An abelian Gauss diagram is braid-admissible if and only if it determines a virtual closed braid diagram, up to diagram isotopy and detour moves.*

Proof. By Proposition 2.3.8, an abelian Gauss diagram on $\mathbb{Z}$ determines a unique virtual knot diagram in the annulus up to diagram isotopy and detour moves. Besides, the "if" part is clear. Propositions 4.2.5 and 4.2.6 together prove the converse for diagrams with a positive refinement (Definition 4.2.4), and Corollary 4.2.13 shows that this is enough. □

Remark 4.2.3. Note that for diagrams that are known to be represented by real knots, there is a more direct proof: one only needs considering the Seifert circles. If their homology classes in $\mathbb{Z} \simeq H_1(\mathbb{R} \times \mathbb{S}^1)$ are all positive, then they must be equal to 1, and one easily sees that the knot is a closed braid. However, this does not work with virtual knots, since the "Seifert circles" obtained by smoothing all (even the virtual) crossings do not actually correspond to loops in G.

4.2.1 Positive admissible T-diagrams are represented by braids

Definition 4.2.4. A T-diagram is called *non-negative* if it only has $\oplus$ markings, *positive* if it is non-negative with at least one marking.

Let T be a positive diagram. We say that an arrow has *level 1* if each of its endpoints is directly preceded by a ($\oplus$) marking. Remove every arrow of level 1. Those of level 1 in the new diagram are said to have *level 2* in T. By induction we define the arrows of *level k* in T. Of course some arrows may have no level at all.

This definition is highly inspired from the topology of braids: assuming that T is the T-diagram of a braid, the level of an arrow is the altitude of the corresponding crossing, in such a parametrization that every crossing has a positive integral altitude as low as possible.

Proposition 4.2.5. *A positive T-diagram is admissible if and only if each of its arrows has a well-defined level.*

Proof. Note that if there are no arrows, then the diagram is admissible and the result is true. We assume from now on that T has at least one arrow.

For positive diagrams, being admissible is equivalent to satisfying the property that every nontrivial and orientation respecting loop meets at least one marking. So assume that each arrow has a level, but that some loop fails to meet any marking. There must be at least one arrow involved in that loop. If not, then it would go all the way around the whole circle, and meet markings since the diagram is positive: that is a contradiction. Remove the arrows that are not involved in the loop. Those remaining had a well defined level, so they still have one in the new diagram, and so at least one of them, say A, has level 1 in the new diagram. It means that each endpoint of A is directly preceded by a marking. Since our loop goes along A, and respects the orientation of the circle, it must meet one of them: that is a contradiction.

Conversely, assume that some arrow has no level, and remove all of those that have one. In this new diagram, pick a marking that is not directly followed by another, *i.e.* that is directly followed by the endpoint of an arrow. Start drawing a path at this endpoint, going along the arrow. The other endpoint cannot be also preceded by a marking, otherwise the arrow would have a level. So go back along the circle until the next endpoint of an arrow that is directly preceded by a marking. Then iterate those two steps: the path must eventually loop, since there is a finite number of arrows, and that loop avoids every marking. Thus the diagram is not admissible. □

Proposition 4.2.6. *A positive T-diagram can be represented by a virtual braid if and only if each of its arrows has a well-defined level.*

Note: it is to be understood that an isotopy of a braid diagram always stays within the set of braid diagrams – and as usual, involves no Reidemeister moves.

Proof. Every real crossing of a virtual braid that may be isotoped into the lowest one corresponds to an arrow of level 1 in the associated T-diagram. Removing these arrows amounts to replacing the real crossings by virtual ones. Until there is no more real crossing, there will always be a lowest one. This proves the "only if" part.

Assume that each arrow of a positive diagram has a level. Let k be the global marking of the circle, and let l be the maximal level of the arrows. Cut the circle at every marking, so as to obtain a diagram based on a union of k segments, and embed it into $\mathbb{R} \times [0, l+1]$, in such a way that the segments are oriented from bottom to top, and such that each arrow of level i is contained in $\mathbb{R} \times \{i\}$. The fact that each arrow has a level is equivalent to the existence of such an embedding. Now, at each level, make the strands cross each other as indicated by the arrows, by a homotopy that keeps the $i + 1/2$-levels untouched. Declare virtual every additional crossing needed to do that.

Finally, add to the top a totally virtual braid corresponding to the permutation defined by the way the strands were originally glued together in the circle, so that the resulting braid determines the required T-diagram. □

4.2.2 Admissible implies positive

The goal here is to show that admissible abelian Gauss diagrams always admit positive refinements. It essentially relies on a technical algebraic fact (Proposition 4.2.11) that requires some definitions.

Definition 4.2.7 (units)**.** Let $M = \mathbb{Z}^n = \bigoplus \mathbb{Z}e_i$. We call $\varepsilon = \sum \varepsilon_i e_i$ a *unit* if for every i, $\varepsilon_i \in \{-1, 0, 1\}$. Units are partially ordered by the relation

$$\varepsilon \leq \eta \iff \forall i, \varepsilon_i \in \{0, \eta_i\}\,.$$

With any $x \in M$ is associated a unit $\varepsilon(x)$ defined by $\varepsilon_i(x) = sign(x_i)$, with the convention $sign(0) = 0$.

Let V be a submodule of M. For any $v \in V$, define

$$V_v = V \cap \bigoplus \varepsilon_i(v)\mathbb{N}e_i,$$

and define $V_v^{\mathbb{1}}$ as the finite set of all units contained in V_v.

Example. Assuming that $(-3, 0, 5) \in V \subset \mathbb{Z}^3$,

$$\begin{array}{rcl} V_{(-3,0,5)} & = & V \cap [(-\mathbb{N}) \times \{0\} \times \mathbb{N}]\,, \\ V^{\mathbb{1}}_{(-3,0,5)} & = & V \cap [\{-1, 0\} \times \{0\} \times \{0, 1\}]\,. \end{array}$$

There are obvious equivalences:

$$V_v \subset V_w \;\Leftrightarrow\; v \in V_w \;\Leftrightarrow\; \varepsilon(v) \leq \varepsilon(w).$$

Definition 4.2.8. Say that V has property $\mathbb{1}^+$ if each $v \in V$ is a linear combination of the elements of $V_v^{\mathbb{1}}$, with non negative coefficients. It is a property that depends on a basis of M, that will be omitted if there is no ambiguity.

Here is the example that will be useful:

Lemma 4.2.9. *Let X be a finite cellular complex, $C_1(X, \mathbb{Z})$ its $\mathbb{Z}$-module of 1-chains endowed with its natural basis of 1-cells, and $V := Z_1(X, \mathbb{Z})$ the submodule of 1-cycles. Then V has property $\mathbb{1}^+$.*

Proof. Write $C_1(X, \mathbb{Z}) = \oplus_{i=1}^n \mathbb{Z}e_i$, and pick $v = \sum v_i e_i \in V$. Let γ be a path in X corresponding as a 1-chain to $\varepsilon_{i_1}(v)e_{i_1}$, where i_1 is such that $v_{i_1} \neq 0$. If the two endpoints of e_{i_1} are glued together in X, then γ is a loop and we stop here. Otherwise, since v is a cycle, there must be some i_2 such that $v_{i_2} \neq 0$ and $\varepsilon_{i_2}(v)e_{i_2}$ is a path that starts where γ ends. So we put $\gamma = \varepsilon_{i_1}(x)e_{i_1} + \varepsilon_{i_2}(x)e_{i_2}$, and iterate this process until γ meets a vertex for the second time. Then we forget what happened before γ first met that vertex. What remains is the class a simple loop, and it is a unit of V_v. Repeating this with $v - \gamma$, and so on, we split v as a sum of units of V_v. □

Lemma 4.2.10. *Assume that $V \subset M = \bigoplus_{i=1}^n \mathbb{Z}e_i$ has property $\mathbb{1}^+$. Then for any i, $V \oplus \mathbb{Z}e_i$ still has property $\mathbb{1}^+$.*

Proof. Put $W := V \oplus \mathbb{Z}e_i$, and let $w = v + ke_i \in W$ with $v \in V$ and $k \in \mathbb{Z}$. By assumption v may be written as

$$v = \sum_{l \in L} v_l,$$

where the v_l's are units in $V_v^{\mathbb{1}}$. Of course some of them can coincide. Note that $\varepsilon_j(w) = \varepsilon_j(v)$ for $j \neq i$.

Case 1: $\varepsilon_i(v) \in \{0, \varepsilon(k)\}$. Then $\varepsilon(v) \leq \varepsilon(w)$. Hence the v_l's lie in W_w, and so does the unit $\varepsilon(k)e_i$, so we are happy with

$$w = \sum v_l + |k| \left(\varepsilon(k)e_i\right).$$

Case 2: $\varepsilon_i(v) = -\varepsilon(k)$. Put $L' := \{l \in L \mid \varepsilon_i(v_l) \neq 0\}$. Notice that

$$\begin{array}{ll} \forall\, l \in L', & v_l + \varepsilon(k)e_i \text{ is a unit of } W_v, \\ \forall\, l \in L \setminus L', & v_l \text{ is a unit of } W_w. \end{array}$$

▷ If $|k| < \sharp L'$, then $\varepsilon_i(w) = \varepsilon_i(v)$, which implies that $\varepsilon(v_l) \leq \varepsilon(w)$ and v_l is a unit of W_w even for $l \in L'$, and if we pick any k elements of L', say $l_1, \ldots, l_k$, then

$$w = \sum_{j=1}^{k} \left(v_{l_j} + \varepsilon(k)e_i\right) + \sum_{l \in L' \setminus \{l_1, \ldots l_k\}} v_l + \sum_{l \notin L'} v_l.$$

▷ If $|k| = \sharp L'$, then simply

$$w = \sum_{l \in L'} (v_l + \varepsilon(k)e_i) + \sum_{l \notin L'} v_l.$$

▷ If $|k| > \sharp L'$, then $\varepsilon_i(w) = \varepsilon(k)$, which means that $\varepsilon(k)e_i$ is a unit of W_w, and

$$w = \sum_{l \in L'} (v_l + \varepsilon(k)e_i) + \sum_{l \notin L'} v_l + \left(|k| - \sharp L'\right) \left(\varepsilon(k)e_i\right).$$

In any case one has a positive decomposition of w along units of W_w. □

The main interest of property $\mathbb{1}^+$ is the following

Proposition 4.2.11. *Assume that $V \subset M = \bigoplus_{i=1}^{n} \mathbb{Z}e_i$ has property $\mathbb{1}^+$, and fix an element $v_0 \in V$. Then any group homomorphism $\phi : V \to \mathbb{Z}$ such that $\phi(V_{v_0}) \subset \mathbb{N}$ extends to a homomorphism $\Phi : M \to \mathbb{Z}$ such that $\Phi(M_{v_0}) \subset \mathbb{N}$.*

Proof. For $k \in \mathbb{Z}$, $\varepsilon(k)$ stands for the sign of k (again $\varepsilon(0) = 0$). Fix i such that $e_i \notin V$, and set $W = V \oplus \mathbb{Z}e_i$. For the sake of simplicity, let us write V_0, W_0, etc. instead of V_{v_0}, W_{v_0}, etc. By Lemma 4.2.10, W still has property $\mathbb{1}^+$. We show below that ϕ extends into a map $\psi : W \to \mathbb{Z}$ such that $\psi(W_0) \subset \mathbb{N}$. The lemma follows by induction.

Set $\psi_{|V} = \phi$. The goal is to give a value to $\psi(e_i)$ so that $\psi(W_0) \subset \mathbb{N}$. Every element $w = v + ke_i \in W_0$ with $k \neq 0$ gives a condition, namely $\psi(e_i) \geq -\frac{1}{k}\phi(v)$

if $k > 0$, $\psi(e_i) \leq -\frac{1}{k}\phi(v)$ if $k < 0$. Let us first look at the conditions yielded by $k = \pm 1$. Set

$$\mathcal{K}_{-1} = \{\phi(v) \mid v \in V,\ v - e_i \in W_0\}, \text{ and}$$
$$\mathcal{K}_{+1} = \{-\phi(v) \mid v \in V,\ v + e_i \in W_0\}.$$

Then all the $k = \pm 1$-conditions are satisfied if and only if

$$\sup \mathcal{K}_{+1} \leq \psi(e_i) \leq \inf \mathcal{K}_{-1}. \tag{4.1}$$

Let $w_1 = v_1 + e_i$ and $w_2 = v_2 - e_i$ lie in W_0. Then

$$\begin{aligned} v_1 + v_2 = w_1 + w_2 &\implies v_1 + v_2 \in W_0 \cap V = V_0 \\ &\implies -\phi(v_1) \leq \phi(v_2). \end{aligned}$$

This proves that

$$\sup \mathcal{K}_{+1} \leq \inf \mathcal{K}_{-1}. \tag{4.2}$$

Hence, since $\mathcal{K}_{-1}$ and $\mathcal{K}_{+1}$ are subsets of $\mathbb{Z}$, it is possible for $\psi(e_i)$ to be an integer and satisfy (4.1) as soon as $\inf \mathcal{K}_{-1} \neq -\infty$ and $\sup \mathcal{K}_{+1} \neq +\infty$. We show that this is always true by discussing the value of $\varepsilon_i(v_0)$.

1. $\varepsilon_i(v_0) = +1$.
In that case, $v_0 - e_i \in W_0$. Then $\mathcal{K}_{-1}$ is not empty, and (4.2) implies that $\sup \mathcal{K}_{+1} \neq +\infty$. Moreover, for every $v \in V$ such that $v - e_i \in W_0$, $\varepsilon_i(v_0) = +1$ implies that $(v - e_i) + e_i$ still lies in W_0. Hence $v \in V \cap W_0 = V_0$. Since $\phi(V_0) \subset \mathbb{N}$, this proves that $\mathcal{K}_{-1}$ is a subset of $\mathbb{N}$, and $\inf \mathcal{K}_{-1} \neq -\infty$.

2. $\varepsilon_i(v_0) = -1$.
This case is symmetric to the previous one.

3. $\varepsilon_i(v_0) = 0$.
If $\mathcal{K}_{-1}$ and $\mathcal{K}_{+1}$ are empty, there is nothing to prove. Assume that $\mathcal{K}_{-1} \neq \varnothing$, and let $v \in V$ be such that $w = v - e_i \in W_0$. By the $\mathbb{1}^+$ property of V, v can be decomposed as a sum of units $\sum_l v_l$ with $v_l \in V_v^{\mathbb{1}}$. Since $\varepsilon_i(v_0) = 0$, the i-th coordinate of w must be 0, hence that of v must be 1, and exactly one of the v_l's has a non-zero i-th coordinate. All of the other v_l's lie in $V \cap W_w \subset V \cap W_0 = V_0$. Since $\phi(V_0) \subset \mathbb{N}$, it follows that all $\phi(v_l)$'s, except at most one, are non-negative. This shows that $\mathcal{K}_{-1}$ is bounded below by the least value of ϕ on the finite set $V_v^{\mathbb{1}}$.

Assuming that $\mathcal{K}_{+1}$ is not empty, one shows exactly similarly that it is bounded above.

So it is possible that $\psi(e_i)$ satisfies all $k = \pm 1$-conditions. Now we claim that these elementary conditions are enough for all the others to hold. Indeed, let $k \in \mathbb{Z}$ and $v \in V$ be such that $w = v + ke_i \in W_0$. Throughout the proof of Lemma 4.2.10, we actually showed that not only such a w is a sum of units of W_w, but also these units are of the form $v_l + e_i$, $v_l - e_i$, v_l, where the v_l's lie in $V_v^{\mathbb{1}}$ (recall that $0 \in V_v^{\mathbb{1}}$). But $w \in W_0$ implies that $W_w \subset W_0$, and a unit of one of these forms lying in W_0 has non-negative image by ψ (precisely thanks to the $k = \pm 1$-conditions). It follows that w has non-negative image by ψ, which terminates the proof. □

Proposition 4.2.12. *An abelian Gauss diagram has a non-negative refinement if and only if it is weakly admissible.*

Corollary 4.2.13. *Any admissible abelian Gauss diagram has a positive refinement.*

Proof of the proposition. The "only if" part is clear since the $\mathbb{Z}$-marking of an ER class is the sum of markings that it meets, counted positively. For the converse, let G be a weakly admissible diagram of degree n, and denote its edges by $e_1, \dots, e_{2n}$. Denote by $\bar{G}$ the cellular complex obtained by shrinking separately every arrow of G to a point. As usual the homology is integral. Since the arrows of G are contractible, there is a natural isomorphism

$$H_1(G) \xrightarrow{\sim} H_1(\bar{G}).$$

Since $\bar{G}$ does not have 2-cells, there is a natural embedding $H_1(\bar{G}) \hookrightarrow \mathbb{Z}^{2n} = \bigoplus \mathbb{Z}e_i$ that induces, together with the above isomorphism, an embedding

$$\iota : H_1(G) \hookrightarrow \bigoplus \mathbb{Z}e_i.$$

Set $V := \iota(H_1(G))$. Lemma 4.2.9 applied to $\bar{G}$ implies that V has property $\mathbb{1}^+$ with respect to the basis $\{e_i\}$.

Set

$$\begin{array}{rccc} \phi : & V & \longrightarrow & \mathbb{Z} \\ & v & \longmapsto & \mu(\iota^{-1}(v)) \end{array},$$

where $\mu : H_1(G) \to \mathbb{Z}$ denotes the decorating map of G.

Finally, set $v_0 = \sum e_i \in V$. One sees that $V_0 = V \cap \mathbb{N}^{2n}$ corresponds through ι to the set of ER homology classes in $H_1(G)$. Hence the weak admissibility of G implies that ϕ maps V_0 into $\mathbb{N}$. Proposition 4.2.11 applies and gives an extension $\Phi : \mathbb{Z}^{2n} \to \mathbb{Z}$ such that $\Phi(\mathbb{Z}_0^{2n}) \subset \mathbb{N}$. Since here $\mathbb{Z}_0^{2n} = \mathbb{N}^{2n}$, decorating each ($i$-th) edge of G with $\Phi(e_i)$ "$\oplus$" markings gives the required non-negative refinement. □

4.2.3 Asymptotic admissibility

Looking at the Energy formula (2.4) with braid-admissibility in mind, one may desire to understand when a diagram features an ER loop with negative energy – and thus is inadmissible for any large enough value of the global $\mathbb{Z}$-marking $\mu(K)$ (decorating the class of the circle, $[K]$). It happens that "almost" all diagrams do:

Definition 4.2.14. Say that a diagram G has a *rightmost point*, or is *descending*, if there is a point on its base circle that is located to the right of each of its arrows.

Theorem 4.2.15. *A Gauss diagram contains no ER loop with negative energy if and only if it is descending. The proportion of such diagrams, among those of degree n, lies in the interval $\left[\frac{n+1}{2^n}, \frac{n}{2^{n-1}}\right]$, and these bounds are optimal.*

Descending knot diagrams are well-known for being unknotted in the classical case (of real knots in $\mathbb{S}^3$) – for real knots in $\mathbb{S}^3$. For virtual knots (and also of course for real knots in a thickened surface) this is no longer true: see for instance the nontrivial virtual trefoil on Fig.4 from [17].

Proof. Let us begin with the second statement, which is easier. Since the ratio does not involve the π-markings, we may ignore them and focus on the arrow orientations. For any of the $2n$ edges in a Gauss diagram, there is exactly one way (among 2^n) to orient the arrows so that the diagram is descending with respect to that edge. At least $n+1$ of these $2n$ descending diagrams are pairwise distinct (the extreme case happens for those configurations where no two arrows intersect), and it also happens that all $2n$ of them are pairwise distinct – for instance when any two arrows intersect.

As for the first statement, the "if" part follows from the definitions: if G has a rightmost point, then the energy of an ER loop is simply the number of times it meets that point.

The "only if" part relies on the following:

Lemma 4.2.16. *A non descending Gauss diagram must contain a simple ER loop, respecting the orientation of the arrows it meets, and meeting at least two.*

Such a loop has positive torsion by Theorem 2.3.22. But it also has opposite torsion and energy by relation (2.6), so the proof will be over with the lemma. □

Proof of Lemma 4.2.16. The non existence of a rightmost point ensures that there is a *minimal* set of arrows, X, such that each point on the circle is on the left of at least one arrow in X. We are going to show that there is a loop as announced, meeting once every arrow in X. It is obvious that X must have at least 2 elements.

Fact 1: Heads and tails of the arrows in X alternate in the order induced by the orientation of the circle.

Indeed, if two heads are consecutive, call the arrows A and B according to the local order of their heads. If A and B do not intersect, then X is not minimal: B may be removed. So A and B must intersect. But then call P and Q two generic points right before the heads of A and B respectively. P is on the left of some arrow C in X, obviously different from A and B. Then Q must be on the left of C too. So again X is not minimal: A may be removed, B and C take care of it. The proof that tails cannot be consecutive is similar.

Fact 2: No arrow in X can be isolated (Fig.4.9(a)).

Indeed, call such an arrow A and P the point right before the head of A. P must be on the left of some arrow in X, which can only be parrallel to A as the dashed arrow on the picture, therefore contradicting the minimality of X.

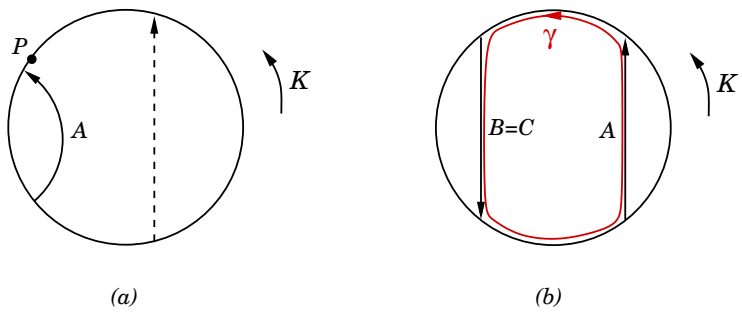

Figure 4.9: First cases in Lemma 4.2.16

Now pick $A \in X$ and call B the arrow whose tail is right after the head of A, and C the one whose head is right before the tail of A.

If $B = C$, then by minimality $X = \{A, B\}$, and the lemma is true (Fig.4.9(b)). Now assume that $B \neq C$. In that case one easily sees that by minimality of X, A and B must "intersect", as well as A and C. If B and C also intersect, then we have a trefoil, and the lemma is true (Fig.4.10(a)). If B and C do not intersect, then they look like Fig.4.10(b), and again by minimality there can't be any other arrow end to the left of A than there are on this picture.

So we have proved that

1. either X contains 3 elements or less and the lemma is true,
2. or every arrow in X has exactly two endpoints on its left, in a configuration exactly similar to Fig.4.10(b).

In this last case, one can draw a loop with the required properties as indicated on Fig.4.10(c), running over all the arrows in X.

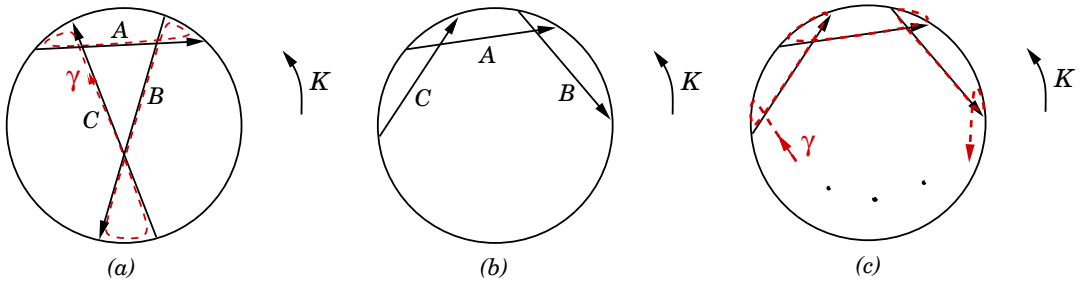

Figure 4.10: The ER loop constructed in the proof of Lemma4.2.16

□

Finally, in terms of asymptotic behaviour, the following holds:

Theorem 4.2.17. *Let G be a decorated Gauss diagram on $\mathbb{Z}$ with parameter $\mu(K)$ as a global $\mathbb{Z}$-marking.*

- → *If G is not descending, then it is inadmissible for $\mu(K)$ large enough.*
- → *If G is descending, then the set of values of $\mu(K)$ for which G is admissible is either empty, or of the form $\{n \in \mathbb{N} \mid n \geq n_0\}$. Moreover the last case happens if and only if every simple ER loop avoiding the rightmost point has positive homology class.*

Remark 4.2.18. In the above theorem, the condition in the first point does not depend on the markings of G, but m_0 does (as well as n_0 in the second point).

4.3 How to take care of Reidemeister moves – a conjecture

Recall that the edges *of a Gauss diagram G are the 1-cells complementary to its arrows. A homology class in $H_1(G)$ is called* ER *(edge-respecting) if, as a 1-chain,*

it has non-negative coordinate along each edge of G.

The major drawback of Theorem 4.2.2 is that it is rigid: one would like to understand not only when a diagram is that of a closed braid, but when it is *equivalent to that of a closed braid* up to Reidemeister moves. Since the theorem gives a criterion in terms of ER classes in $H_1(G)$, it is natural to wonder what happens to these classes when a Reidemeister move is performed, more precisely to the set $\mu_{ER}(G)$ of all $\mathbb{Z}$-markings of ER classes.

Conjecture. *Let G_0 be a Gauss diagram with minimal number of arrows in its class modulo* R*-moves. Then for any G of the same knot type as G_0,*

$$\mu_{ER}(G_0) \subset \mu_{ER}(G).$$

In more usual terms of knot diagrams, this being true would imply that if a knot diagram has minimal number of real crossings in its virtual knot type, and if it is not a closed braid diagram (up to diagram isotopy and detour moves), then it is neither a closed braid diagram up to Reidemeister moves. Also, a similar assertion would hold replacing "closed braid diagram" with "diagram contained in a little disc".

This section is devoted to discuss some aspects of a possible perspective towards that conjecture.

4.3.1 Trace graphs

Lemma 4.2.9 allows one to think of an ER class as a *simple loop* γ in a knot diagram that always respects the diagram orientation and may "turn" at the real crossings (see Fig.2.3 – note that the left and right examples are not possible for an ER loop). If a Reidemeister move happens, involving no real crossing where γ turns, then γ "survives" the move: that is, there is a loop in the new knot diagram that naturally corresponds to γ and that has the same homology class in $H_1(\mathbb{R}\times\mathbb{S}^1)$. When the crossings at which γ turns *are* involved, it can happen that γ does not obviously (*i.e. locally*) survive. In that case, one has to take a larger point of view and see if the homology class of γ is still represented by another loop. Fig.4.11 shows the most basic example: from a local viewpoint, it looks like the red loop "dies" during the last Reidemeister II move. However, at a larger scale, it is clear that there is a crossing to "rescue" it.

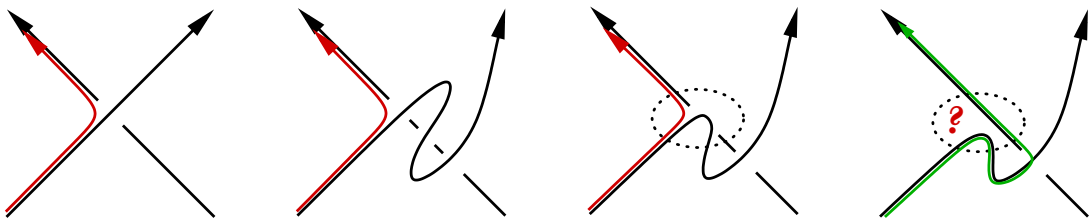

Figure 4.11: Should the red path be considered dying in the process?

Another example is depicted in Fig.4.12. At first glance it looks like the red loop survives the move. However, looking carefully, one sees that the little part near the

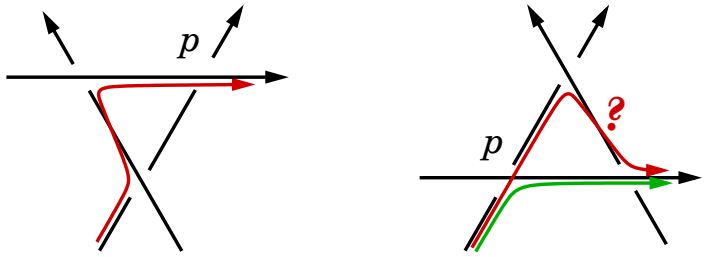

Figure 4.12: p is called a "stealing crossing" for that move

interrogation mark does not respect the orientation. Fortunately, the green loop is ER and has the same homology class as the red one.

So it appears that understanding the future of a loop during a sequence of Reidemeister moves demands to understand what happens globally to the real crossings during the sequence, especially those at which the loop turns. An adapted tool for that is the *trace graph* associated with a sequence of moves. It was first introduced in [11], in the special case of a knot isotopy induced by a full rotation of the solid torus around its core.

Definition 4.3.1. Let D_0 be a virtual knot diagram in the annulus $\mathbb{R}\times\mathbb{S}^1$, and consider a smooth sequence $\{D_t\}$ of diagram isotopies, detour moves and Reidemeister moves from D_0 to another diagram D_1. With such data is associated a *trace graph* $\mathrm{TG}(\{D_t\})$, that consists in the closure of the set of all points $(x,\theta,t)\in\mathbb{R}\times\mathbb{S}^1\times[0,1]$ such that D_t has a usual real crossing at (x,θ).

Topologically, a trace graph is a *non generic* immersion of a finite number of segments. Let $\{D_t\}$ be a 1-parameter sequence as above, featuring a finite number of Reidemeister moves at times $0<t_1<\ldots<t_k<1$. Then the restriction of $\mathrm{TG}(\{D_t\})$ over a time interval $\Delta=[t_i+\varepsilon,t_{i+1}-\varepsilon]$ is a *generalized braid* in $\mathbb{R}\times\mathbb{S}^1\times\Delta$ based on the sets of real crossings of $D_{t_i+\varepsilon}$ and $D_{t_{i+1}-\varepsilon}$ (see Definition 2.2.7). On the other hand, the restriction of $\mathrm{TG}(\{D_t\})$ over a neighborhood of a critical point t_i can take the following forms – ordered consistently with the three types of Reidemeister moves (see Fig.4.13):

→ R-I: Birth or death of an isolated strand,
→ R-II: Cap or cup (smooth extremum of a strand),
→ R-III: Triple point (three strands meet in a single point).

For the sake of simplicity, we usually represent only the projections of trace graphs on the two coordinates (θ,t). Hence, besides the critical points described above, *regular crossings* may appear (with the usual over/under decoration), when two real crossings of the knot diagram D_t have the same θ coordinate.

Remark 4.3.2. With that definition, a 1-parameter family $\{D_t\}$ is far from being uniquely determined by D_0 and the trace graph. For instance, when a Reidemeister I birth happens, there is neither information about what branch of the knot is concerned, nor what should be the writhe of the new crossing or the Whitney index of the new knot diagram.

Definition 4.3.3. A *strand* is a maximal smooth component of a trace graph.

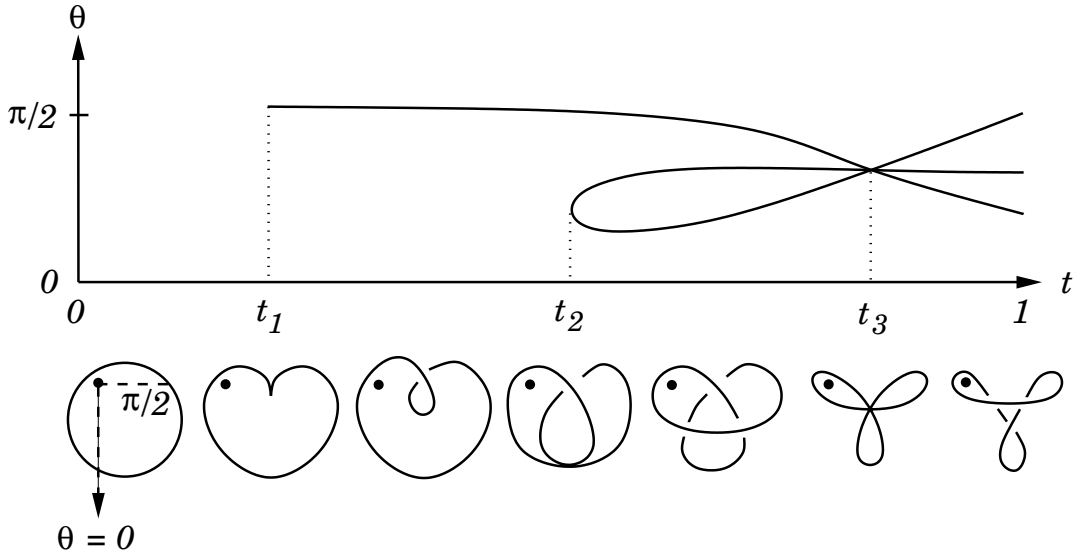

Figure 4.13: Projection of a trace graph on the annulus (θ, t) – the dots in the knot diagrams represent the "hole" of the annulus (x, θ).

This notion is the first step towards formalizing the informal statement that the remaining crossing in the last diagram of Fig.4.11 "rescues" the one at which the red loop used to turn. Indeed, the trace graph of this local sequence of moves is composed of a single strand, with a *zigzag* shape (see Definition 4.3.5 and Fig.4.18). The main result of this section is that zigzags can always be avoided – which is clear, for instance, in the sequence of Fig.4.11.

4.3.2 A normal form for trace graphs

Consider a knot diagram that is generic except for one crossing where the two branches are tangent to each other. These self tangencies can be thought of as infinitesimal triples of crossings (see Fig.4.14). In all this section, every statement is expressed in terms of classical diagrams with sometimes such triples of crossings very close to each other, but one should keep in mind the self-tangent point of view.

A number of new "Reidemeister moves" naturally arise from that definition, but only two of them will be useful here : T_0, which changes the type of self-tangency, and T_3, which is akin to the third Reidemeister move where one crossing is self-tangent. Fig.4.15 shows a few representative examples. Among T_3 moves, we distinguish between $\mathrm{T}_3^{(3)}$ and $\mathrm{T}_3^{(5)}$, according to the number of edges of the polygon in the picture.

There is a nice way to realize these new moves as a composition of classical Reidemeister moves.

To perform T_0, one creates a little loop by R-I and make it travel along the whole picture before killing it by R-I again. A crucial point is the fact that one can choose on which local branch of the knot to create the initial little loop. The picture at the end will be the same, but, from the trace graph point of view, it changes the names of the two extremal crossings. For this reason we also distinguish between T_0^{above} and T_0^{below}, corresponding to the higher (resp. lower) branch.

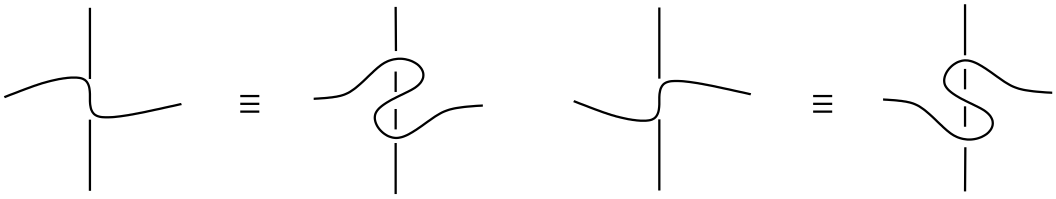

Figure 4.14: Self tangencies

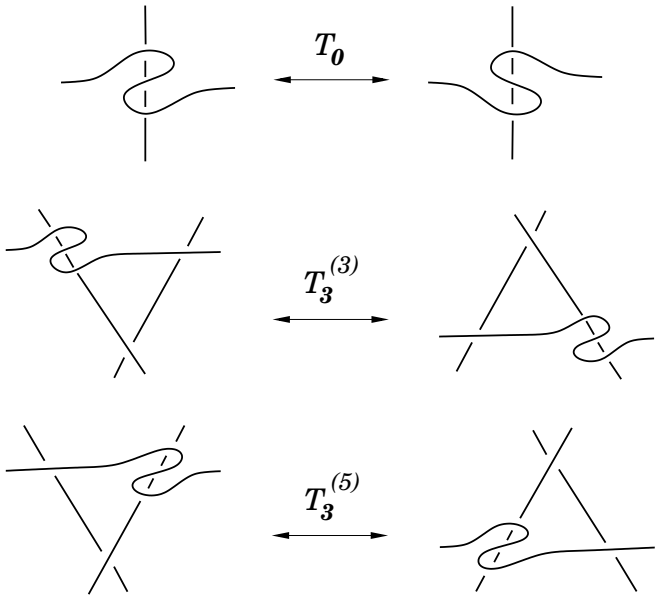

Figure 4.15: Tangent Reidemeister moves

Definition 4.3.4. The strand which is completely contained in the trace graph of an expanded T_0-move is called a *short* strand.

$T_3^{(3)}$ is realized as the composition of three R-III moves (see Fig.4.17). As for $T_3^{(5)}$, it is nothing but the conjugate of $T_3^{(3)}$ by T_0.

Definition 4.3.5. A time interval $[t_0, t_1]$ is generic for a given trace graph if the projection from the graph to the time axis has no critical point over t_0 or t_1. It induces a *restricted trace graph*. A *zigzag* is a strand in a restricted trace graph, which meets the boundary points of the restriction interval, and which has exactly two critical points between them.

A strand which contains no zigzags is called a *good* strand. Figs.4.18 and 4.21 shows representative examples.

Proposition 4.3.6 (combing)**.** *Two knot diagrams of the same virtual knot type can always be connected by a trace graph with only good strands. Moreover, if D and D' are regularly equivalent (Definition 3.4.6), then they can be connected by a trace graph that contains only good strands and whose every R-I move belongs in a short strand.*

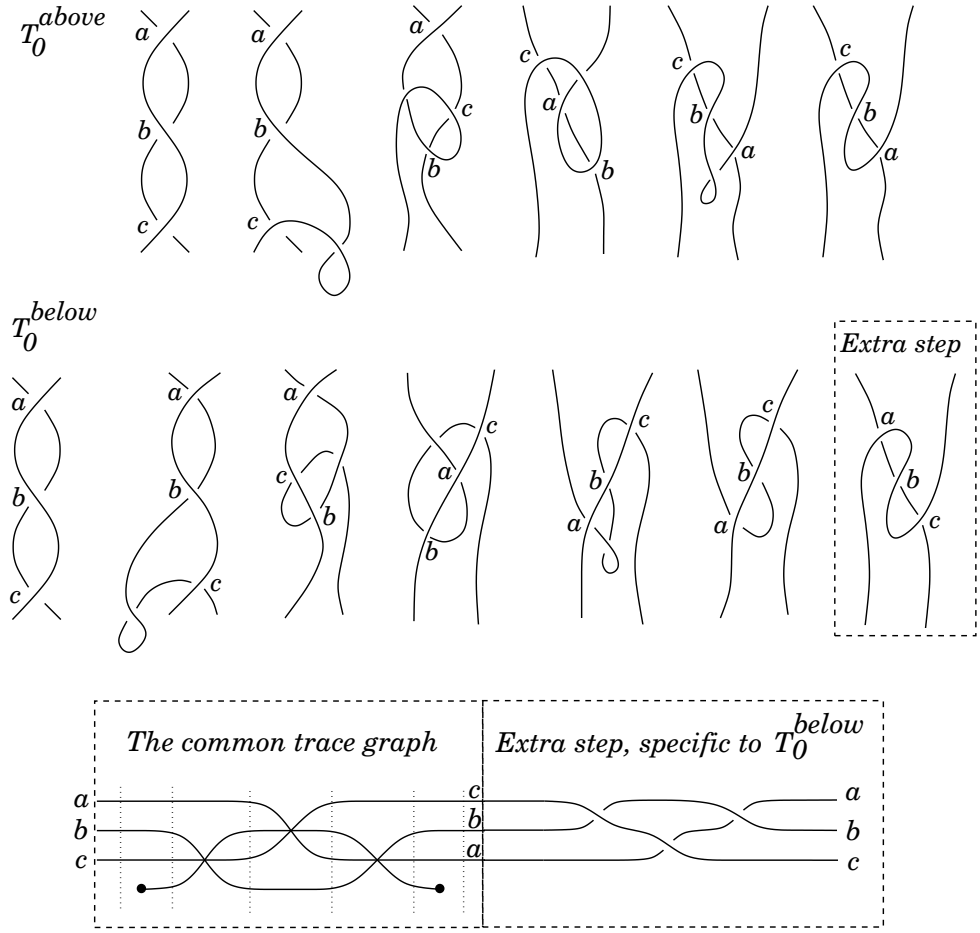

Figure 4.16: Reidemeister sequence and trace graph of an expanded T_0 move

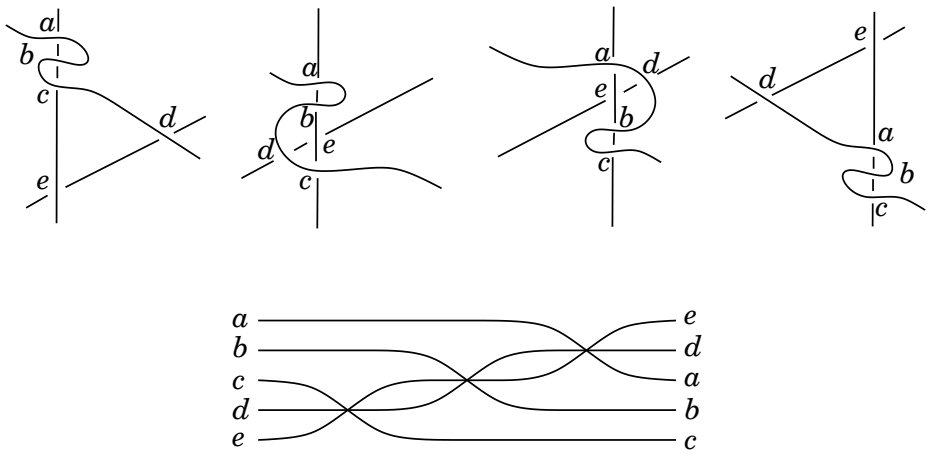

Figure 4.17: Reidemeister sequence and trace graph of an expanded $\mathrm{T}_3^{(3)}$ move

Proof. Consider an arbitrary sequence of moves between D and D'. If it contains zigzags, we are going to comb them algorithmically by inserting appropriate sequences of moves, in such a way that every R-I birth or death added is part of a short strand. Let $[t_0, t_1]$ be a time interval that features exactly one zigzag, and such

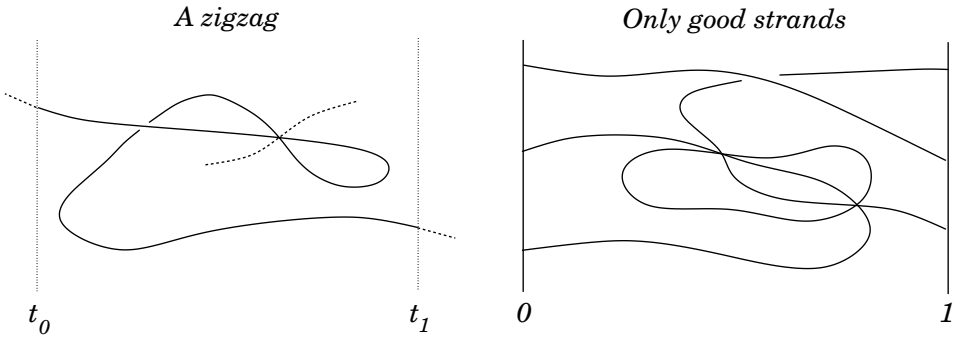

Figure 4.18: A zigzag vs good strands

that no Reidemeister move happens between t_0 and the R-II birth of the zigzag, or between the R-II death and t_1. We take notations for times and crossings as indicated by Fig.4.19.

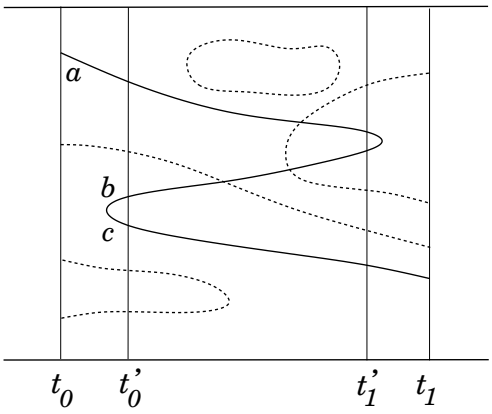

Figure 4.19: An innermost zigzag - notations for the proof of 4.3.6

Start with the knot diagram at t_1'. We see a and b just about to cancel each other. At that point, instead of proceeding to t_1, replace a by a self-tangent crossing, consisting of a triple $\{a, \overline{a}, a'\}$, "looking" outside of the R-II-bigon (Fig.4.20). Then slide a and $\overline{a}$ along the bigon to make them join b. One gets the same picture as one had at t_1', except a has been replaced with a' and b has been replaced with the triple $(b, a, \overline{a})$. Now from that fake t_1' situation, perform the moves that lie between t_0' and t_1' in the reverse direction, back to a fake t_0' (perhaps using R-I moves to perform $T_3^{(5)}$, but those are always part of short strands). There c finds itself in front of the triple $(b, a, \overline{a})$, and using T_0 moves if necessary we can assume that b may be slided right in front of c in a position to be cancelled with an R-II move. Make b and c actually cancel each other (notice that they were born together, so we just added a good strand). Then the diagram is exactly the same as it was at t_0', except for the names of the crossings (from the trace graph point of view): a has been replaced with a', b with $\overline{a}$, and c has been replaced with a. Therefrom, follow the initial sequence of moves up to t_1: a' and $\overline{a}$ cancel each other (hence creating yet another good strand), and a survives all along the new trace graph.

One can see on Fig.4.20 that the total number of R-II caps and cups lying on

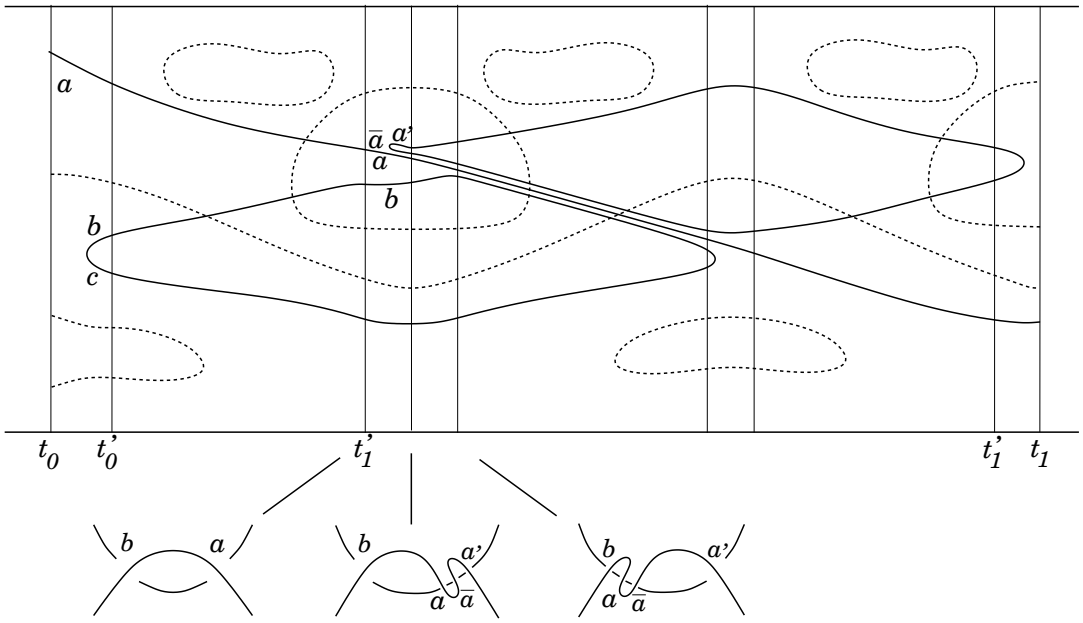

Figure 4.20: Combing an innermost zigzag

bad strands in the whole trace graph has decreased. This proves the first assertion. For the second, it suffices to observe that in the combing process, the only moments when R-I moves may appear are when T_0 or $T_0^{(5)}$ moves are performed. But these moves only generate short strands by definition.

□

This proposition minimizes in some sense the combinatorial complexity of R-I and R-II in trace graphs. It is reasonable to hope that in such a position, the combinatorics of triple points (R-III) will be easier to handle.

4.3.3 Some ideas that do not work (yet)

Getting rid of the short strands

Looking at the decomposition of T_0 moves into classical Reidemeister moves (Fig.4.16), one could try to get rid of the necessity of R-I moves by giving birth to *two* little loops instead of one, using the Whitney trick, then performing the expanded T_0, and then making the two little loops meet again and cancel with the same Whitney trick.

Why this does not work is because the Whitney trick, as well as the step of making the two loops meet at the end, involve a little loop getting across another branch, as in Fig.4.21. This process adds a zigzag in the trace graph, and one cannot remove it without adding short strands again – see Fig.4.22. However, short strands have essentially no effect on the set of ER loops and their homology classes, so they can be ignored.

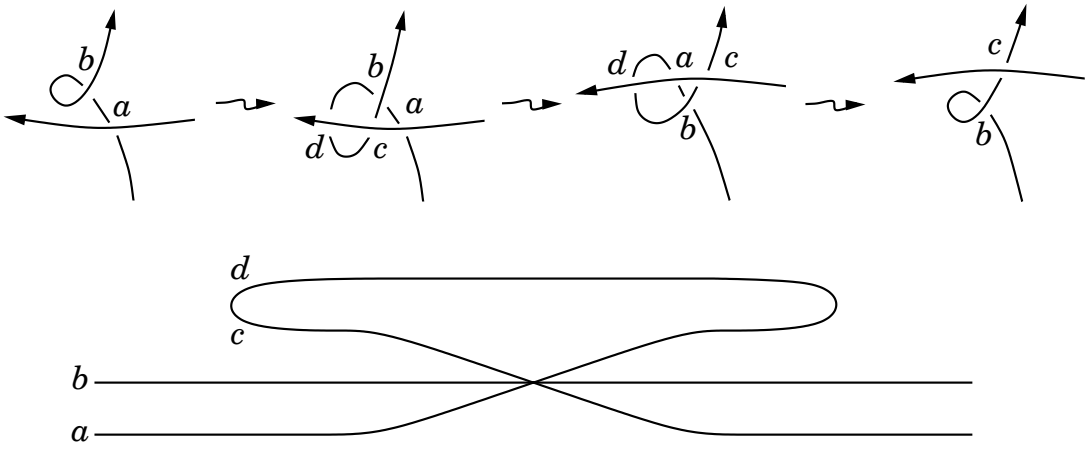

Figure 4.21: Elementary example of a zigzag

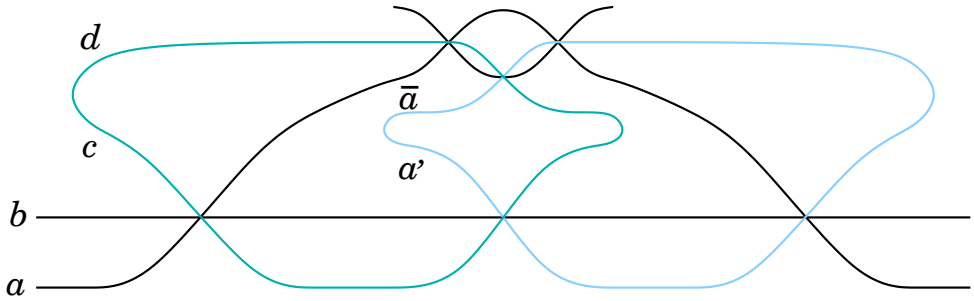

Figure 4.22: Combing the zigzag from Fig.4.21

About the set of R-III moves involved in a close combed strand

Definition 4.3.7. A *close combed strand* in a trace graph is a strand which is homeomorphic with a circle, such that the projection from that strand to the time axis has only two critical points.

The combing process produces trace graphs with only this kind of strands, besides those with zero or one critical point.

Let us consider again the example from Fig.4.12. This *stealing* process happens every time a simple loop turns twice in a Reidemeister III picture. Conversely, if a loop happens to turn only once, then:

- → Of course it has a way to survive naturally the move, by keeping on turning at the same crossing.
- → Depending on the move, it may have the "choice" to stop turning at that crossing, and turn at the two others instead. For instance in Fig.4.12 (from right to left), the green loop can choose to keep turning at p, or to become the red loop.

Why is this choice important? Because it can happen that a strand thieves and becomes the only turn of a loop, and then goes dying in an R-II move, hence a priori killing that loop. *Unless* before this R-II move there is another triple point, where the loop can choose to get away from the soon-to-be dead strand.

Here is a conjectural (informal) principle that could be of significant help if one

could formalize it – which will not be done here:

What a close combed strand steals, it always somehow gives it back.

It is possible to prove that the number of R-III encountered by a single close combed strand is always even. Hence the most naive (still informal) version of the above principle would be: "it is possible to group the triple points met by a given strand into pairs, in such a way that what is stolen by the strand at one point is given back at its match."

Let us present an enlightening example. Consider the red path at time t_0 from Fig.4.23. First of all, it is clear that this path should not rely on the present local picture if it hopes to live in every diagram. But let us disregard this fact. At least from this local point of view, the path does not survive the sequence of moves: at t_1 there is no way it can cross the interrogation mark while respecting the orientation of the knot. In other words, during this sequence of moves, the close (light blue) strand steals something from the red loop, that it does not give back eventually.

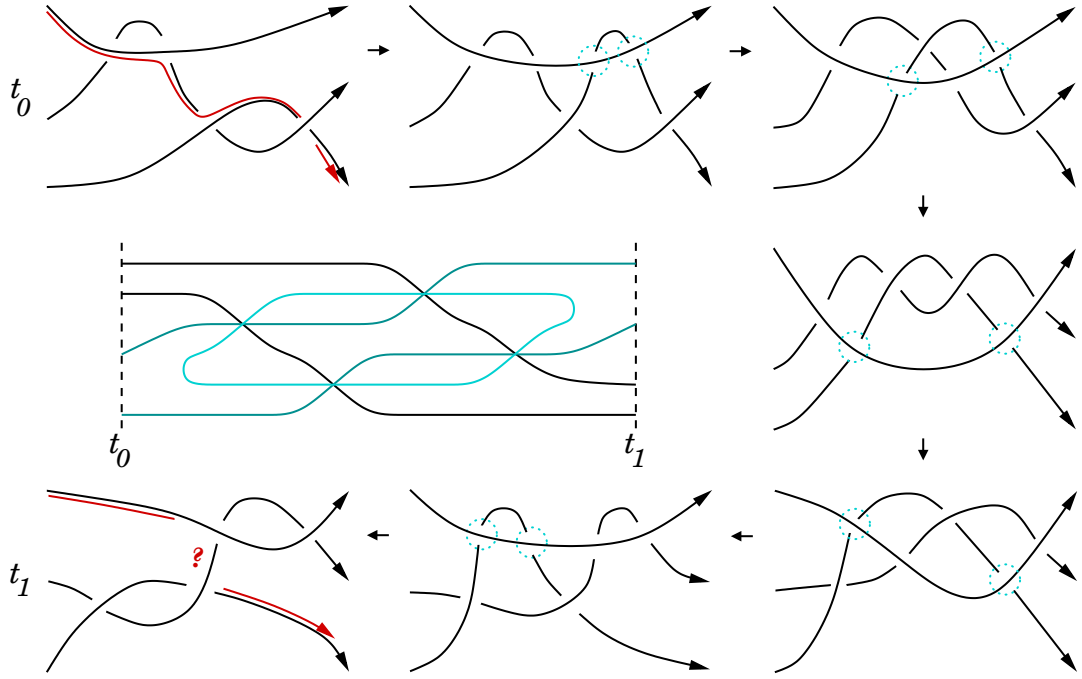

Figure 4.23: A single closed strand in a combed trace graph can *locally* kill a path

There is no *local* rescue in this example, as there were in Figs.4.11 and 4.12. But to construct it, it appeared necessary to use from the beginning a couple of crossings that could be killed by R-II. Hence, if this situation at t_0 appears while the diagram at time $t = 0$ had minimal number of crossings – as it does in the conjecture – then something significant must have happened *before* t_0. What this teaches us is that time should not be considered absolute: one has to allow rescuings to go back in time, and then forward again. This remark could have been made right after the example of Fig.4.11, but Fig.4.23 shows that it remains relevant even after the combing process.

Here is a draft plan to formalize the "rescuing" process:

1. Glue all knot diagrams of a given knot type together, "à la Vassiliev".
2. For every knot diagram D of this type, there is a natural map $H_1(D) \to H_1(X)$. Define the *reduced homology group* $H_1^{red}(D)$ as the image of this map.
3. Homologies in X define maps $H_1^{red}(D) \to H_1^{red}(D')$ for any two diagrams D and D'. Here there is a difficulty finding an *order* on the diagrams so that these maps form a direct system.
4. The conjecture reasonably becomes: "if a diagram D has minimal number of crossings, then $H_1^{red}(D)$ is naturally isomorphic to the direct limit of the above system".

A slightly different approach, maybe more promising, is the following: instead of gluing together knot diagrams, consider the actual embeddings of the circle in a thickened surface, with additional *arcs* joining every two preimages of a crossing. This gives a trivalent graph, which is nothing but an embedding of the Gauss diagram (see an example on Fig.4.24). It happens that this graph is bipartite (it is a necessary condition for a Gauss diagram to be realizable by a usual knot, see [17]). Hence it is what L.Lewark calls a *knotted web* [20]. To get a nice way of gluing these graphs together, one may take inspiration from the *foams* from [20], which are cobordisms between webs.

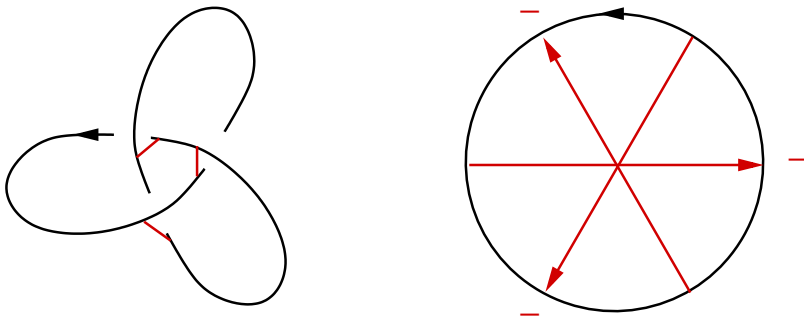

Figure 4.24: An embedded Gauss diagram of a trefoil

Chapter 5

Invariants of non generic homotopies

[1]

For a long time knot theory was just the study of non-singular knots up to isotopy. V.A.Vassiliev [30] has introduced a new point of view: instead of studying individual knots he has considered the space of all smooth immersions of a circle, including singular knots. The discriminant of that space has a natural stratification. The level 0 of Vassiliev's theory, that of finite-type invariants described in Section 3.1, is usually expressed using only those strata of the discriminant that correspond to immersions with only ordinary double points as singularities.

The present chapter is the starting point for the study of more complicated strata of the discriminant, by means of invariants of non generic homotopies. A generic homotopy between two classical knots in $\mathbb{R}^3$ would intersect the discriminant only in the interior of codimension 1 strata. Here we consider *triple homotopies*, that is homotopies that meet the discriminant only in *ordinary triple points* (which are a kind of codimension 3 strata), and only with *coherent* directions (Definition 5.1.2). Any two knots can be connected by such a homotopy (see [8]).

We define the *index* $\mathrm{ind}(\gamma)$ of such a homotopy γ, and prove that it is invariant under boundary-fixing homotopy of γ. Hence it defines a 1-cocycle (in the sense of braid-like triple loops up to homotopy), which is shown to be non trivial. On another hand, we define a weighted index, the *writhe* of a triple homotopy, and show that the Casson invariant of a knot (v_2) can be recovered as the writhe of a triple homotopy from that knot to the unknot. In other words, the writhe be regarded as the "derivative" of the Casson invariant with respect to triple points. As a corollary we obtain a very simple proof of the fact that passing a coherent triple point always changes the knot type.

1. This chapter is a joint work with T.Fiedler, that was published in the Journal of Knot Theory and its Ramifications [12].

5.1 Triple homotopies

Let $\mathbb{R}^4$ be the euclidean space with coordinates (x, y, z, t). Let K_0 be a non singular knot (i.e. an embedded circle) in $(x, y, z, 0)$. A homotopy of K_0 is a cylinder $\{K_t, t \in [0, 1]\}$ immersed in $\mathbb{R}^4$. It can be regarded as a 1-parameter family of knot diagrams with respect to the projection $(x, y, z, t) \mapsto (x, y, t)$.

Let Σ be the discriminant of all *singular* knots in $\mathbb{R}^3$ (*i.e.* maps f whose image $f(\mathbb{S}^1) \subset \mathbb{R}^3$ is not a submanifold). Σ has a natural stratification (compare [30]). The strata of codimension 1, $\Sigma^{(1)} \subset \Sigma$ are formed by all knots that have exactly one ordinary double point. Let Σ_{triple} be the union of all those strata that correspond to knots that have exactly one ordinary triple point as a singularity.

Definition 5.1.1. An ordinary triple point p of a homotopy $\mathbb{S}^1 \times [0, 1] \to \mathbb{R}^4$ is called *coherent* if all three branches intersect at p pairwise with the same intersection index. In other words, the three crossings on any side of the triple point must have the same writhe (see Fig.5.1 and Fig.5.2).

Definition 5.1.2. A homotopy of a knot K_0 is called a *triple homotopy* if it intersects Σ only in Σ_{triple}, where the intersection is coherent and not tangential. It is called *elementary* if it involves exactly one triple point. It is called *regular* if moreover the isotopy part of it is regular (i.e. involves no Reidemeister move of type I) with respect to the projection $(x, y, z, t) \mapsto (x, y, t)$.

Remark 5.1.3. Notice that being coherent is a property of the *homotopy* and not only of the stratum it crosses. For that reason, we will often refer to a *triple point* not only as the datum of a stratum but also as the local behaviour of a knot homotopy on each side of that stratum.

It is easy to see that generically a coherent triple point in a homotopy corresponds to a 1-parameter family of diagrams as shown in Fig.5.1 and Fig.5.2) (compare [8]). We call the family in Fig.5.1 a *braid-like move* and that in Fig.5.2 a *star-like move*.

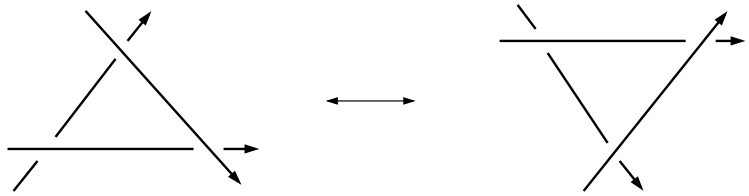

Figure 5.1: Braid-like moves

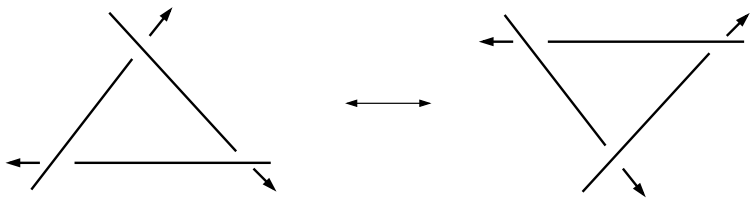

Figure 5.2: Star-like moves

The following is proved in [8], where it is attributed to M.Heusener.

Lemma 5.1.4. *Every knot can be unknotted by a triple homotopy.*

Corollary 5.1.5. *Every knot can be unknotted by a homotopy with only coherent braid-like triple points.*

Proof of the corollary. The proof amounts to Fig.5.3 below. The second kind of star-like moves is obtained from this one by reversing all the orientations. The picture remains the same otherwise.

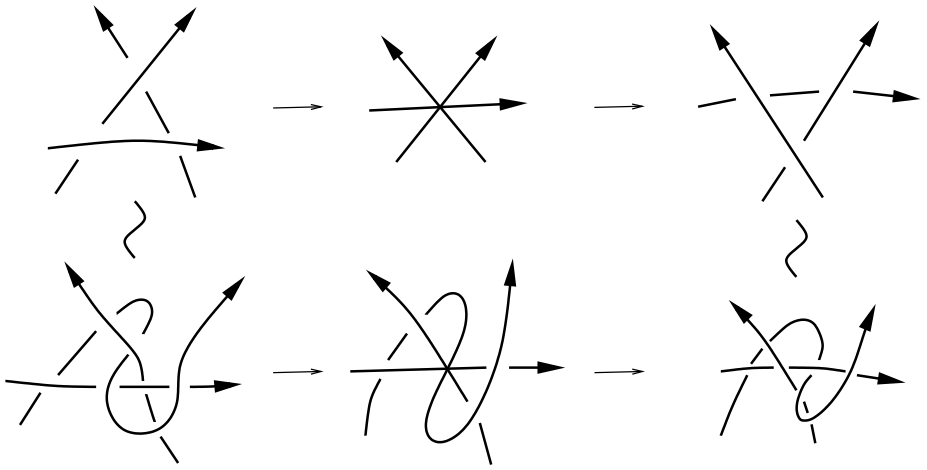

Figure 5.3: Exchanging braid-like and star-like moves

□

Definition 5.1.6. A *homotopy of a triple homotopy* is a homotopy $\{h_s, s \in [0,1]\}$ with fixed end points and such that h_s is a triple homotopy for fixed s except for a finite number of values of s where it either intersects Σ in the intersection of two strata of Σ_{triple} (Fig.5.4a) or in an ordinary quadruple point (Fig.5.4b), or it intersects Σ in an adjacent stratum of higher codimension (Fig.5.4c and Fig.5.4d), or it becomes tangential to Σ_{triple} (Fig.5.5).

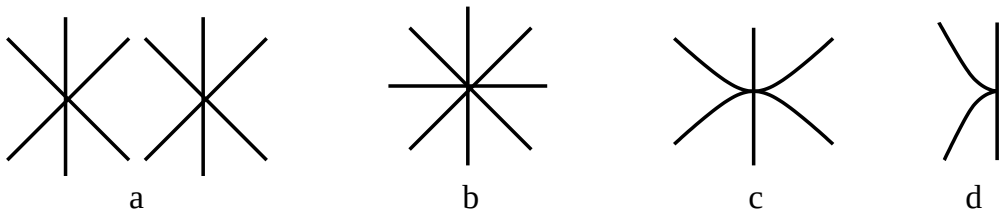

Figure 5.4: The four strata one may cross when homotoping a homotopy

In the last case, the singular knot diagram alone is not enough to see what happens, one needs to draw the local behaviour of the knot homotopy.

In other words, we add to the ordinary triple points all strata of higher codimension corresponding to singular knots without double points. *A triple homotopy may become tangent to Σ_{triple} during a homotopy, but always in a coherent way.*

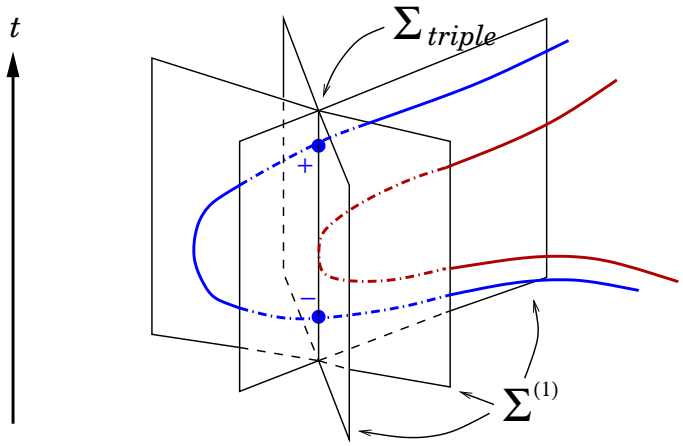

Figure 5.5: Tangency with Σ_{triple}

5.2 A non trivial triple loop

The *writhe* of a diagram is defined as usual as the sum of the signs of all crossings. Notice that the sum of the signs of the three involved crossings changes from $+3$ to -3 for both moves on Fig.5.3.

Let $\{K_t, t \in [0,1]\}$ be a triple homotopy.

Definition 5.2.1. The *index of a triple point* p, $\text{ind}(p)$, is defined to be $+1$ if the writhe increases by $+6$ for increasing parameter t, and -1 otherwise. The *index of the triple homotopy* $\text{ind}(\{K_t\})$ is defined as the sum of $\text{ind}(p)$ over all triple points in $\{K_t\}$.

Theorem 5.2.2. *The index* $\text{ind}(\{K_t\})$ *is invariant under boundary-fixing homotopy of the triple homotopy* $\{K_t\}$.

Remark 5.2.3. The index takes its values in an abelian group. It follows that $\text{ind}(\{K_t\})$ is also invariant under *homologies* of triple homotopies (which can be defined as cobordisms between cylinders).

Proof. We have to prove that the index of each little loop around a stratum shown in Fig.5.4 is zero.

Cases $1a$, $1b$ and $1c$ are easy to deal with: indeed, a generic little loop around one of these strata can be assumed to contain only triple crossings and *regular* isotopies (that do not make use of Reidemeister I moves). The writhe increase for a regular path is linearly dependent on its index, which implies that a regular *loop* has index 0.

As for the tangency case, the result is clear since the two additional intersection points that (dis)appear when a homotopy crosses a tangency have opposite indices (see Fig.5.5).

To treat the case $1d$ (a cusped triple point), we show the 18 possible resolutions, divided into five different local knot types (see Fig.5.6).

Remark 5.2.4. There are essentially two possible orientations for the cusped triple point (see Fig.5.7). Fig.5.6 only shows one case, the other one is exactly similar.

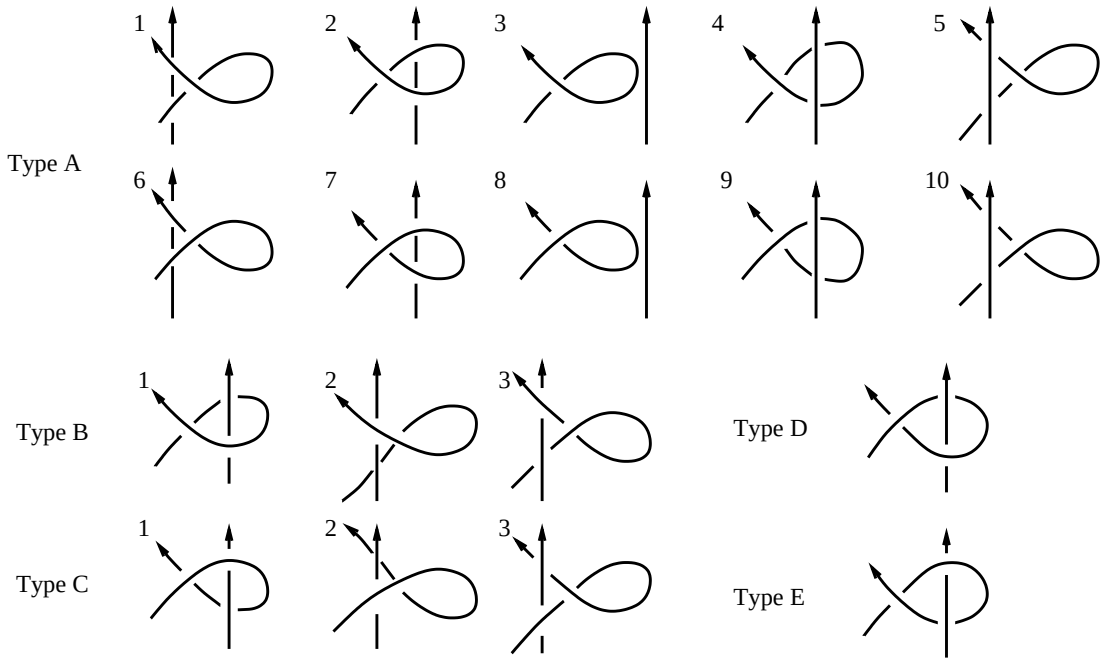

Figure 5.6: Resolutions of a cusped triple point

Diagrams of type A cannot contain a coherent triangle, therefore cannot be involved in a loop. Fig.5.7 shows the *elementary* paths between the remaining diagrams, consisting either of going across a triple point, or of a little isotopy, for both possible orientations of the strands.

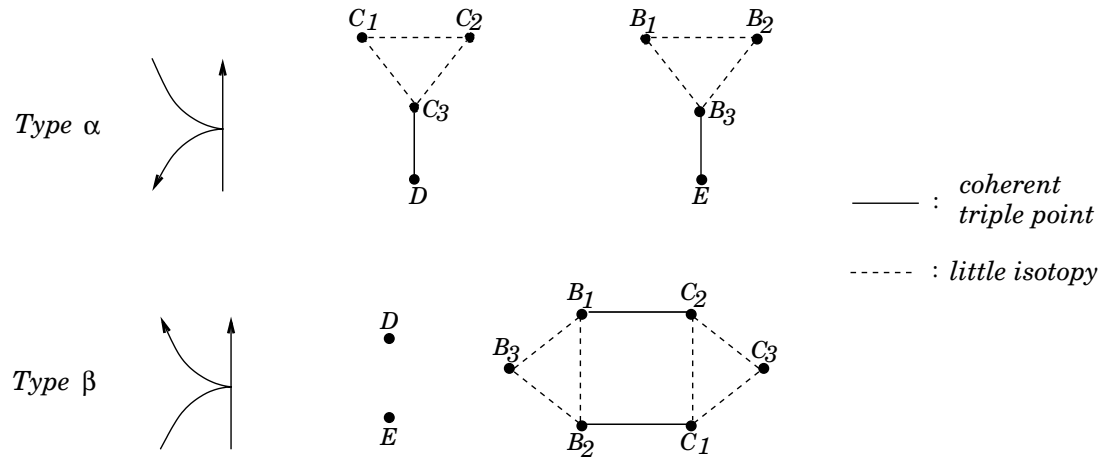

Figure 5.7: The graphs of little paths near a cusped triple point

The only loops appearing on the first graph of Fig.5.7 (type α) consist of isotopies, and we may ignore them. The second graph (type β) contains one possibly non trivial loop, namely the square $B_1 \to B_2 \to C_1 \to C_2 \to B_1$, whose index is clearly zero.

Remark 5.2.5. Among the five knot types (A,B,C,D,E) shown on Fig.5.6, some might be equivalent (for instance in the case of a nugatory crossing), but these

unpredicted equivalences cannot be achieved by a little isotopy within the depicted part of $\mathbb{R}^3$.

□

Proposition 5.2.6. *There are two triple unknottings of the right trefoil that are not homotopic as triple unknottings.*

Proof. First, notice that if we know a triple homotopy between two knots K_0 and K_1, then for any knot L we can deduce from it a triple homotopy from the connected sum $K_0 \sharp L$ to $K_1 \sharp L$ *with the same index*.

Fig.5.8 shows a positive elementary path from the trivial knot to the right trefoil 3_1^r. On one hand, it proves that we may unknot 3_1^r with index -1. On the other hand, thanks to the connected sum property, it gives a path of index 2

$$3_1^r \xrightarrow{+2} 3_1^r \sharp 3_1^r \sharp 3_1^r.$$

Fig.5.9 shows a negative path from $3_1^r \sharp 3_1^r$ to 4_1, from which we deduce

$$3_1^r \sharp 3_1^r \sharp 3_1^r \xrightarrow{-1} 4_1 \sharp 3_1^r.$$

Figs.5.10 and 5.11 successively give

$$4_1 \sharp 3_1^r \xrightarrow{-1} 3_1^l \xrightarrow{+1} \text{unknot}.$$

Finally, we have two triple unknottings of 3_1^r with indices +1 and -1. But the index is a homotopy invariant by Theorem 1.

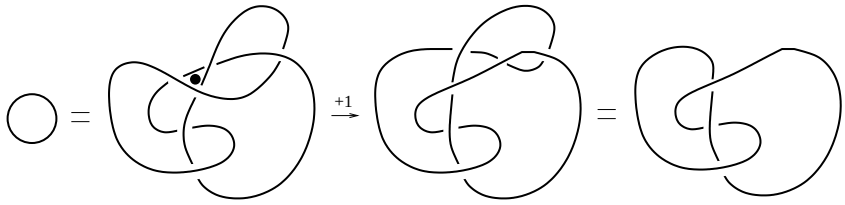

Figure 5.8: Unknot to trefoil

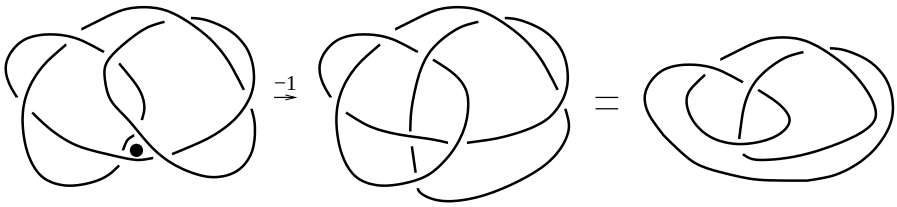

Figure 5.9: Trefoils to eight

□

Corollary 5.2.7. *There are triple loops that are not homotopic – as triple homotopies – to regular triple loops.*

Proof. The proof of Proposition 5.2.6 implies the existence of a triple loop with index non zero. But as we mentioned in the proof of Theorem 5.2.2, a regular loop must have index zero. □

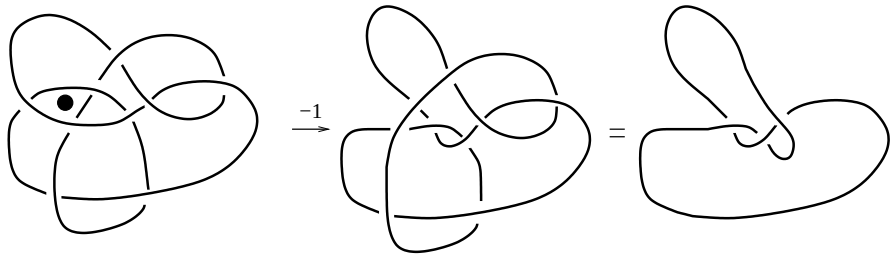

Figure 5.10: Eight ♯ trefoil to trefoil

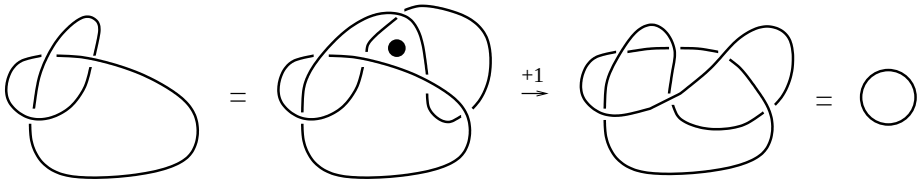

Figure 5.11: Left trefoil to unknot

5.3 A new formula for the Casson invariant

From now on, we only consider triple homotopies with braid-like triple points (recall Corollary 5.1.5). Let K be a singular knot with a triple point that corresponds to a braid-like move. Given a generic projection $\mathbb{R}^3 \to \mathbb{R}^2$, there is a natural way to associate a Gauss diagram to K:

- → As usual the regular crossings correspond to arrows, with a sign and an orientation.
- → There are three *unoriented and unsigned arrows* (chords) in a triangle shape, corresponding to the triple point.

Definition 5.3.1. The *writhe of K with respect to p*, denoted by $W(K,p)$, is defined as the sum of the signs of all the arrows that intersect the triangle in the Gauss diagram of K. Let $\{K_t\}$ be a triple homotopy. For some values $t_1, \ldots, t_m$ of t, K_{t_i} contains a triple point p_i. $W(\{K_t\})$ is then defined as the sum of $\mathrm{ind}(p_i)W(K_{t_i}, p_i)$ over all i.

This definition seems to depend on a choice of a projection, since it involves Gauss diagrams. It actually does not, as a corollary of Theorem 5.3.2 below.

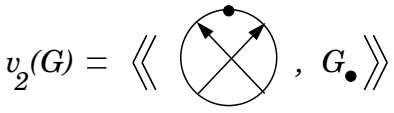

Figure 5.12: Based arrow diagram formula for v_2

Let $v_2(K)$ be the Vassiliev invariant of degree 2 (normalized to be 0 for the unknot and +1 for the trefoil). We use the expression of v_2 as an arrow diagram formula for long knots, given in [27] (Theorem 1) and reproduced here on Fig.5.12. It fits in the framework described in the paragraph "Long knots" (Subsection 3.2.1). Let us recall how this works. Here v_2 denotes the based arrow diagram from Fig.5.12. $G_\bullet$ is

an arbitrary based Gauss diagram (on the trivial group, since the knots considered live in the sphere $\mathbb{S}^3$). The map

$$G_\bullet \mapsto \langle\langle v_2, G_\bullet \rangle\rangle = \langle S(v_2), I(G_\bullet)\rangle$$

sums up the number of times the configuration v_2 happens in $G_\bullet$, weighted with the product of the signs of the two arrows involved. First, one shows that it is invariant under R moves that happen far away from the base point. Then by Proposition 3.2.4, this implies that choosing any base point on the Gauss diagram of a *real* knot, and then computing $\langle\langle v_2, \cdot \rangle\rangle$, gives a result that is independent from the choice of the base point, and defines a real knot invariant – which, in the present case, is the Casson invariant.

Theorem 5.3.2. *For any triple homotopy $\{K_t\}$ that contains only braid-like coherent triple points,*

$$W(\{K_t\}) = v_2(K_1) - v_2(K_0).$$

Remark 5.3.3. This should be regarded as a formula for the "first derivative" of the Casson invariant with respect to coherent braid-like triple points – in the same way Vassiliev invariants are defined through the derivatives with respect to ordinary double points. Note that the formula does not hold in the case of non coherent triple points, and neither even for coherent *star-like* triple points.

Proof. Consider an elementary triple homotopy $\{K_t\}$ (see Fig.5.13). To compute $v_2(K_1) - v_2(K_0)$ one may restrict one's attention to couples of arrows in which at least one arrow from the triple is implied (other couples contribute equally in $v_2(K_1)$ and $v_2(K_0)$, given the choices of base points made on Fig.5.13). Let $w(X, Y)$ denote the sum of the writhes of all the arrows whose tail lies in zone X and head in zone Y. The above description of v_2 yields

$$\begin{aligned} v_2(K_1) - v_2(K_0) &= (w(B,A) + w(B,C) + w(C,B)) - (-w(A,C) - w(A,B) - w(C,A)) \\ &= W(\{K_t\}). \end{aligned}$$

□

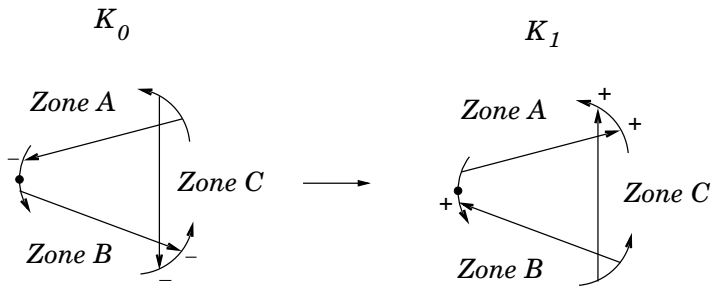

Figure 5.13: An elementary triple homotopy

Proposition 5.3.4. *The writhe $W(K, p)$ of a braid-like move is always odd.*

As a corollary of this Proposition and Theorem 5.3.2, one gets

Corollary 5.3.5. *Passing a coherent triple point always changes the knot type.*

Remark 5.3.6. This corollary was already proved in [8], using Rokhlin's $\mathbb{Z}/2\mathbb{Z}$-valued quadratic form associated to an orientable characteristic surface in an orientable 4-manifold.

Proof of Proposition 5.3.4. Let us compute again the difference $v_2(K_1) - v_2(K_0)$ (with the notations of Theorem 5.3.2), this time the special point lying between the two arrow ends of the branch that separates zone A and zone C. One gets

$$W(\{K_t\}) = 1 + 2w(B, A) + 2w(B, C) + w(A, C) + w(C, A).$$

It remains to show that $w(A, C) + w(C, A)$ is even. Consider the knot K_1 with two crossings of the triple smoothed as indicated by Fig.5.14. A, B and C have become the three components of a link, and one sees that $w(A, C)$ and $w(C, A)$ are both equal to the linking number of A and C.

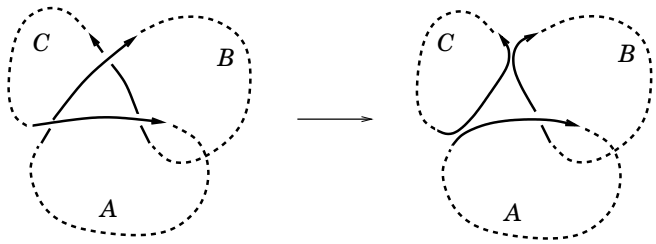

Figure 5.14: Smoothings

□

Bibliography

[1] Dror Bar-Natan. On the Vassiliev knot invariants. *Topology*, 34(2):423–472, 1995.

[2] Joan S. Birman and Xiao-Song Lin. Knot polynomials and Vassiliev's invariants. *Invent. Math.*, 111(2):225–270, 1993.

[3] Sergei Chmutov, Michael Cap Khoury, and Alfred Rossi. Polyak-viro formulas for coefficients of the Conway polynomial. *J. Knot Theory Ramifications*, 18(6):773–783, 2009.

[4] Sergei Chmutov and Michael Polyak. Elementary combinatorics of the HOMFLYPT polynomial. *Int. Math. Res. Not. IMRN*, (3):480–495, 2010.

[5] Micah W. Chrisman. Twist lattices and the Jones-Kauffman polynomial for long virtual knots. *J. Knot Theory Ramifications*, 19(5):655–675, 2010.

[6] Micah W. Chrisman. On the Goussarov-Polyak-Viro finite-type invariants and the virtualization move. *J. Knot Theory Ramifications*, 20(3):389–401, 2011.

[7] Thomas Fiedler. A small state sum for knots. *Topology*, 32(2):281–294, 1993.

[8] Thomas Fiedler. Triple points of unknotting discs and the Arf invariant of knots. *Math. Proc. Cambridge Philos. Soc.*, 116(1):119–129, 1994.

[9] Thomas Fiedler. *Gauss diagram invariants for knots and links*, volume 532 of *Mathematics and its Applications*. Kluwer Academic Publishers, Dordrecht, 2001.

[10] Thomas Fiedler. Gauss diagram invariants for knots which are not closed braids. *Math. Proc. Cambridge Philos. Soc.*, 135(2):335–348, 2003.

[11] Thomas Fiedler and Vitaliy Kurlin. A 1-parameter approach to links in a solid torus. *J. Math. Soc. Japan*, 62(1):167–211, 2010.

[12] Thomas Fiedler and Arnaud Mortier. On homotopies with triple points of classical knots. *J. Knot Theory Ramifications*, 21(4):1250038, 10 p., 2012.

[13] Mikhail Goussarov. Finite-type invariants are presented by gauss diagram formulas, 1998. Translated from Russian by O. Viro.

[14] Mikhail Goussarov, Michael Polyak, and Oleg Viro. Finite-type invariants of classical and virtual knots. *Topology*, 39(5):1045–1068, 2000.

[15] S. A. Grishanov and V. A. Vassiliev. Fiedler type combinatorial formulas for generalized Fiedler type invariants of knots in $M^2 \times \mathbf{R}^1$. *Topology Appl.*, 156(14):2307–2316, 2009.

[16] Christian Kassel and Vladimir Turaev. *Braid groups*, volume 247 of *Graduate Texts in Mathematics*. Springer, New York, 2008. With the graphical assistance of Olivier Dodane.

[17] L. H. Kauffman. Virtual Knot Theory. *ArXiv Mathematics e-prints*, November 1998.

[18] Louis H. Kauffman. *On knots*, volume 115 of *Annals of Mathematics Studies*. Princeton University Press, Princeton, NJ, 1987.

[19] Jean Lannes. Sur les invariants de Vassiliev de degré inférieur ou égal à 3. *Enseign. Math. (2)*, 39(3-4):295–316, 1993.

[20] Lukas Lewark. *Khovanov-Rozansky homologies, knotted weighted webs and the slice genus*. PhD thesis, Université Paris Diderot, France, 2013.

[21] A. Mortier. Gauss diagrams of real and virtual knots in the solid torus. *ArXiv e-prints*, January 2012.

[22] A. Mortier. Polyak type equations for virtual knots in the solid torus. *ArXiv e-prints*, October 2012. To appear in *J. Knot Theory Ramifications*.

[23] Olof-Petter Östlund. A combinatorial approach to vassiliev knot invariants. U.U.D.M. Project Report, 1996:P7.

[24] Michael Polyak. Talk at Swiss Knots 2011 – "3 stories about 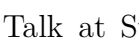 ". `http://drorbn.net/dbnvp/SK11_Polyak.php`. Videography by Pierre Dehornoy and Dror Bar-Natan.

[25] Michael Polyak. On the algebra of arrow diagrams. *Lett. Math. Phys.*, 51(4):275–291, 2000.

[26] Michael Polyak. Minimal generating sets of Reidemeister moves. *Quantum Topol.*, 1(4):399–411, 2010.

[27] Michael Polyak and Oleg Viro. Gauss diagram formulas for Vassiliev invariants. *Internat. Math. Res. Notices*, (11):445ff., approx. 8 pp. (electronic), 1994.

[28] Michael Polyak and Oleg Viro. On the Casson knot invariant. *J. Knot Theory Ramifications*, 10(5):711–738, 2001. Knots in Hellas '98, Vol. 3 (Delphi).

[29] Fionntan Roukema. Goussarov-Polyak-Viro combinatorial formulas for finite type invariants. *ArXiv e-prints*, November 2007.

[30] V. A. Vassiliev. Cohomology of knot spaces. In *Theory of singularities and its applications*, volume 1 of *Adv. Soviet Math.*, pages 23–69. Amer. Math. Soc., Providence, RI, 1990.

[31] V. A. Vassiliev. Combinatorial formulas for cohomology of spaces of knots. In *Advances in topological quantum field theory*, volume 179 of *NATO Sci. Ser. II Math. Phys. Chem.*, pages 1–21. Kluwer Acad. Publ., Dordrecht, 2004.

Summary

A knot is an embedding of a circle into a 3-dimensional manifold. When this manifold is the sphere, knots can be described combinatorially using Gauss diagrams. Forgetting about the actual knots, one can study Gauss diagrams independently: this is called virtual knot theory. In the first part we define a general version of virtual knots that depends on a group G endowed with a $\mathbb{Z}/2$-valued homomorphism w. When G and w are suitably chosen, this version generalizes knot theory in a given thickened surface – i.e. a 3-manifold endowed with a line bundle projection onto a surface. Besides encoding knots, Gauss diagrams can also encode Vassiliev's finite-type knot invariants. A complete set of criteria is given to detect these invariants in the present framework. Notably, the criterion for Reidemeister III gives a positive answer to a conjecture of Polyak. Several examples are given, including an improvement of Grishanov and Vassiliev's theorem on planar chain invariants.

The third part is a draft investigating a plan to find an algorithm that tells whether a knot in the solid torus is isotopic to a closed braid. The first step is achieved: it consists of a characterization of Gauss diagrams of closed braids. We state and investigate a conjecture which predicts that for diagrams with minimal number of crossings, this first step is enough.

The last part is a joint work with T.Fiedler, investigating invariants of non generic loops in the space of all immersions of a circle into the 3-space. This space is infinite dimensional, stratified by the degree of non genericity of an immersion. Vassiliev's theory was based on adding to the usual knots all strata with only ordinary double points as singularities. Here we forbid these double points and regard only some higher codimensional strata with a certain kind of triple points. We show that the resulting space is not simply connected, by exhibiting a non trivial 1-cocycle. Weighting this cocycle gives a new formula for the Casson invariant, using triple unknottings.

Keywords: Virtual knots – Gauss diagrams – Polyak algebra – Finite type invariants – Braids – Casson invariant.

MSC classes: 57M25, 57M99.

Résumé

Un nœud est un plongement du cercle dans une variété de dimension 3. Dans la sphère $\mathbb{S}^3$, les nœuds peuvent être codés combinatoirement par des diagrammes de Gauss. Ceux-ci peuvent être étudiés indépendamment, en oubliant les véritables nœuds: c'est ce qu'on appelle la théorie des nœuds virtuels. En première partie nous définissons une version générale de nœuds virtuels, dépendant d'un groupe G muni d'un morphisme à valeurs dans $\mathbb{Z}/2$. Lorsque ces paramètres sont bien choisis, la théorie obtenue généralise les nœuds dans une surface épaissie quelconque (c'est-à-dire un fibré en droites réelles sur une surface). Outre l'encodage des nœuds, les diagrammes de Gauss sont aussi un outil puissant pour décrire les invariants de type fini de Vassiliev. En seconde partie, nous donnons un ensemble complet de critères pour détecter ces invariants. Notamment, le critère d'invariance sous Reidemeister III est une réponse positive à une conjecture de M.Polyak. Parmi les exemples donnés figure une nouvelle preuve et une généralisation du théorème de Grishanov-Vassiliev sur les invariants par chaînes planaires.

La troisième partie est une ébauche de plan visant à trouver un algorithme pour décider si un diagramme donné dans l'anneau $\mathbb{R} \times \mathbb{S}^1$ représente une tresse fermée dans le tore solide, à isotopie près. La première étape est franchie, consistant à trouver un critère reconnaissant les diagrammes de Gauss des tresses fermées. Nous conjecturons que ce critère suffit pour les diagrammes à nombre minimal de croisements, et proposons des pistes dans cet objectif.

La dernière partie est un travail commun avec T.Fiedler, explorant les propriétés d'objets non génériques liés à l'espace de toutes les immersions du cercle dans $\mathbb{R}^3$. Cet espace est de dimension infinie, stratifié par le degré de non généricité des immersions. Alors que la théorie de Vassiliev se cantonne à l'étude des strates contenant uniquement des points doubles ordinaires, ici nous interdisons ces points doubles et autorisons uniquement un certain type de points triples. Nous montrons que l'espace qui en résulte n'est pas simplement connexe en exhibant un 1-cocycle non trivial. Une pondération de ce 1-cocycle fournit une nouvelle formule pour l'invariant de Casson des nœuds.

Mots-clés : Nœuds virtuels – Diagrammes de Gauss – Algèbre de Polyak – Invariants de type fini – tresses – invariant de Casson.